Non-perturbative access to Casimir-Polder potentials for nontrivial geometries in QED

Diploma Thesis

Institute of Theoretical Physics
Quantum Field Theory

submitted by:	Frank Glowna
field of study:	physics
student ID:	76961
advisor:	Prof. Dr. Holger Gies
second advisor:	Priv.-Doz. Dr. Maarten DeKieviet

Diploma thesis submitted by Frank Glowna, born in Tharand, Germany.

May 14, 2010
corrected version June 7, 2010

Abstract

A non-perturbative quantum field theoretical handling of Casimir forces in QED for nonplanar surfaces is reviewed and applied to certain geometries. The possible extension to general dielectrics is shown, but the main focus lies on perfectly conducting surfaces. Boundary conditions are derived for a non-local and local implementation into the formalism, whereby the latter one is used. At first, Casimir's result for two plain plates is obtained. Then, the propagator for a sphere of arbitrary radius, which is needed within the method, is derived, studied, and inverted analytically. Three different coordinate choices are discussed, whereby the general inverse propagator for the sphere is found. The standard Casimir-Polder result for an atom in front of a plain plate is calculated. At last, the method is applied to a sphere in front of a uniaxial corrugated surface. To obtain the Casimir energy for this setup, the corresponding propagator for the corrugated surface and the numerical method is presented.

Contents

1 Introduction

1.1 From historical background to the actual work

The understanding of the nature of forces has, of course, a long history. But the birth of quantum mechanics first leads to significant results in the development of a theory of the origin of atomic and interatomic forces. One of the big results of quantum mechanics is, for example, the change of a classical vacuum to a quantum vacuum. In this one, thanks to Heisenberg's uncertainty principle, we know that energy can fluctuate over short instances of time. Therefore the quantum vacuum has the so-called zero-point energy. These fluctuations now lead to physical effects. In 1930 London [1,2] showed that a force between molecules possessing electric dipole moments should fall off with the distance d between the molecules as $\frac{1}{d^6}$. The simple argument for this gives the interaction energy H_{int} for two such dipoles which is $\frac{1}{d^5}$ for short distances. Now taking fluctuations into account, the energy is given by the mean value $\langle H_{\text{int}} \rangle$ and the first order of perturbation theory vanishes, because the dipoles are oriented randomly. Thus, the short distance behaviour starts with the second order which gives the $\frac{1}{d^6}$. In 1948 Casimir [3] shifted the idea from an action at a distance between molecules to a local action of fields. According to that, the above phenomenon can equally be discussed in terms of fluctuating fields.

He considered two parallel, infinitely large and ideally conducting plates in vacuum at zero temperature, separated by a distance d. Now the idea is that electromagnetic fields or photons that emerge between the plates have to obey certain boundary conditions on the surfaces. Thus the allowed number of fluctuation modes between the surfaces is restricted, whilst on the outside the number of permissible modes is higher. This boundary conditions, of course, are dictated by the vacuum Maxwell's equations. In the end, Casimir's results for the energy and the force per unit area are

$$E_{\text{Casimir}} = -\frac{\hbar c \pi^2}{720} \frac{1}{d^3} \qquad F_{\text{Casimir}} = -\frac{\partial}{\partial d} E_{\text{Casimir}} = -\frac{\hbar c \pi^2}{240} \frac{1}{d^4} \,. \tag{1.1}$$

This change of viewpoint now opens up a new field of phenomena, which is referred to as the Casimir effect. For an overview, see [4]. Nowadays, forces arising from fluctuations are all called Casimir forces, and in the special case of long-range interactions between neutral atoms or molecules due to their common interaction with the electromagnetic radiation field, the forces are called Casimir-Polder or van der Waals forces [5]. But also non quantum mechanical fluctuations like density fluctuations in liquids [6] lead to "critical Casimir forces", which have been observed recently [7].

So why are influences of structures that interesting to the community? Although Casimir and Casimir-Polder forces are very small, they have been measured with high precision for macroscopic objects [8, 9, 10, 11, 12, 13], for mesoscopic configurations [14, 15], and also indirectly for atom-atom van der Waals interactions [16]. To compare these results with the theory, it is necessary to take into account temperature, boundary effects like those from finite surfaces or edge effects, general dielectrics and so forth. Also the corrugation of the surfaces could be theoretically optimised to increase the intensity of such forces. All together, Casimir forces find practice in nanoscale engineering [17, 18], chemistry, biology, but also in cosmology.

1.2 Current state of research

So far, calculations for nontrivially shaped geometries in the sense of Casimir Polder potentials were done with the so-called proximity force approximation (PFA) [19, 20]. In this, corrugated surfaces are replaced piecewise by flat segments and thus can be used for any configurations. But of course, Casimir deliberately chose two parallel plates because fluctuation induced forces are inherently non-additive. Hence, in the end, PFA is only an approximation, which has to be used with care. Therefore, various techniques are desired by the Casimir community [21, 22, 23, 24, 25, 26, 27, 28, 29] to describe Casimir forces.

Another non-perturbative formalism, firstly introduced by Bordag, is a functional approach. With this, the Casimir energy density can be calculated out of the partition function by introducing a delta functional into it, which carries the boundary conditions on the surfaces [30]. This formalism was extended to corrugated dielectric surfaces for abelian scalar fields [31], in which the only approximation is that the dielectric sphere, which represents an atom, has a very small radius compared to the mean distance to the corrugated surface. So the corrugation itself can be arbitrarily raised and lowered without loss of correctness in accordance with the numerical precision.

On the experimental side, diverse measurements of Casimir forces were done, too. For example, in Heidelberg at the atomic beam spin echo (ABSE)-apparatus, Casimir experiments were done with ^{3}He atoms which were quantum reflected [11, 32] by the attractive Casimir Polder potential of an atom and a structured plate [33]. For instance, a sinusoidal corrugation appears as a surface effect of thick gold atom layers, but also a sawtooth structure was tried out. For the latter, an interesting effect was found, which may only be explained by short distance Casimir Polder forces. The observed power n with which the force decreases, depends on the incident direction in the fol-

lowing way: Along the ridges, $n = 6$ was found, under an angle of 45 degrees to the ridges, the potential changes with $n = 4$ and orthogonal to the ridges the n was 5. This is of course a strongly geometric sensitive effect and could hardly be described by above methods.

1.3 Topic of this thesis

The task of this thesis is to extend the above non-perturbative technique [31] for nontrivial geometries from scalar fields to abelian vector fields, or precisely to the electrodynamic case in QED. Thus, the scalar dielectric boundary conditions become, according to Maxwell's equations, dictated boundary conditions, which also carry surface information, and the propagator for the scalar fields changes to the free photon propagator, which is a matrix in the end.

2 Casimir forces for abelian gauge fields

2.1 Preliminaries

Quantum field theory can be formulated with the functional integral formalism. In this formulation, fields are not treated as operators but as common functionals, which have to obey Hamilton's principle. Starting with the generating functional or partition function $\mathcal{Z}$, every quantity of interest can be obtained. In this sense, the Casimir force can be obtained by the energy density of the fluctuating field, which is determined by the logarithm of $\mathcal{Z}$. Additionally, boundary conditions on the surfaces have to be set, which then give restrictions on $\mathcal{Z}$. For the energy altogether, $\ln \mathcal{Z}$ will be reformulated in a more convenient way, which also provides space for physical interpretations.

2.2 Vector field theory with boundaries

2.2.1 The "free" partition function

In QED, the partition function is defined as

$$\mathcal{Z} = \int \mathcal{D}A e^{-S_E[A_\mu]}\,, \tag{2.1}$$

where $\mathcal{D}A$ symbolises $\prod_{\mu,x} dA_\mu(x)$, the path integral over the field strength of every component of the electromagnetic vector field potential A_μ at every point x in space and time and S_E is the Euclidean action after a Wick rotation to imaginary time.[1] This is still the "free" vacuum formulation, where no boundary conditions are imposed. Now the action-integral in QED is the Maxwell-Yang-Mills action $S = \int (\mathcal{L}_0 + J^\mu A_\mu) dx$, where $\mathcal{L}_0 = -\frac{1}{4} F_{\mu\nu} F^{\mu\nu}$ is the Lagrangian, $F^{\mu\nu} = \partial^\mu A^\nu - \partial^\nu A^\nu$ is the electromagnetic field strength tensor and J_μ are external charge and current sources which are set to zero in the following (see section 2.2.3). This action S is constructed in that way, that after variation of the Lagrangian, the inhomogeneous Maxwell's equation $\partial_\mu F^{\mu\nu} = J^\nu$, or without external currents and charges:

$$\partial_\mu F^{\mu\nu} = 0\,, \tag{2.2}$$

is resulting. Later, the free photon propagator is needed, which is in principle the inverse of this equation (2.2) corresponding to A_μ. Thus it is necessary

[1] A so-called Wick rotation is the formal transfer from a real valued time t to the pure imaginary axis $t \to -i\tau$ of the complex plane. τ afterwards is an imaginary time, which is usefull for calculations because the flat space Minkowski metric diag $(-,+,+,+)$ becomes an Euclidian metric diag $(+,+,+,+)$.

to insert the definition of $F_{\mu\nu}$ in $\partial_\mu F^{\mu\nu} = 0$ and the equation

$$(g_{\mu\nu}\Box - \partial_\mu\partial_\nu)A^\nu = 0 \tag{2.3}$$

is obtained. This equation of motion also could have been obtained with a Lagrangian of the quadratic form $\mathcal{L} = \frac{1}{2}A^\mu L_{\mu\nu}A^\nu$ with $L_{\mu\nu} = g_{\mu\nu}\Box - \partial_\mu\partial_\nu$. Now the inverse of $L_{\mu\nu}$ would be needed, but due to a zero-eigenvalue[2] the inverse does not exist. The reason for this is that $\mathcal{L}$ is still invariant under the gauge transformation $A_\mu \to A_\mu + \partial_\mu\Lambda$. The integral in equation (2.1) runs over all fields and thus in particular over all configurations which differ only by such a gauge transformation. Every gauge contains the same physics, so they will be integrated over infinitely many gauges of the same physics, which would result in an infinite contribution to the partition function. To fix this problem, the gauge has to be fixed. This can be done by introducing a gauge fixing term to the Lagrangian $\mathcal{L} = \mathcal{L}_0 + \mathcal{L}_{GF}$. Here $\mathcal{L}_{GF} = \frac{1}{2\alpha}(\partial_\mu A^\mu)^2$ is used, where $\alpha \in \mathbb{R}$ is a free parameter parameterising an orbit in the space of possible gauges. For example, $\alpha = 1$ is known as the Feynman gauge or $\alpha \to 0$ is known as the Landau gauge. With the use of the Feynman gauge, most calculations become very easy and therefore it will be used in this thesis. However, with this gauge fixing, the number of degrees of freedom is still not equal to the number of physical degrees of freedom. But QED is an abelian gauge theory and therefore a fully fixed gauge[3] is not needed. Additional gauge freedoms will be discussed later in chapter 2.5.

The new choice of $\mathcal{L}$ can now easily be transformed to

$$\mathcal{L} = \frac{1}{2}A^\mu(g_{\mu\nu}\Box + (\frac{1}{\alpha} - 1)\partial_\mu\partial_\nu)A^\nu\,, \tag{2.4}$$

where the so-called "non-Maxwell-equation of motion" [34] appears.

$$\left[\Box + (\frac{1}{\alpha} - 1)\partial^\mu\partial_\nu\right]A^\nu = 0 \tag{2.5}$$

This one has no zero-eigenvalues and therefore can be inverted in the next section. But before, the operator in the squared brackets in (2.5) can be rewritten to a form in which it becomes a functional operator depending on two points.

$$L^{\mu\nu}(x,y) = -\delta^4(x-y)\left[\Box + (\frac{1}{\alpha} - 1)\partial^\mu\partial_\nu\right](x) \tag{2.6}$$

The global minus is only convention.

[2] $L_{\mu\nu}\partial^\mu\Lambda = (\partial_\nu\Box - \partial_\mu\partial^\mu\partial_\nu)\Lambda = (\partial_\nu\Box - \Box\partial_\nu)\Lambda = 0$

[3] "Fully fixed gauge" means the number of degrees of freedom equals the number of physical degrees of freedom.

2.2.2 Free photon propagator

The free photon propagator $G^{\nu\kappa}$ is given by the functional inverse of the operator $L_{\mu\nu}(x,y)$:

$$\int_y L_{\mu\nu}(x,y)G^{\nu\kappa}(y,z) = \delta(z-x)\delta^\kappa_\mu\,, \tag{2.7}$$

an analogue to the usual matrix inverse $\sum_j M^{-1}_{ij}M_{jk} = \delta_{ik}$. The integral replaces the matrix product. Now inserting the definition of $L_{\mu\nu}$ (2.6), the integral (2.7) can be carried out and the above non-Maxwell-equation of motion acting on $G^{\nu\kappa}$ is obtained.

$$L_{\mu\nu}(x)G^{\nu\kappa}(x,z) = \delta(z-x)\delta^\kappa_\mu \tag{2.8}$$

Afterwards both sides have to be transformed to momentum space $z-x \to p$, because $L_{\mu\nu}(x)$ becomes diagonal there and can be inverted like a usual matrix. Of course, this "free" system with no boundary conditions is still translation invariant and therefore a change to momentum space is allowed in all four dimensions. Now on the left side a Fourier transformation integral appears. By partial integrations, the differential operators in L can be shifted to act on the e^{ipx} term and thus will be replaced by ip.

$$\int \frac{d^4p}{(2\pi)^4}e^{-ip(z-x)}\delta^\kappa_\mu = L_{\mu\nu}(x)\int \frac{d^4p}{(2\pi)^4}G^{\nu\kappa}(p)e^{-ip(z-x)} \tag{2.9}$$

$$= -\int \frac{d^4p}{(2\pi)^4}G^{\nu\kappa}(p)\left[\Box + (\frac{1}{\alpha}-1)\partial^\mu\partial_\nu\right]e^{-ip(z-x)} \tag{2.10}$$

$$= \int \frac{d^4p}{(2\pi)^4}G^{\nu\kappa}(p)\left[p^2 + (\frac{1}{\alpha}-1)p^\mu p_\nu\right]e^{-ip(z-x)} \tag{2.11}$$

In the end,

$$G^{\nu\kappa}(p)\left[g_{\mu\nu}p^2 + (\frac{1}{\alpha}-1)p_\mu p_\nu\right] = \delta^\kappa_\mu \tag{2.12}$$

is left and the matrix inverse is

$$G^{\nu\kappa}(p) = \frac{1}{p^2}\left[g^{\nu\kappa} + (\alpha-1)\frac{p^\nu p^\kappa}{p^2}\right]. \tag{2.13}$$

After a simple back transformation to position space $p \to x$, the resulting $G^{\nu\kappa}(x)$ becomes

$$G^{\nu\kappa}(x) = \frac{1}{(2\pi)^2}\left[\frac{1}{2}(\alpha+1)\frac{g^{\nu\kappa}}{x^2} - (\alpha-1)\frac{x^\nu x^\kappa}{x^4}\right], \tag{2.14}$$

which in Feynman gauge ($\alpha = 1$) becomes the well known free photon propagator

$$G^{\nu\kappa}(x) = \frac{1}{(2\pi)^2}\frac{g^{\nu\kappa}}{x^2}\,. \tag{2.15}$$

With an Euclidian metric, $g^{\nu\kappa} = \delta^{\nu\kappa}$, the "scalar" propagator $G(x)$ can be defined:

$$G^{\nu\kappa}(x) = \delta^{\nu\kappa}G(x) \qquad\qquad G(x) = \frac{1}{(2\pi)^2}\frac{1}{x^2}\,. \tag{2.16}$$

2.2.3 Boundary conditions for perfectly conducting surfaces

The whole formulation and calculation is based on boundary conditions, which have to be realised on some surfaces. In the case of QED, they are given by Maxwell's equations. So, in general, the boundary conditions for the electromagnetic fields on a noncharged, nonmoving and nonrotating surface are given by $\vec{n} \times (\vec{E}_2 - \vec{E}_1) = 0$ and $\vec{n} \cdot (\vec{B}_2 - \vec{B}_1) = 0$, where the indices 1 and 2 represent the inside and the outside of the conductor, and $\vec{n}$ is the normal vector of the boundary surface. For a perfect conductor the fields inside vanish. Therefore, in the simplest situation, the only conditions are $\vec{n}\times\vec{E} = 0$ and $\vec{n}\cdot\vec{B} = 0$ at the outside. However, in the following calculations, it is useful to utilize the electromagnetic field tensor $F^{\mu\nu} = \partial^\mu A^\nu - \partial^\nu A^\nu$, or better the dual electromagnetic field tensor $\tilde{F}^{\mu\nu} = \frac{1}{2}\epsilon^{\mu\nu\alpha\beta}F_{\alpha\beta}$, because it is much more manageable and also a formulation for general coordinate systems. In flat Minkowski space and Cartesian coordinates with the metric $(-,+,+,+)$, $\tilde{F}$ has the explicit form

$$\tilde{F}^{\mu\nu} = \begin{pmatrix} 0 & B_1 & B_2 & B_3 \\ -B_1 & 0 & -E_3 & E_2 \\ -B_2 & E_3 & 0 & -E_1 \\ -B_3 & -E_2 & E_1 & 0 \end{pmatrix}\,. \tag{2.17}$$

With the help of $n^\mu := (0, \vec{n})$, the product $n_\mu\tilde{F}^{\mu 0} = 0 \Leftrightarrow \vec{n}\cdot\vec{B} = 0$ and $n_\mu\tilde{F}^{\mu i} = 0 \Leftrightarrow \vec{n}\times\vec{E} = 0$ can be obtained. So the projection of $\tilde{F}$ on n has to be zero on the surface of the above perfect conductor and thus, the boundary conditions are:

$$n_\mu\tilde{F}^{\mu\nu} = n_\mu\epsilon^{\mu\nu\alpha\beta}\partial_\alpha A_\beta = 0\,. \tag{2.18}$$

2.2.4 Restricted partition function for perfectly conducting surfaces

Now having the boundary conditions and the free Euclidean action with the invertable free photon propagator, the partition function for describing a system of vacuum fluctuations together with surfaces that influence these fluctuations, can be formulated. This partition function with boundary conditions, now called $\mathcal{Z}_{\mathrm{BC}}$, can be received by simply cutting out the states, which do not fulfil the conditions. This can be done with a Dirac delta functional, which has to be zero in all cases where the boundary condition (2.18) is not achieved [30]:

$$\mathcal{Z}_{\mathrm{BC}} = \int \mathcal{D}A \prod_{\nu,a,x_a} \delta\left(n^a_\gamma(x_a)\tilde{F}^{\gamma\nu}(x_a)\right) e^{-S_E(A_\mu)} \,. \tag{2.19}$$

The index a labels the surfaces, so x_a are the spacetime coordinates on the surface a and $n^a(x_a)$ is the normal vector on the surface a at the point x_a. The product is used to place the delta functional for all 4 conditions at each point in spacetime, where these conditions have to be fulfilled and thus $\mathcal{Z}$ is restricted to a special area in the phase space. But this formulation of the partition function is not very suitable. To get rid of the delta functional, every delta function in the product $\prod_{\nu,a,x_a}$ can be replaced by its Fourier representation

$$\delta\left(n^a_\gamma(x_a)\tilde{F}^{\gamma\nu}(x_a)\right) = \int d\left(\Psi^a_\nu(x_a)\right) e^{i\Psi^a_\nu(x_a)n^a_\gamma(x_a)\tilde{F}^{\gamma\nu}(x_a)} \,. \tag{2.20}$$

Afterwards, the product of the exponential functions can be rewritten as the exponential function of the summation of all exponents. This summation becomes an integral in the sense of continuous summands. So $\mathcal{Z}_{\mathrm{BC}}$ becomes

$$\mathcal{Z}_{\mathrm{BC}} = \int \mathcal{D}\Psi\mathcal{D}A e^{i\sum_a \int_{S_a} dx_a \Psi^a_\nu n^a_\gamma \tilde{F}^{\gamma\nu}} e^{-S_E(A_\mu)} \,, \tag{2.21}$$

where the path integral $\mathcal{D}\Psi = \prod_{\nu,a,x_a} d\Psi^a_\nu(x_a)$ appears. The integrals in this expression have to be rewritten this way that only Gaussian integrals have to be solved, in order to calculate them analytically. This will be done in the next steps for the $\mathcal{D}A$ path integral.

To get Gaussian integrals, the exponent has to become quadratic in the fields A and Ψ. Thus one can take the Euclidean action integral in the non-Maxwell formulation with the help of $L^{\mu\nu}(x,y)$ in (2.6). With this Lagrangian, the action integral becomes

$$S_E(A_\mu) = \frac{1}{2}\int d^4x d^4y A_\mu(x) L^{\mu\nu}(x,y) A_\nu(y) \,. \tag{2.22}$$

Equation (2.22) is quadratic in A. In a next step, the dual field strength tensor $\tilde{F}^{\gamma\nu}$ in (2.21) is written out in terms of A and hence replaced by $\epsilon^{\gamma\nu\alpha\beta}\partial_\alpha A_\beta$. This exponent obviously becomes linear in A. Therefore all A_μ have to be split up in this way that afterwards, "the square can be completed". More precisely, another delta function $\delta^4(x-x_a)$ and an integral $\int dx$ have to be inserted in the exponential term:

$$i\sum_a \int_{S_a} dx_a \Psi^a_\nu n^a_\gamma \tilde{F}^{\gamma\nu} = i\sum_a \int_{S_a} dx_a \Psi^a_\nu(x_a) n^a_\gamma(x_a)\epsilon^{\gamma\nu\alpha\beta}\partial_\alpha A_\beta(x_a) \tag{2.23}$$

$$= \int dx \sum_a \int_{S_a} dx_a i\Psi^a_\nu(x_a) n^a_\gamma(x_a)\epsilon^{\gamma\nu\alpha\beta}\left[\partial_\alpha A_\beta(x_a)\right]\delta^4(x-x_a)\,, \tag{2.24}$$

and $A_\mu(x_a)$ becomes free of x_a:

$$\int dx \sum_a \int_{S_a} dx_a i\Psi^a_\nu(x_a) n^a_\gamma(x_a)\epsilon^{\gamma\nu\alpha\beta}\left[\partial_\alpha A_\beta(x)\right]\delta^4(x-x_a)\,. \tag{2.25}$$

By a partial integration, the differential operator ∂_α now acts on the delta function. Then, everything which belongs to $\int dx_a$ can be called a current term $J^\mu(x)$ for simplicity:

$$\int dx \underbrace{\sum_a \int_{S_a} dx_a(-i)\Psi^a_\nu(x_a) n^a_\gamma(x_a)\epsilon^{\gamma\nu\alpha\beta}\left[\partial_\alpha\delta^4(x-x_a)\right]}_{J^\beta(x)} A_\beta(x)\,. \tag{2.26}$$

In the end, the whole partition function looks like

$$\mathcal{Z}_{\mathrm{BC}} = \int \mathcal{D}\Psi\mathcal{D}A e^{\int d^4x J^\beta(x)A_\beta(x) - \frac{1}{2}\int d^4x d^4y A_\mu(x) L^{\mu\nu}(x,y) A_\nu(y)} \tag{2.27}$$

$$J^\beta(x) = \sum_a \int_{S_a} dx_a(-i)[\partial_\alpha\delta^4(x-x_a)]\Psi^a_\nu(x_a) n^a_\gamma(x_a)\epsilon^{\gamma\nu\alpha\beta}\,. \tag{2.28}$$

$J^\beta(x)$ has the physical meaning of a current on the surfaces, which is induced by the vacuum fluctuations A_μ. The complete exponential term in (2.27) now can be rewritten in the way that Gaussian integrals appear for the $\mathcal{D}A$. Here, the superindex notation lends itself to do this in a clear way. The superindex with capital letters combines the space-time vector $x = (x_0, x_1, x_2, x_3)$ and the Lorentz indices $\alpha = (0, 1, 2, 3)$ to $A = (x, \alpha)$. So, according to Einstein's summation convention, indices appearing twice have to be summed over and integrated. With this, the exponent of (2.27) becomes

$$J^A A_A - \frac{1}{2}A_A L^{AB} A_B = -\frac{1}{2}\tilde{A}_A L^{AB}\tilde{A}_B + \frac{1}{2}J_A L^{-1\,AB} J_B\,, \tag{2.29}$$

where $\tilde{A}_A$ stands for $A_A - (L^{-1}J)_A$.[4] At this point, the necessity for an invertable $L_{\mu\nu}$ operator becomes clear. Now the path integral for $\mathcal{D}A$ is shifted to a path integral for $\mathcal{D}\tilde{A}$ and the Gaussian integrals for all $\tilde{A}$ at each point in the space-time are reached. They can be collected by a constant $\mathcal{Z}_0$, because they are independent of the geometry of the problem. This normalisation constant will cancel out later, especially when the Casimir force will be calculated. Effectively, the partition function with imposed boundary conditions becomes

$$\mathcal{Z}_{\mathrm{BC}} = \mathcal{Z}_0 \int \mathcal{D}\Psi e^{\frac{1}{2}J^A L^{-1}_{AB} J^B} \,. \tag{2.30}$$

At this point, $\mathcal{D}\Psi$ can be replaced by $\mathcal{D}J_{\mathrm{surface}}$. The appearing Jacobi determinant would be independent of the distance of the objects, therefore would not contribute to the Casimir force and could be absorbed by $\mathcal{Z}_0$, too. Thus, this partition function would be finished and one could work with it. This was done by T. Emig in [29] for example, who received this term in a different way. But to go straight forward and also analogue to [31], a propagator for Ψ will be obtained. Using the definition of J (2.28), the $J^A L^{-1}_{AB} J^B$ term can be transformed by partial integrations to a more useful object with $M^{\mu\nu}_{ab}(x_a, y_b)$ being the Greens function of the problem. $M^{\mu\nu}_{ab}(x_a, y_b)$ also is the propagator of a "bounded photon" propagating from a point x_a of the surface a to a point y_b of the surface b.

$$J^A L^{-1}_{AB} J^B = -\sum_{a,b} \int_{S_a, S_b} \Psi^a_\mu(x_a) M^{\mu\nu}_{ab}(x_a, y_b) \Psi^b_\nu(y_b) \tag{2.31}$$

$$M^{\mu\nu}_{ab}(x_a, y_b) = n^a_\gamma(x_a) n^b_{\gamma'}(y_b) \epsilon^{\gamma\mu\alpha\beta} \epsilon^{\gamma'\nu\alpha'\beta'} \left[\partial_\alpha(x) \partial'_{\alpha'}(y) L^{-1}_{\beta\beta'}(x, y)\right]\Big|_{\substack{x = x_a \\ y = y_b}} \tag{2.32}$$

Here, ∂ means the derivative for x and ∂' is the one for y. From section 2.2.2, $L^{-1}_{\beta\beta'}$ is known as the free photon propagator $G_{\beta\beta'}$.

Because of these conditions on the surfaces, the rank of $M^{\mu\nu}_{ab}$ is not 4. The $3 + 1$ space-time is the reason for the 4×4 matrix, but the normal vector of the surface enforces M to act on a $2 + 1$ subspace. Therefore the maximal rank of M is 3. Assuming there is a coordinate system, in which the zero eigenvalue of M is written on the diagonal, the corresponding entries are zero and so there is no propagation of Ψ in this direction. But then the integrals in (2.31) are not suppressed by an exponential term and therefore become infinity. These infinities can be neglected because the Casimir force

[4] Of course also $(L^{-1}J)_A$ contains a summation and integration: $(L^{-1}J)_A = L^{-1}_{AC} J^C$.

only depends on differences of the energy. Another point of view is that these infinities are also part of the free photon field and would be absorbed by the normalization constant $\mathcal{Z}_0$. To avoid such problems, $M_{ab}^{\mu\nu}$ has to be projected onto the subspace, where the propagating fields Ψ exist.

In a last step, because the term in (2.31) is already quadratic in Ψ, the $\mathcal{D}\Psi$ can be carried out and the result for $\mathcal{Z}_{\mathrm{BC}}$ for any number of surfaces is

$$\mathcal{Z}_{\mathrm{BC}} = \mathcal{Z}_0 \left[\det(\mathcal{M}_{\mathrm{BC}})\right]^{-\frac{1}{2}} . \tag{2.33}$$

The 2π constants arising from this Gaussian integrals will also be absorbed by $\mathcal{Z}_0$, because they cancel out when calculating the force.

This result for $\mathcal{Z}_{\mathrm{BC}}$ can be obtained by first defining the matrix $\mathcal{M}_{\mathrm{BC}}$ as the combined super-propagator of one field $\Psi(x)$ where $x \in S_1 \otimes \ldots \otimes S_n$ and then integrating over Gaussian integrals of the form $\int d\Psi e^{-\frac{1}{2}\Psi \mathcal{M}_{\mathrm{BC}} \Psi}$, too. For the situation with only two surfaces, $\mathcal{M}_{\mathrm{BC}}$ simplifies to

$$\mathcal{M}_{\mathrm{BC}} = \begin{pmatrix} M_{11} & M_{12} \\ M_{21} & M_{22} \end{pmatrix} \quad \Psi = \begin{pmatrix} \Psi_1 \\ \Psi_2 \end{pmatrix}, \tag{2.34}$$

or, for example, with three surfaces it becomes

$$\mathcal{M}_{\mathrm{BC}} = \begin{pmatrix} M_{11} & M_{12} & M_{13} \\ M_{21} & M_{22} & M_{23} \\ M_{31} & M_{32} & M_{33} \end{pmatrix} \quad \Psi = \begin{pmatrix} \Psi_1 \\ \Psi_2 \\ \Psi_3 \end{pmatrix}. \tag{2.35}$$

2.2.5 Extension to dielectric surfaces - the boundary conditions

The above described method is, of course, not restricted only to ideal conducting surfaces. As it was pointed out in [35], boundary conditions can also be found for general dielectrics. To obtain them, the Helmholtz equation

$$[\vec{\nabla}^2 + \varepsilon(\omega)\omega^2]\vec{B}(\omega, \vec{x}) = 0 \tag{2.36}$$

for the magnetic field $\vec{B}$ can be used, which directly follows from the Maxwell's equations. Inside a volume V with surface S the general frequency dependent dielectric function $\varepsilon(\omega)$ is considered. Now including the free Green's function, which has to satisfy

$$[\vec{\nabla}^2 + \varepsilon(\omega)\omega^2]G^{\varepsilon}(\omega, \vec{x}, \vec{x}') = \delta(\vec{x} - \vec{x}') \tag{2.37}$$

inside the medium, equations (2.36) and (2.37) can be combined due to Green's second identity to

$$\int_{\vec{x}' \in S} [\vec{B}(\vec{x}')\vec{\nabla}'_n G^{\varepsilon}(\vec{x}, \vec{x}') - G^{\varepsilon}(\vec{x}, \vec{x}')\vec{\nabla}'_n \vec{B}(\vec{x}')] = \begin{cases} \vec{B}(\vec{x}) & , \vec{x} \in V \\ 0 & , \vec{x} \notin V . \end{cases} \tag{2.38}$$

The frequency ω is neglected, $\vec{n}' = \vec{n}(\vec{x}')$ denotes the surface normal vector pointing into the vacuum and $\vec{\nabla}'_n = \vec{n}'\vec{\nabla}'$ is the derivative of $\vec{x}'$ in normal direction. With the use of vector identities, equation (2.38) can be transformed to

$$\int_{\vec{x}'\in S}\Big[-i\omega\varepsilon\vec{n}'\times\vec{E}(\vec{x}')+(\vec{n}'\times\vec{B}(\vec{x}'))\times\vec{\nabla}'+(\vec{n}'\vec{B}(\vec{x}'))\vec{\nabla}'\Big]G^{\varepsilon}(\vec{x},\vec{x}')=0\,, \quad (2.39)$$

where $\vec{x}$ is set to lie outside of V. This equation now states that the tangential component of the electric field as well as the tangential and normal components of the magnetic field have to be continuous across the boundary surface, which is the case for a dielectric boundary without surface charges or currents. Therefore, it can be used as a nonlocal boundary condition. That means, even for a complex structured surface S with coordinates $\vec{x}'$, a second surface R playing the role of an auxiliary surface with coordinates $\vec{x}$ can be introduced, which carries the conditions (2.39) (see Fig. 2.1).

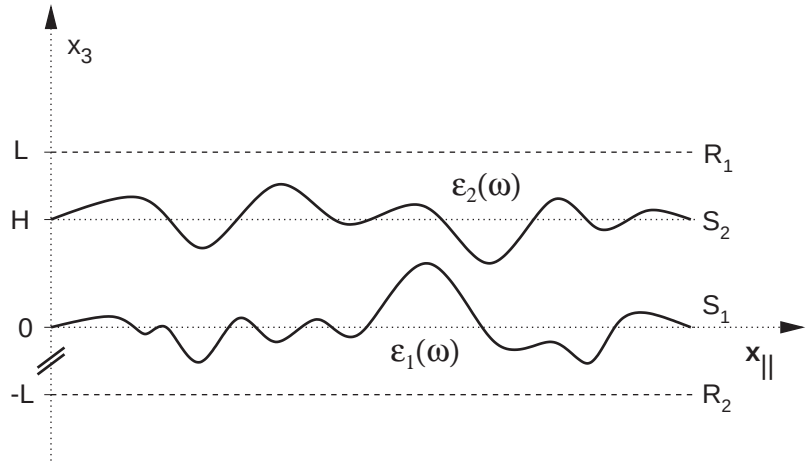

Fig. 2.1: Two dielectric media bounded by their surfaces S_a are filling two half spaces. With each physical surface S_a comes an auxiliary surface R_a, on which the non-local boundary conditions are implemented. This figure is taken from [35].

However to be able to use the above formalism, equation (2.39) has to become a condition for the electromagnetic vector field potential A and not for the electromagnetic fields themselves. Hence, the relations[5] $E^i = -p_0 A^i - i\partial^i A^0$ and $B^i = \epsilon^{ijk}\partial_j A_k$ have to be inserted in (2.39) and the complete term can

[5]The Wick rotation has to be considered.

be expressed as an integral

$$\int_{\vec{x}'_a \in S_a} L^{aj}_{\mu}(\vec{x}'_a, \vec{x}_a) A^{\mu}(\vec{x}_a) = 0\,, \tag{2.40}$$

with L^{aj}_{μ} being an operator acting on A^{μ} at each point $\vec{x}_a \in R_a$, whereby a is called the surface index. This operator can be expressed in component notation after some simplifications:

$$L^{aj}_{\mu}(\vec{x}'_a, \vec{x}_a) = n^a_{\gamma}(\vec{x}'_a) \left[(-i)\epsilon^{j\gamma\alpha\beta} + \frac{1}{p_0 \varepsilon_a} \epsilon^{0\gamma\sigma\rho} \epsilon^{0\sigma\alpha' j} \epsilon^{0\rho\alpha\beta} \partial'_{\alpha'} \right] G^{\varepsilon_a}_{\beta\mu}(\vec{x}'_a, \vec{x}_a) \partial_{\alpha}\,. \tag{2.41}$$

The derivatives $\partial' \equiv \partial_{x'}$ and $\partial \equiv \partial_x$ act on G^{ε_a} and A respectively. By inserting (2.40) and (2.41) into the delta functional in $\mathcal{Z}_{\mathrm{BC}}$ of section 2.2.4 and expanding the delta into its Fourier representation, the appearing integral over the auxiliary surface R_a can be used to shift the derivative ∂ to act on G^{ε_a} due to a partial integration. Then, the symmetry $\partial G(x' - x) = -\partial' G(x' - x)$ can be utilised to transform the vector field potential $A(\vec{x}_a)$ on the auxiliary surface R_a to a vector field potential $A(\vec{x}'_a)$ on the surface S_a with the transformation $\int_{\vec{x}_a \in R_a} G^{\varepsilon_a}_{\beta\mu}(\vec{x}'_a, \vec{x}_a) A^{\mu}(\vec{x}_a) = A_{\beta}(\vec{x}'_a)$. This step leads to a partition function, which also could be obtained by using the local boundary condition

$$n^a_{\gamma}(\vec{x}_a) \left[(-i)\epsilon^{j\gamma\alpha\beta} + \frac{1}{p_0 \varepsilon_a} \epsilon^{0\gamma\sigma\rho} \epsilon^{0\sigma\alpha' j} \epsilon^{0\rho\alpha\beta} \partial_{\alpha'} \right] \partial_{\alpha} A_{\beta}(\vec{x}_a)\,,\ \vec{x}_a \in S_a \tag{2.42}$$

in first place. As a cross-check, by taking the limit $\varepsilon \to \infty$, the dielectric surface becomes an ideal conductor and thus (2.42) leads to the previously found boundary condition[6] (2.18).

Therefore, in the end, when Casimir forces have to be calculated for nontrivial geometries, what can be chosen are, for example, a plain surface with a complicated nonlocal boundary condition (2.40) and (2.41) or the complicated shaped surface with a local boundary condition (2.42).

[6] ... in $\Psi_0 = 0$ gauge. See section 2.5.

2.3 Obtaining the Casimir energy from the partition function

With the above considerations, everything of the physical system is known. For example, one can ask for the ground state energy $\langle 0|H|0\rangle$ of the photon field in presence of surfaces, which is the Casimir energy. Because the partition function also has the definition

$$\mathcal{Z} = \mathrm{Tr}\left[e^{itH}\right] = \sum_n e^{-\tau E_n}\,, \tag{2.43}$$

where $\tau = -it$ is the complex Euclidean time, the ground state energy $E = E_0$ can be obtained by taking the limit $\tau \to T_E := \infty$ from $\ln \mathcal{Z}$, whereby T_E is the "overall Euclidean timelength".

$$\ln \mathcal{Z} = -ET_E \tag{2.44}$$

This equation is of course written in natural dimensions $\hbar = c = 1$. Otherwise, with the correct dimensions and the above partition function, the energy is given by

$$E = -\frac{\hbar c}{T_E} \ln \mathcal{Z}_{\mathrm{BC}}\,. \tag{2.45}$$

$\mathcal{Z}_{\mathrm{BC}}$ is infinity and so the energy, too. However, due to being interested in the Casimir force, which is minus the gradient of E, a constant can be subtracted from the energy. This constant could be the ground state energy of the free photon field, so $\mathcal{Z}_{\mathrm{BC}}$ just has to be divided by the free $\mathcal{Z}$. But this expression is still infinity, because of the zero eigenvalues in $\mathcal{M}_{\mathrm{BC}}$ resulting from the surfaces. To remove those infinities, it is better to normalise $\mathcal{Z}_{\mathrm{BC}}$ by $\mathcal{Z}_\infty$, which has the same zero eigenvalues. $\mathcal{Z}_\infty$ is the $\mathcal{Z}_{\mathrm{BC}}$, where the surfaces have infinite distance. Thus the Casimir energy is defined as

$$E_{\mathrm{Cas}} = -\frac{\hbar c}{T_E} \ln \frac{\mathcal{Z}_{\mathrm{BC}}}{\mathcal{Z}_\infty}\,, \tag{2.46}$$

which leads to a finite energy density in the end, the energy per surface area. The surface distance independent $\mathcal{Z}_0$ cancels out now.

2.4 Casimir energy in the propagator formulation

With the help of (2.33), (2.46) and using $\ln\det = \mathrm{Tr}\ln$, the Casimir energy is given by

$$E_{\mathrm{Cas}} = \frac{\hbar c}{2T_E} \mathrm{Tr} \ln \frac{\mathcal{M}_{\mathrm{BC}}}{\mathcal{M}_\infty}\,. \tag{2.47}$$

As for $\mathcal{M}_\infty$, the surface distance goes to infinity, the free photon propagator connecting two separate surfaces, becomes zero and therefore also $M_{ab}^{\mu\nu}$ becomes zero for all $a \neq b$. Thus $\mathcal{M}_\infty$ is

$$\mathcal{M}_\infty = \begin{pmatrix} M_{11} & 0 \\ 0 & M_{22} \end{pmatrix}. \tag{2.48}$$

Taking the product $\mathcal{M}_\infty^{-1}\mathcal{M}_{\mathrm{BC}}$ leads to an equation of the form $\mathbb{1} + \Delta\mathcal{M}$, where

$$\Delta\mathcal{M} = \begin{pmatrix} 0 & \Delta\mathcal{M}_{12} \\ \Delta\mathcal{M}_{21} & 0 \end{pmatrix} \tag{2.49}$$

or in general

$$\Delta\mathcal{M}_{ab} = \begin{cases} M_{aa}^{-1}M_{ab} & , a \neq b \\ 0 & , a = b \end{cases}. \tag{2.50}$$

Now, the logarithm can be expanded into a Taylor series at $\Delta\mathcal{M} = 0$. Carrying out the trace over the discrete surface indices leads to

$$E_{\mathrm{Cas}} = -\frac{\hbar c}{2T_E}\sum_{n=2}^{\infty}\frac{(-1)^n}{n}\operatorname{Tr}\left[\Delta\mathcal{M}^n\right]. \tag{2.51}$$

The first summand $n = 1$ is the sum of all selfinteractions and therefore becomes zero in this formalism. For all other n, $\operatorname{Tr}[\Delta\mathcal{M}^n]$ is the sum of all combinations of propagations around a complete circle passing n surfaces. Especially for two surfaces, the summands with an odd n are zero[7] and the one with an even n are $2\operatorname{Tr}[(\Delta\mathcal{M}_{12}\Delta\mathcal{M}_{21})^n]$. Thus in this case, the Casimir energy specialises to

$$E_{\mathrm{Cas}} = -\frac{\hbar c}{2T_E}\sum_{n=1}^{\infty}\frac{1}{n}\operatorname{Tr}\left[(\Delta\mathcal{M}_{12}\Delta\mathcal{M}_{21})^n\right] \tag{2.52}$$

and hence the force is always attractive. Such a simple result, of course, cannot be obtained in general, as it can be seen in the case with only one more surface. Then the first two summands are $\operatorname{Tr}[\Delta\mathcal{M}_{12}\Delta\mathcal{M}_{21} + \Delta\mathcal{M}_{23}\Delta\mathcal{M}_{32} + \Delta\mathcal{M}_{31}\Delta\mathcal{M}_{13}] + \operatorname{Tr}[\Delta\mathcal{M}_{12}\Delta\mathcal{M}_{23}\Delta\mathcal{M}_{31} + \Delta\mathcal{M}_{13}\Delta\mathcal{M}_{32}\Delta\mathcal{M}_{21}]$.

2.5 Additional gauge freedoms

It is known that a photon has only two degrees of freedom corresponding to the two directions transverse to the propagation direction. This holds

[7] There does not exist a complete circle consisting of an odd number of propagators.

also for the "bounded photon" and thus the propagator matrices M_{ab} only need to have rank two. However, as mentioned before, QED is an abelian field theory and therefore there is no need for a fully fixed gauge. Only the invertibility of (2.3) has to be achieved to obtain a propagator. Therefore, the Feynman gauge was introduced. On the other hand, a different gauge may lead to different simplifications within the calculations and to a different convergence behaviour[8]. Therefore, one more gauge should be found.

$A_0 = 0$ **gauge**

Since there was no matter included in the setup, the Coulomb gauge could be a good idea. This one can be obtained by setting $A_0 = 0$ additionally to the Feynman gauge $\partial_\mu A^\mu = 0$. The reason for this is the following:

The connection between electromagnetic fields $\vec{E}$ and $\vec{B}$, and the vector field potential A^μ is given by the well known equations

$$E^i = -\partial^i A^0 + \partial^0 A^i \qquad\qquad B^i = \epsilon^{ijk}\partial_j A_k \,. \tag{2.53}$$

Therefore the vector potential A^μ has the gauge freedom $A'^\mu = A^\mu + \partial^\mu \Lambda$. If A'^0 is set to zero by a gauge fixing, $\Lambda(\vec{x}, t)$ can be fixed by simply integrating over $A^0(\vec{x}, t)$ up to an integration constant $\lambda(\vec{x})$.

$$\Lambda(\vec{x}, t) = -\int^t A^0(\vec{x}, t')dt' + \lambda(\vec{x}) \tag{2.54}$$

Feynman gauge $\partial_\mu A^\mu = 0$ now leads to

$$0 \stackrel{!}{=} \partial_i A'^i = \partial_i A^i + \Delta\Lambda \tag{2.55}$$

$$= \partial_i A^i(\vec{x}, t) - \int^t \Delta A^0(\vec{x}, t')dt' + \Delta\lambda(\vec{x}) \tag{2.56}$$

and λ gets fixed by a simple Poisson equation if (2.56) does not depend on the time. But this is implicitly declared by the Feynman gauge. As a consistency check the time derivative of (2.56) can be taken.

$$0 \stackrel{!}{=} \partial^0\partial_i A^i - \partial^0 \int^t \Delta A^0(\vec{x}, t')dt' \tag{2.57}$$

$$\stackrel{\partial_\mu A^\mu = 0}{=} -\partial_0\partial^0 A^0 - \Delta A^0 = -\Box A^0 \tag{2.58}$$

[8] As seen in (2.50), the functional inverse propagator M_{ab}^{-1} will be needed. This inverse cannot be obtained analytically, in general, and thus one will have to set restrictions or truncations on these propagators. Here, "convergence behaviour" is meant in the sense of this truncation.

So A^0 has to obey the vacuum equation of motion (2.5) with $\alpha = 1$ as assumed. Thus in the case of vacuum, the so-called Weyl gauge, $A_0 = 0$, is allowed. However, since there is no matter in the vacuum, a boundary is introduced. At this boundary, the fields have to obey some conditions which lead to a current term in the action. So, after changing the free action to a bounded one, $A_0 = 0$ is not allowed because this action can be obtained also by introducing matter into the vacuum. The current term can be interpreted as matter. In contrast, in the case of two parallel plates, this gauge does not change the result because the plates are translation invariant with respect to all three surface directions.[9] But because this is not obvious, an allowed $A_0 = 0$ gauge will be assumed with care.

$\Psi_0 = 0$ gauge

However, there exists a second possible gauge. For the auxiliary fields Ψ on the surfaces similar equations hold. The electromagnetic current J is connected to Ψ by a 4D rotation of $n\Psi$ after a partial integration in equation (2.28).[10]

$$J^\beta(x) = i \sum_a \epsilon^{\alpha\gamma\nu\beta} \partial_\alpha [n^a_\gamma \Psi^a_\nu] \tag{2.59}$$

$$= i \sum_a [\underbrace{\epsilon^{\alpha\gamma\nu\beta} (\partial_\alpha n^a_\gamma)}_{0} \Psi^a_\nu + \epsilon^{\alpha\gamma\nu\beta} n^a_\gamma \partial_\alpha \Psi^a_\nu] \tag{2.60}$$

The first term vanishes because of stationarity of the surfaces: The normal vector n_γ does not depend on time and $n_0 = 0$, so one is left with $\operatorname{rot} \vec{n}$. But this is also zero.[11] Obviously a gradient term and a normal vector term can be added to Ψ so $\Psi^a_\nu \to \Psi'^a_\nu = \Psi^a_\nu + \partial_\nu \Lambda^a + n_\nu \Gamma^a$ is a gauge freedom for all surfaces a independent of each other. For the next considerations, the surface index a will be neglected for simplicity.

In the following certain conditions are checked, which maybe simplify the propagator M_{ab}. Since Ψ is a field on the surface, $n^\nu \Psi'_\nu = 0$[12] and $n^\mu \partial_\mu \Psi'_\nu = 0$[13] would be possible. These conditions would lead to $n^\nu \partial_\nu \Lambda + \Gamma = -n^\nu \Psi_\nu$ and $n^\mu \partial_\mu \partial_\nu \Lambda + n^\mu \partial_\mu n_\nu \Gamma = -n^\mu \partial_\mu \Psi_\nu$ which are always solvable. By choosing

[9] See section 3.3.

[10] Due to the surface integral, this partial integration can only be done for the surface derivatives. But due to the ϵ tensor, ∂_α has to be orthogonal to the normal vector and thus it is only a derivative of surface variables.

[11] $\vec{n}$ could be expressed by a single gradient of a potential whose equipotential surface is the surface itself. A normal vector field has no rotation.

[12] The normal component of Ψ can be assumed to be zero.

[13] There should be now flow of Ψ leaving the surface.

$n^\nu \partial_\nu \Lambda = 0$, $\Gamma = -n^\nu \Psi_\nu$ solves the system and leaves space for a third condition. Because n^0 is zero, this solution is no restriction for Ψ_0. Hence Ψ_0 can be arbitrary chosen, for instance, $\Psi_0 = 0$ would simplify the used Matrix propagators very much due to being able to even ignore the time components. In addition, this gauge also lowers the rank of M_{ab}.

Therefore, the task is to show that Λ can be found in such a way that $\Psi_0' = 0$ is always satisfied. At first, Λ can be obtained up to an integration constant by integrating over Ψ_0.

$$\Lambda(\vec{x}, t) = -\int^t \Psi_0(\vec{x}, t')dt' + \lambda(\vec{x}) \tag{2.61}$$

This constant is determined by the following linear differential equation which can be solved always, if the right-hand side does not depend on time.

$$\partial_i \lambda(\vec{x}) = \Psi_i' - \Psi_i + \partial_i \int^t \Psi_0(\vec{x}, t')dt' \tag{2.62}$$

But taking the time derivative of (2.62) leads to zero, because

$$i\epsilon^{0\gamma i\beta} n_\gamma \partial_0 \left(\Psi_i' - \Psi_i + \partial_i \int^t \Psi_0 dt' \right) = i\epsilon^{0\gamma i\beta} n_\gamma (\partial_0 \Psi_i' - \partial_0 \Psi_i + \partial_i \Psi_0) \tag{2.63}$$

$$= J'^\beta - J^\beta = 0\,. \tag{2.64}$$

Thus the Weyl gauge for the Ψ is allowed always in the case of no time dependend normal vectors. Of course, only a change in the boundary conditions would lead to a change in this gauge freedom.

A physical interpretation of this gauge is this: The propagating photons have two degrees of freedom and therefore, only two boundary conditions are needed. For example $n_\mu \tilde{F}^{\mu i} = 0$ with $i = 1, 2, 3$ can be chosen, which means $\vec{n} \times \vec{E} = 0$. By writing out the $\vec{E}$ in normal and tangential components, the surface normal vector automatically sets one of this three equations to zero and thus they are only two conditions. Now, the Fourier transformation of $n_\mu \tilde{F}^{\mu i} = 0$ leads to a Ψ, which has no time component.[14]

[14] Another interpretation comes with the comprehension of Ψ being for the surfaces the analogue to the vector field potential A for the vacuum. In other words, a being, living only on the surface, does not recognise the surface. Thus, for this object, the fluctuating field Ψ is simply the same as for us a fluctuating A field in a free vacuum. Now, in a vacuum with no matter inside, there are no external charges or currents and therefore A_0 can be set to zero. For a field on the surfaces, this means $\Psi_0 = 0$ gauge is a result of no external surface charges and currents.

3 Casimir force for two parallel plates

In the year 1948, H. B. G. Casimir [3] predicted an attractive force between two parallel perfectly conducting plain plates. This result was also reobtained by many people afterwards and will be calculated in the following with the above propagator formulation, too. Corresponding to (2.52), the propagator between the surfaces therefore will be calculated.

3.1 Setup

Two parallel perfectly conducting plain plates, in the following denoted as 1 and 2, are placed at a distance H above each other. The lower one lies on the (x_1, x_2) plane. The used coordinates are Cartesian ones. A figure of this is shown in Fig. 3.1. The normal vectors on this surfaces have to face each other by convention and thus are $n^a_\gamma = (-1)^{a+1}\delta^3_\gamma$, where a indicates the surface number.

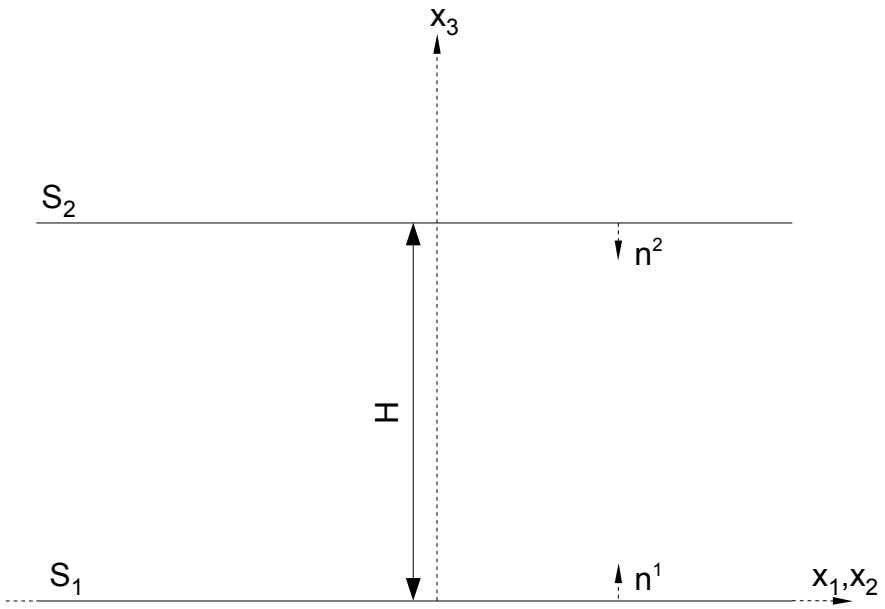

Fig. 3.1: Two parallel perfectly conducting plates are placed at a distance H with n^1 and n^2 being the normal vectors of the plates S_1 and S_2. Additionally, the Cartesian coordinates x_1 and x_2 are the coordinates on the plates.

3.2 The propagator between two parallel plates

With this setup and the use of (2.32), the corresponding propagator matrix can be calculated. But to get the Casimir energy (2.52), also the functional inverse of this matrix is needed. Therefore, the translation invariance in $\underline{x} = (x_0, x_1, x_2)$ direction should be used. Because of this invariance, the propagator $M(\underline{x}, \underline{x}')$ is diagonal in momentum space and can easily be functionally inverted by calculating the usual matrix inverse of the Fourier transformed propagator $M(\underline{p})$ with $\underline{x} - \underline{x}' \to \underline{p}$. This $M(\underline{p})$ can be obtained by transforming the free photon propagator $G_{\beta\beta'} = \frac{\delta_{\beta\beta'}}{4\pi^2(x-x')^2}$ to $G_{\beta\beta'}(\underline{p}, x_3 - x_3')$ in momentum space and inserting it into (2.32).

$$M^{\mu\nu}_{ab}(x_a, x_b') = n^a_\gamma n^b_{\gamma'} \epsilon^{\gamma\mu\alpha\beta} \epsilon^{\gamma'\nu\alpha'\beta'} \partial_\alpha \partial'_{\alpha'} \frac{1}{(2\pi)^3} \int_{\underline{p}} G_{\beta\beta'}(\underline{p}, x_3^a - x_3'^b) e^{-i\underline{p}(\underline{x}_a - \underline{x}_b')} \tag{3.1}$$

$$= \frac{1}{(2\pi)^3} \int_{\underline{p}} M^{\mu\nu}_{ab}(\underline{p}, x_3^a - x_3'^b) e^{-i\underline{p}(\underline{x}_a - \underline{x}_b')} \tag{3.2}$$

With

$$G_{\beta\beta'}(\underline{p}, x_3 - x_3') = \delta_{\beta\beta'} \frac{1}{2|\underline{p}|} e^{-|\underline{p}||x_3 - x_3'|} \tag{3.3}$$

and the plate normal vectors, M_{ab} can be obtained:

$$M^{\mu\nu}_{ab}(\underline{p}, H) = (-1)^{a+b} \epsilon^{3\mu\alpha\beta} \epsilon^{3\nu\alpha'\beta'} \delta_{\beta\beta'} \tilde{p}_\alpha \tilde{p}_{\alpha'} \frac{1}{2|\underline{p}|} e^{-|\underline{p}||H(a-b)|} \,. \tag{3.4}$$

$\tilde{p}$ is the modified momentum $(p_0, p_1, p_2, -i|\underline{p}|\,\mathrm{sign}(H(a-b)))$. However, its third component $\tilde{p}_3$ is not needed because in this case the ϵ tensor is zero. After a simplification, in the case of only Feynman gauge, the M results in:

$$M^{\mu\nu}_{ab}(\underline{p}, H) = \frac{(-1)^{a+b}}{2|\underline{p}|} \left(\delta^{\alpha\alpha'} \underline{p}^2 - \underline{p}^\alpha \underline{p}^{\alpha'} \right) \perp^\mu_\alpha \perp^\nu_{\alpha'} e^{-|\underline{p}||H(a-b)|} \,. \tag{3.5}$$

$\perp^\mu_\alpha = (\delta^\mu_\alpha - \delta^3_\alpha \delta^\mu_3)$ and $\perp^\nu_{\alpha'} = (\delta^\nu_{\alpha'} - \delta^3_{\alpha'} \delta^\nu_3)$ are two projectors on the surface. Thus there are no propagations of Ψ leaving the surfaces. Furthermore, M_{ab} is rank(2). In the special case of additional Coulomb gauge[15], M_{ab} can be

[15]Feynman gauge $\partial_\mu A^\mu = 0$ and $A_0 = 0$ leads to Coulomb gauge $\partial_i A^i = 0$. This can be realised by setting G_{00} to zero or restricting the summations on β and β' in (2.32) to go from 1 to 3.

written out to

$$M_{ab}(\underline{p},H) = \frac{(-1)^{a+b}}{2|\underline{p}|} e^{-|\underline{p}||H(a-b)|} \begin{pmatrix} {p_1}^2+{p_2}^2 & -p_0\,p_1 & -p_0\,p_2 & 0 \\ -p_0\,p_1 & {p_0}^2 & 0 & 0 \\ -p_0\,p_2 & 0 & {p_0}^2 & 0 \\ 0 & 0 & 0 & 0 \end{pmatrix}, \quad (3.6)$$

which has rank(2), too. Also, with additional $\Psi_0 = 0$ gauge, the time components of (3.5) or (3.6) have to be set to zero and M_{ab} still remains rank(2).

According to (2.52), M_{aa} has to be inverted on the non-zero-eigenvalue subspace so that $M_{aa}^{-1} M_{aa} = \underline{\mathbb{1}}$ [16]. This inverse can be obtained by a principal axis transformation of M_{aa}, an inversion of this diagonalised matrix, and a backtransformation afterwards. Thus it is the same like inverting the eigenvalues or calculating the Moore-Penrose or pseudo-inverse of a Hermitian matrix (see appendix D). With these methods, the inverse propagator in the case of only Feynman gauge results in:

$$M_{aa}^{-1\,\mu\nu}(\underline{p},H) = \frac{2}{|\underline{p}|^3} \left(\delta^{\alpha\alpha'} \underline{p}^2 - \underline{p}^\alpha \underline{p}^{\alpha'} \right) \perp_\alpha^\mu \perp_{\alpha'}^\nu , \quad (3.7)$$

with additional $A_0 = 0$ gauge:

$$M_{aa}^{-1}(\underline{p},H) = \frac{2}{|\underline{p}|^3} \begin{pmatrix} p_1^2+p_2^2 & -p_0\,p_1 & -p_0\,p_2 & 0 \\ -p_0\,p_1 & \frac{p_1^2 p_2^2 + (p_0^2+p_2^2)^2}{p_0^2} & -\frac{p_1 p_2 (p_0^2+\underline{p}^2)}{p_0^2} & \\ -p_0\,p_2 & -\frac{p_1 p_2 (p_0^2+\underline{p}^2)}{p_0^2} & \frac{p_1^2 p_2^2 + (p_0^2+p_1^2)^2}{p_0^2} & 0 \\ 0 & 0 & 0 & 0 \end{pmatrix}, \quad (3.8)$$

or with additional $\Psi_0 = 0$ gauge:

$$M_{aa}^{-1}(\underline{p}) = \frac{2}{|\underline{p}| p_0^2} \begin{pmatrix} 0 & 0 & 0 & 0 \\ 0 & p_0^2+p_1^2 & p_1\,p_2 & 0 \\ 0 & p_1\,p_2 & {p_0}^2+p_2^2 & 0 \\ 0 & 0 & 0 & 0 \end{pmatrix}, \quad (3.9)$$

or with additional A_0 and $\Psi_0 = 0$ gauge:

$$M_{aa}^{-1}(\underline{p}) = \frac{2|\underline{p}|}{p_0^2} \begin{pmatrix} 0 & 0 & 0 & 0 \\ 0 & 1 & 0 & 0 \\ 0 & 0 & 1 & 0 \\ 0 & 0 & 0 & 0 \end{pmatrix}. \quad (3.10)$$

[16] After the principal axis transformation of M_{aa} the $\underline{\mathbb{1}}$ is a rank(2) $\mathbb{1}$.

3.3 Casimir energy for two parallel plates

With these matrices, the Casimir energy (2.52) for the parallel plates setup can be easily calculated. Multiplying the inverse propagator matrix of one surface with the propagator matrix from one surface to the other, $\Delta\mathcal{M}_{12}$ and $\Delta\mathcal{M}_{21}$ result in $\underline{\mathbb{1}}e^{-|\underline{p}||H|}$. With those terms, $\mathrm{Tr}[(\Delta\mathcal{M}_{12}\Delta\mathcal{M}_{21})^n]$ can be calculated, especially for all n.

$$\mathrm{Tr}[(\Delta\mathcal{M}_{12}\Delta\mathcal{M}_{21})^n] = \mathrm{Tr}[\underline{\mathbb{1}}e^{-|\underline{p}||2nH|}] \tag{3.11}$$

Carrying out the trace over the matrix indices of $\underline{\mathbb{1}}$ leads to an additional factor 2. The trace over the continuous space time indices is an integral over the surface coordinates. Thus, also the Fourier transformation of $\Delta\mathcal{M}$ back to position space has to be mentioned.

$$\begin{aligned}\mathrm{Tr}[(\Delta\mathcal{M}_{12}\Delta\mathcal{M}_{21})^n] &= \int_{\underline{x}} \frac{1}{(2\pi)^3} \int_{\underline{p}} 2e^{-|\underline{p}||2nH|} e^{-i\underline{p}(\underline{x}-\underline{x}')}{}_{|\underline{x}'=\underline{x}} \\ &= \underbrace{\int_{\underline{x}}}_{=T_E A} \frac{1}{(2\pi)^3} \int_{\underline{p}} 2e^{-|\underline{p}||2nH|} \\ &= \frac{1}{4\pi^2 n^3 |H|^3} T_E A\end{aligned} \tag{3.12}$$

T_E is the overall length in Euclidian time direction, which cancels out after inserting (3.12) in (2.51). A is the overall surface area. Taking (2.51) divided by the surface area A results in the Casimir energy density for this setup.

$$\rho_{\mathrm{Cas}} = -\frac{\hbar c}{2^3\pi^2|H|^3} \sum_{n=1}^{\infty} \frac{1}{n^4} \tag{3.13}$$

In a last step the convergent sum $\sum_{n=1}^{\infty} \frac{1}{n^4}$ can be replaced by $\frac{\pi^4}{90}$, so the well known Casimir energy density for two parallel plates [3] is obtained. Furthermore, the Casimir force density is minus the gradient of the Casimir energy density corresponding to the relative position, or more precisely $f_{\mathrm{Cas}} = -\partial_H \rho_{\mathrm{Cas}}$.

$$\rho_{\mathrm{Cas}} = -\frac{\pi^2\hbar c}{720|H|^3} \qquad\qquad f_{\mathrm{Cas}} = -\frac{\pi^2\hbar c}{240|H|^4} \tag{3.14}$$

In this special case, where M_{ab} (3.5) is translation invariant in all three surface directions and therefore is in full momentum space, the full knowledge about M_{aa}^{-1} is not needed. The exponential term in M_{aa} is 1 and thus the one in

M_{ab} remains after taking the product $M_{aa}^{-1}M_{ab}$. Only the rank of M_{aa} has to be known, which gives the factor 2 in (3.12). With that, the possibility to calculate the right energy out of the scalar case by multiplying it with a two [31] becomes clear. Also, this is the reason for the correct result within the unallowed $A_0 = 0$ gauge, since this gauge does not change the rank of M_{aa}.

4 Casimir-Polder force for an atom and a plain plate

Casimir-Polder forces are the Casimir forces for atoms or atoms including setups. These atoms can be represented by spheres, which can be assumed to be perfectly conducting for simplicity. Thus, they are ideal for studying within this formalism. As mentioned in the introduction, Casimir-Polder forces for situations like two or three atoms or an atom in front of a plain plate are already obtained by others. Their results can be used for comparison. Because the (inverse) propagator matrix for a perfectly conducting plain plate is already known and to have the smallest amount of work, it is convenient to chose the plain plate sphere setup in the following. But afterwards, also other configurations with a sphere can be obtained. Then, the sphere part is no problem anymore. Of course, the propagators from a sphere to other surfaces are needed, too, but these calculations are almost easy in comparison with obtaining the inverse propagator of any surfaces analytically. The surface normal vectors only have to be put in equation (2.32).

4.1 Setup

In this chapter, a perfectly conducting sphere with radius R above a perfectly conducting plain plate has to be studied. Their mean distance is denoted by H, where "mean" means the shortest distance between the center of the sphere and the plate. Again, Cartesian coordinates for the surfaces are used. But additionally, the sphere implies spherical coordinates and thus their surface angles φ and θ, abstracted by Ω, will be needed, too. This is shown in Fig. 4.1. The plate with surface index 1 is placed in the (x_1, x_2) plane and the sphere indexed by 2 has its center at the point $(x_0, 0, 0, H)$ for all times. Again, the normal vectors have to face each other by convention, thus n^2 points outside the sphere.

$$n^1_\gamma = \delta^3_\gamma = \begin{pmatrix} 0 \\ 0 \\ 0 \\ 1 \end{pmatrix} \qquad n^2_{\gamma'}(\Omega) = \begin{pmatrix} 0 \\ \cos\varphi \sin\theta \\ \sin\varphi \sin\theta \\ \cos\theta \end{pmatrix} \tag{4.1}$$

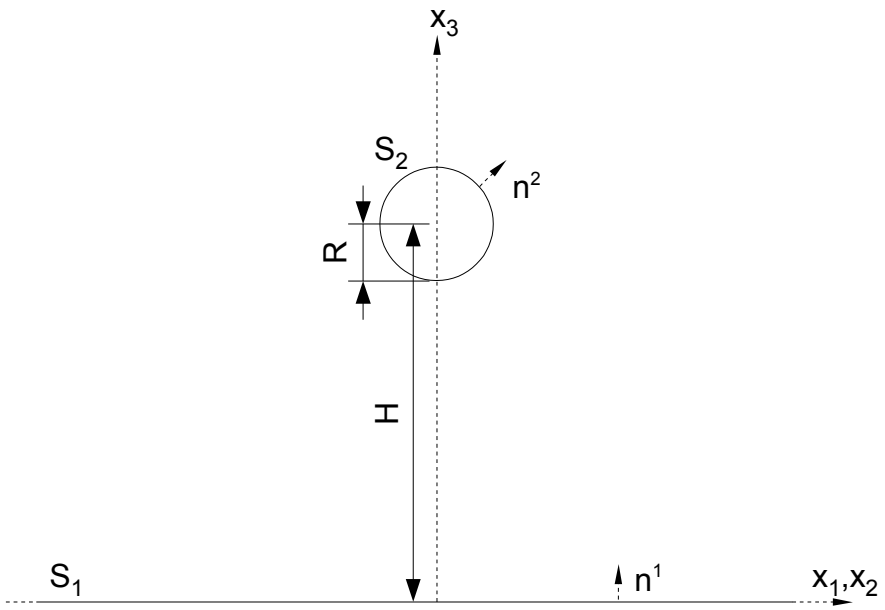

Fig. 4.1: A plain plate and a sphere of radius R on top of it are set on a distance H. Both are assumed to be perfect conductors. The Coordinates for the plate are Cartesian and those for the sphere are spherical ones. x_1 and x_2 are the coordinates on the plate, θ and ϕ are the coordinates on the sphere. n^1 and n^2 are the corresponding normal vectors.

4.2 Preliminaries

The change in the symmetry of the problem leads to a slightly different strategy to achieve the Casimir energy, as it was done in chapter 3. The sphere propagator now cannot be functional inverted in momentum space because it is not translation invariant. At first one should recall equation (2.52), the Casimir energy for the special case of two surfaces:

$$E_{\mathrm{Cas}} = -\frac{\hbar c}{2T_E} \sum_{n=1}^{\infty} \frac{1}{n} \operatorname{Tr} \left[(\Delta\mathcal{M}_{12}\Delta\mathcal{M}_{21})^n \right] . \tag{4.2}$$

The matrix product and the trace are an integration over all surface variables additionally to the summation of the space-time indices. Hence, again, the usage of a momentum space would simplify this equation. A translation

invariance for all surfaces is only given in time direction, so it is convenient to transform the times to frequencies. Additionally, the plate is translation invariant with respect to x_1 and x_2 and therefore M_{11}^{-1} will be used in its momentum space representation. But for the sphere, surface integrals have to be carried out later on. They can be done for all n in equation (4.2), but an analytical result like (3.14) does not exist. Hence, only the first dominant contributions can be calculated. These are given by the monopole, dipole and quadrupole order, and so forth, and thus the power of $\frac{R}{H}$ is an adapted criterion. From the scalar case [31], it is known that the first orders are given by the first summands in equation (4.2) and so one could restrict oneself to the first summand. This corresponds to the propagation of a photon from one surface to the other and back, and consequently rendering one propagation "loop". As a result, the 1-loop Casimir energy[17] is given by

$$E_{\mathrm{Cas}}^{1\text{ loop}} = -\frac{\hbar c}{2T_E}\mathrm{Tr}\left[\Delta\mathcal{M}_{12}\Delta\mathcal{M}_{21}\right]. \tag{4.3}$$

$$\begin{aligned}\mathrm{Tr}\left[\Delta\mathcal{M}_{12}\Delta\mathcal{M}_{21}\right] = &\int_{\underline{x}}\int_{\underline{x}'}\int_{x''}\int_{x'''} \\ &\mathrm{tr}\left[M_{11}^{-1}(\underline{x},\underline{x}')M_{12}(\underline{x}',x'')M_{22}^{-1}(x'',x''')M_{21}(x''',\underline{x})\right]\end{aligned} \tag{4.4}$$

$\int_{x''}$ and $\int_{x'''}$ are meant to be surface integrals on the sphere. To simplify this equation, the Fourier integrals (A.1) to (A.4) from appendix A can be inserted. In accordance to the previously used convention, $\underline{p} \equiv (p_0, p_1, p_2) \equiv (p_0, p_{||})$ is used.

$$\begin{aligned}\mathrm{Tr}\left[\Delta\mathcal{M}_{12}\Delta\mathcal{M}_{21}\right] = &\frac{1}{(2\pi)^{10}}\int_{\underline{x}}\int_{\underline{x}'}\int_{t'',\vec{x}''}\int_{t''',\vec{x}'''}\int_{\underline{p}}\int_{\underline{p}'}\int_{p_0''}\int_{\underline{p}'''} \\ &\mathrm{tr}\left[M_{11}^{-1}(\underline{p})M_{12}(\underline{p}',\vec{x}'')M_{22}^{-1}(p_0'',\vec{x}'',\vec{x}''')M_{21}(\vec{x}''',\underline{p}''')\right] \\ &e^{-i\underline{p}(\underline{x}-\underline{x}')}e^{-i\underline{p}'\underline{x}'+ip_0't''}e^{-ip_0''(t''-t''')}e^{-ip_0'''t'''+i\underline{p}'''\underline{x}}\end{aligned} \tag{4.5}$$

In the next step, some of the space time integrals have to be integrated out, which leads to seven delta functions of momenta. Six of the momenta integrals can be carried out, thus afterwards, the trace is determined by only four space surface integrals on the sphere, one time integral and three momentum integrals on the plate.

$$\begin{aligned}\mathrm{Tr}\left[\Delta\mathcal{M}_{12}\Delta\mathcal{M}_{21}\right] = &\frac{R^4}{(2\pi)^3}\int_{\Omega''}\int_{\Omega'''}\int_{t''}\int_{\underline{p}} \\ &\mathrm{tr}\left[M_{11}^{-1}(\underline{p})M_{12}(\underline{p},R,\Omega'')M_{22}^{-1}(p_0,\Omega'',\Omega''')M_{21}(R,\Omega''',\underline{p})\right]\end{aligned} \tag{4.6}$$

[17] The term "1-loop" Casimir energy has nothing to to with the known term "1-loop" used for describing connected Feynman diagrams with only one cycle.

Because of stationarity, the integrand of (4.6) does not depend on the time t''. So the time integral can be carried out and results in the Euclidean timelength T_E, which cancels out with the one in (4.3). The same result can be obtained for all $\mathrm{Tr}\left[(\Delta\mathcal{M}_{12}\Delta\mathcal{M}_{21})^n\right]$. Therefore, T_E cancels also in equation (4.2). After including all translation symmetries, the 1-loop energy is given by

$$E_{\mathrm{Cas}}^{1\text{ loop}} = -\frac{\hbar c}{2}\frac{R^4}{(2\pi)^3}\int_{\Omega''}\int_{\Omega'''}\int_{\underline{p}} \mathrm{tr}\left[M_{11}^{-1}(\underline{p})M_{12}(\underline{p},R,\Omega'')M_{22}^{-1}(p_0,\Omega'',\Omega''')M_{21}(\Omega''',\underline{p})\right]. \tag{4.7}$$

With (4.7) the calculation of the propagator matrices can be started. Indeed, the plain plate propagator M_{11} and its inversion has already been done and can be found in the previous chapter or in appendix C.

4.3 The propagator between a plate and a sphere

To get the Casimir energy for the case of one (see (4.7)) or more loops, the propagator matrices $M_{12}(\underline{p},R,\Omega)$ and $M_{21}(R,\Omega,\underline{p})$, describing the transition of a photon from a point on a plate to another point on a sphere and back, are needed. As it was done in the parallel plates case, they can be obtained by first transforming the free photon propagator to the corresponding momentum space. Afterwards the conditions defined in (2.32) can be imposed. To be specific, the Fourier transformation

$$G(x_0-x_0',x_{||},x_3,\vec{\Omega}) = \frac{1}{(2\pi)^3}\int_{\underline{p}} G(\underline{p},\vec{\Omega})e^{-ip_0(x_0-x_0')-ip_{||}x_{||}} \tag{4.8}$$

can be chosen for $G(x-x')$, with $\vec{\Omega}=\vec{x}'$ being the point on the sphere. This leads to the scalar propagator from the plate to the sphere

$$G(\underline{p},\vec{\Omega}) = \frac{1}{2|\underline{p}|}e^{-|x_3-x_3'||\underline{p}|+ix_{||}'p_{||}}. \tag{4.9}$$

By putting (4.8) and (4.9) times $\delta_{\beta\beta'}$ into (2.32), the Fourier integrals can be extracted and in consequence the integrand is $M_{12}(\underline{p},\Omega)$ in momentum space. With the use of the normal vectors (4.1), M_{12} can be simplified to the following object: In the case of pure Feynman gauge it is

$$M_{12}(\underline{p},\Omega) = \frac{e^{-|\underline{p}||R\cos\theta+H|+iR\sin\theta(\cos\varphi p_1+\sin\varphi p_2)}}{2|\underline{p}|}\times \tag{4.10}$$

$$\begin{pmatrix} c_\theta(p_1^2+p_2^2)-s_\theta(c_\varphi p_1+s_\varphi p_2)i|\underline{p}| & -c_\theta p_0\, p_1 & -c_\theta p_0\, p_2 & s_\theta p_0\,(c_\varphi p_1+s_\varphi p_2) \\ p_0(c_\varphi s_\theta i|\underline{p}|-c_\theta p_1) & c_\theta(p_0^2+p_2^2)-s_\varphi s_\theta p_2 i|\underline{p}| & p_2(c_\varphi s_\theta i|\underline{p}|-c_\theta p_1) & s_\varphi s_\theta p_1 p_2 - c_\varphi s_\theta(p_0^2+p_2^2) \\ p_0(s_\varphi s_\theta i|\underline{p}|-c_\theta p_2) & p_1(s_\varphi s_\theta i|\underline{p}|-c_\theta p_2) & c_\theta(p_0^2+p_1^2)-c_\varphi s_\theta p_1 i|\underline{p}| & c_\varphi s_\theta p_1 p_2 - s_\varphi s_\theta(p_0^2+p_1^2) \\ 0 & 0 & 0 & 0 \end{pmatrix},$$

and together with $\Psi_0 = 0$ on both surfaces it becomes

$$M_{12}(\underline{p},\Omega) = \frac{e^{-|\underline{p}||R\cos\theta+H|+iR\sin\theta(\cos\varphi p_1+\sin\varphi p_2)}}{2|\underline{p}|}\times \tag{4.11}$$
$$\begin{pmatrix} 0 & 0 & 0 & 0 \\ 0 & c_\theta(p_0^2+p_2^2) - s_\varphi s_\theta p_2 i|\underline{p}| & p_2(c_\varphi s_\theta i|\underline{p}| - c_\theta p_1) & s_\varphi s_\theta p_1 p_2 - c_\varphi s_\theta(p_0^2+p_2^2) \\ 0 & p_1(s_\varphi s_\theta i|\underline{p}| - c_\theta p_2) & c_\theta(p_0^2+p_1^2) - c_\varphi s_\theta p_1 i|\underline{p}| & c_\varphi s_\theta p_1 p_2 - s_\varphi s_\theta(p_0^2+p_1^2) \\ 0 & 0 & 0 & 0 \end{pmatrix}.$$

The terms c_θ, s_θ, c_φ and s_φ denote $\cos\theta$, $\sin\theta$, $\cos\varphi$ and $\sin\varphi$ respectively. However, Coulomb gauge can be reached again by restricting β and β' to count from 1 to 3. In this case M_{12} would look like

$$M_{12}(\underline{p},\Omega) = \frac{e^{-|\underline{p}||R\cos\theta+H|+iR\sin\theta(\cos\varphi p_1+\sin\varphi p_2)}}{2|\underline{p}|}\times \tag{4.12}$$
$$\begin{pmatrix} -c_\theta(p_1^2+p_2^2) + s_\theta(c_\varphi p_1 + s_\varphi p_2) i|\underline{p}| & c_\theta p_0\, p_1 & c_\theta p_0\, p_2 & -s_\theta p_0\,(c_\varphi p_1 + s_\varphi p_2) \\ p_0(c_\theta p_1 - c_\varphi s_\theta i|\underline{p}|) & -c_\theta p_0^2 & 0 & c_\varphi s_\theta p_0^2 \\ p_0(c_\theta p_2 - s_\varphi s_\theta i|\underline{p}|) & 0 & -c_\theta p_0^2 & s_\varphi s_\theta p_0^2 \\ 0 & 0 & 0 & 0 \end{pmatrix},$$

but this leads to a wrong Casimir energy in the end. For a clear understanding of these calculations, component $(0,1)$ of M_{12} is explicitly calculated as an example in appendix B.

Now it is an easy task to get the back propagator M_{21}. The scalar propagator from the sphere to the plate $G(\vec{\Omega},\underline{p})$ will be the complex conjugated of $G(\underline{p},\vec{\Omega})$ because of a minus in the Fourier integral. Additionally, the exchange of the points also exchanges the fields in the product $\Psi M \Psi$. Therefore, M_{21} will be equal to the adjoint of M_{12}. This can be calculated out of (2.32), too.

$$M_{21}(\Omega,\underline{p}) = M_{12}^\dagger(\underline{p},\Omega) \tag{4.13}$$

4.4 The c_l coefficients

In the following, it will be necessary to calculate the scalar expansion coefficients $c_{lml'm'}$ of the free scalar propagator $G(p_0,\Omega,\Omega')$ for an expansion into spherical harmonics Y_{lm} at both points $\vec{\Omega}$ and $\vec{\Omega}'$.

$$G(p_0,\Omega,\Omega') = \sum_{lm,l'm'} c_{lml'm'}(R,p_0) Y_{lm}(\Omega) Y^\star_{l'm'}(\Omega') \tag{4.14}$$

G depends only on the distance between the two points and not on any direction. Therefore, it can also be expanded into Legendre polynomials $P_l(\vec{\Omega}\cdot\vec{\Omega}') = P_l(\cos\alpha)$ with α being the angle between the two points

$\Omega \equiv (\theta, \varphi)$ and $\Omega' \equiv (\Theta, \Phi)$ on the sphere.

$$\cos\alpha = \cos\theta\cos\Theta + \sin\theta\sin\Theta\cos(\varphi - \Phi) \tag{4.15}$$

Now the addition theorem for spherical harmonics

$$P_l(\cos\alpha) = \frac{4\pi}{2l+1}\sum_{m=-l..l} Y_{lm}(\Omega)Y^{\star}_{lm}(\Omega') \tag{4.16}$$

shows that $c_{lml'm'}$ has to be diagonal in l, l' and m, m', and also independent from m or m'. Thus, $c_{lml'm'}$ becomes $\delta_{ll'}\delta_{mm'}c_l$ and equation (4.14) changes to

$$G(p_0, \Omega, \Omega') = \sum_{lm} c_l(R, p_0)Y_{lm}(\Omega)Y^{\star}_{lm}(\Omega')\,. \tag{4.17}$$

To obtain c_l coefficients, the integral

$$c_l = 2\pi\int_{-1}^{1} G(\cos\alpha)P_l(\cos\alpha)d(\cos\alpha) \tag{4.18}$$

has to be solved. This can be done by rewriting G as an integral over T, which is called the "proper time" formalism. With

$$G(p_0, \vec{x}) = \frac{1}{4\pi}\frac{e^{-|\vec{p_0}||\vec{x}|}}{|\vec{x}|} \tag{4.19}$$

$$= \int_0^{\infty} \frac{1}{4\sqrt{\pi T}} e^{-\vec{x}^2 T - \frac{p_0^2}{4T}} dT \tag{4.20}$$

and $\vec{x} = R\sqrt{2(1-\cos\alpha)}$, the c_l coefficients can be obtained for arbitrary high l. Afterwards the T integration has to be carried out, which is always possible. Actually, a solution up to the T integration can be given in form of a sum formula. By using

$$P_l(x) = \sum_{k=0}^{\lfloor \frac{l}{2} \rfloor} \frac{(-1)^k(2l-2k)!}{(l-k)!(l-2k)!k!2^l}x^{l-2k} \tag{4.21}$$

and

$$\int_{-1}^{1} x^n e^{rx}dx = (-1)^n\left(\frac{e^{-\frac{1}{2}r}M_{\frac{1}{2}n,\frac{1}{2}(n+1)}(r)}{(n+1)r^{\frac{1}{2}n+1}} + \frac{n\Gamma(n,-r) - \Gamma(n+1)}{r^{n+1}}\right) + \frac{e^r}{r}\,, \tag{4.22}$$

the $d(\cos\alpha)$ integral in (4.18) can be simplified to the following expression:

$$\lambda_l(r) = \frac{e^r}{r} + \sum_{k=0}^{\lfloor \frac{l}{2} \rfloor} \frac{[\Gamma(l-2k,-r)(l-2k) - \Gamma(l-2k+1,r)]\,\Gamma(l-k+\frac{1}{2})}{(-1)^{k+l} 2^{2k-l} \sqrt{\pi} r^{l+1-2k} \Gamma(l-2k+1)\Gamma(k+1)} \tag{4.23}$$

$$c_l = 2\pi \int_0^\infty \frac{\lambda_l(2R^2T)}{4\sqrt{\pi T}} e^{-2R^2T - \frac{p_0^2}{4T}} dT \tag{4.24}$$

The brackets $\lfloor\,\rfloor$ in (4.21) and (4.23) mean rounding down. The integral (4.22) is given by *Maple 11* , where $M_{k,m}(x)$ is the Whittaker M function, and $\Gamma(z,a)$ and $\Gamma(z) = \Gamma(z,0)$ are the incomplete and the usual Gamma function respectively. With (4.24) or (4.18), the first 5 coefficients are:

$$c_0 = \frac{1}{2} \frac{\left(-1 + e^{2|p_0|R}\right) e^{-2|p_0|R}}{R^2 |p_0|} \tag{4.25}$$

$$c_1 = \frac{1}{2} \frac{\left(-e^{2|p_0|R} + e^{2|p_0|R} R^2 {p_0}^2 + 2|p_0| R + 1 + R^2 {p_0}^2\right) e^{-2|p_0|R}}{|p_0|^3 R^4} \tag{4.26}$$

$$c_2 = \frac{1}{2} \frac{\left(e^{2|p_0|R} R^4 p_0^4 - 3e^{2|p_0|R} R^2 p_0^2 + 9e^{2|p_0|R} - 6R^3 |p_0|^3 - R^4 p_0^4 - 18R|p_0| - 9 - 15R^2 p_0^2\right) e^{-2|p_0|R}}{R^6 |p_0|^5} \tag{4.27}$$

$$c_3 = \frac{1}{2} \frac{\left(-6e^{2|p_0|R} R^4 {p_0}^4 + e^{2|p_0|R} R^6 {p_0}^6 + 45e^{2|p_0|R} R^2 {p_0}^2 - 225e^{2|p_0|R} + 210R^3 |p_0|^3 + 405R^2 {p_0}^2 + 66R^4 {p_0}^4 + 450|p_0| R + 225 + 12|p_0|^5 R^5 + R^6 {p_0}^6\right) e^{-2|p_0|R}}{R^8 |p_0|^7} \tag{4.28}$$

$$c_4 = \frac{1}{2} \frac{\left(11025e^{2|p_0|R} + 135e^{2|p_0|R} R^4 p_0^4 - 10e^{2|p_0|R} R^6 p_0^6 + e^{2|p_0|R} R^8 p_0^8 - 1575e^{2|p_0|R} R^2 p_0^2 - 1110R^5 |p_0|^5 - 11550R^3 |p_0|^3 - 4335R^4 p_0^4 - 20R^7 |p_0|^7 - R^8 p_0^8 - 11025 - 20475R^2 p_0^2 - 22050R|p_0| - 190R^6 p_0^6\right) e^{-2|p_0|R}}{R^{10} |p_0|^9} . \tag{4.29}$$

At last, for some arguments later, the leading power of R for each of those coefficients has to be determined. This is R^{-1} for every c_l. A possible proof

of this is given by the equations (4.22), (4.23) and (4.24): The left side of equation (4.22) shows that their right side does not have singularities for all finite r. This integral (4.22) was used to solve (4.18) with (4.20). Thus, all $\lambda_l(r)$ in (4.23) can be verified to have no singularities for finite r. With $r = 2R^2T$ and $\lambda_l(r)$, the integrand in (4.24) can therefore be argued to have only one singularity of the type $T^{-\frac{1}{2}}$. Thus, the dT integral leads to a singularity of the type R^{-1} for all c_l. That means, the leading power of a series expansion at $R = 0$ starts with R^{-1}, as can also be explicitly checked by expanding (4.25) – (4.29).

4.5 Cartesian basis

The last step for receiving the Casimir energy is to calculate the functional inverse matrix propagator for a propagation on the sphere. This inversion cannot be done exactly like in the translation invariant case of a plain plate, but an expansion into multipoles works in the case of a scalar field [31]. This will be done in the following by also trying different expansion schemes.

4.5.1 Sphere-sphere propagator explicitly

Firstly, the free photon propagator $G(p_0, \Omega, \Omega')$ describing the propagation from one point on a sphere to another point on the same sphere has to be obtained. Only the time coordinate can be transformed to momentum space because of stationarity. It results in

$$G(p_0, \Omega, \Omega') = \frac{1}{4\pi}\frac{1}{|\vec{x}|}e^{-|\vec{x}||p_0|}\big|_{\vec{x}=\vec{\Omega}-\vec{\Omega}'} \,. \tag{4.30}$$

This equation has to be inserted into (2.32) to get the propagator matrix $M_{22}^{\mu\nu}(p_0, \Omega, \Omega')$. Contrary to Appendix B there are 12 nontrivial summands for each combination of μ and ν, so the expressions become very large. But in principal, it can be written as

$$M_{22}(p_0, \Omega, \Omega') = \begin{pmatrix} R^{-2}\vec{\mathcal{L}}\vec{\mathcal{L}}'^{\star} & ip_0R^{-1}(\vec{\mathcal{L}}\times\vec{n}')^T \\ -ip_0R^{-1}\vec{n}\times\vec{\mathcal{L}}'^{\star} & p_0^2(\vec{n}'\otimes\vec{n} - \vec{n}\vec{n}'\mathbb{1}_3) + R^{-2}\vec{\mathcal{L}}\otimes\vec{\mathcal{L}}'^{\star} \end{pmatrix} G(p_0, \Omega, \Omega') \tag{4.31}$$

in Cartesian coordinates, where the primed variables correspond to Ω'. $\vec{\mathcal{L}}$ is the usual angular momentum operator $-i\vec{\Omega}\times\vec{\nabla}$, which appears in (2.32) due to $\vec{n}R = \vec{\Omega}$. The product $\otimes$ means $\vec{n}' \otimes \vec{n}$ is the matrix $n_i' n_j$ in components. The evidence is given on the following pages.

However, to get the functional inverse propagator $M_{22}^{-1}(p_0, \Omega, \Omega')$, equation (4.31) needs to be expanded into a functional basis. In the scalar case [31] this was done by expanding their scalar M_{22} into multipoles, or to be specific, into Legendre polynomials $P_l(\cos\alpha)$, where α is the angle between the points $\vec{\Omega}$ and $\vec{\Omega}'$ on the sphere. But, due to (4.31) depending not only on α but also on the direction on the sphere, this does not work in the QED case.

4.5.2 Sphere-sphere propagator expanded into spherical harmonics

Although, there is no expansion of M_{22} into Legendre polynomials, which was used in the scalar case to obtain the expansion into spherical harmonics

by the addition theorem (4.16), a direct expansion of M_{22} into spherical harmonics can be tried. The general expansion coefficient would be a matrix S and M_{22} would have the representation

$$M_{22}^{\mu\nu}(p_0, \Omega', \Omega'') = \sum_{lml'm'} S_{lml'm'}^{\mu\nu}(p_0, R, \{c_i\}) Y_{lm}(\Omega') Y_{l'm'}^{\star}(\Omega'') \,. \tag{4.32}$$

Then the inverse propagator can be calculated by inverting the coefficient matrix as shown in section D:

$$M_{22}^{-1\,\mu\nu}(p_0, \Omega, \Omega') = \frac{1}{R^4} \sum_{lml'm'} S_{lml'm'}^{-1\,\mu\nu}(p_0, R, \{c_i\}) Y_{lm}(\Omega) Y_{l'm'}^{\star}(\Omega') \,. \tag{4.33}$$

Because the $\int_{x'}$ in equation (D.1) is $R^2 \int_{\Omega'}$ and the delta function $\delta(x - x'')$ becomes $R^{-2}\delta(\Omega - \Omega'')$, the R^{-4} appears as a result of the dimensionality. This is in principle the same result as for the scalar case calculated in [31], where the coefficients of the inverse sphere-sphere propagator where calculated by dividing the inverse coefficients $\frac{1}{c_l}$ by R^4.

Indeed, a direct expansion of (4.31) into this basis with the use of $S_{lml'm'}^{\mu\nu} = \int_\Omega \int_{\Omega'} M_{22}^{\mu\nu}(\Omega, \Omega') Y_{lm}^{\star}(\Omega) Y_{l'm'}(\Omega')$ fails due to unsolvable integrals. This problem can be circumvented with the knowledge that G can be easily decomposed into spherical harmonics with coefficients c_l (see (4.17)). All remaining terms and operators in (2.32), which do not belong to G, act on this expansion. Thereby, the indices of the spherical harmonics will simply be lifted and lowered. All modifications can be absorbed afterwards by above coefficient matrix $S_{lml'm'}^{\mu\nu}$. Hence the task is to identify these operators, which, in the end, are the one written in (4.31).

With the use of $x_\gamma^a \equiv R n_\gamma^a$, (2.32) can be rewritten as follows:

$$\begin{aligned} M_{22}^{\mu\nu}(p_0, \Omega, \Omega') = & \underbrace{\left[\frac{1}{iR} x_\gamma \epsilon^{\mu\beta\gamma\alpha} \partial(x)_\alpha\right]}_{\mathcal{T}(x)} \delta_{\beta\beta'} \times \\ & \underbrace{\left[\frac{1}{-iR} y_{\gamma'} \epsilon^{\nu\beta'\gamma'\alpha'} \partial(y)_{\alpha'}\right]}_{\mathcal{T}^\dagger(y)} G(x, y) \Big|_{\substack{\vec{x} = \vec{\Omega} \\ \vec{y} = \vec{\Omega}'}} \,. \end{aligned} \tag{4.34}$$

Thus, the problem can be split up symmetrically into two operators $\mathcal{T}(x)$ and $\mathcal{T}^\dagger(y)$. Then M_{22} results in

$$M_{22}^{\mu\nu}(p_0, \Omega, \Omega') = \mathcal{T}^{\mu\beta}(x) \mathcal{T}_\beta^{\dagger\nu}(y) G(x, y) \Big|_{\substack{x = \Omega \\ y = \Omega'}} \,. \tag{4.35}$$

In a next step, $\mathcal{T}$ can be written out explicitly, whereby the angular momentum operator $\vec{\mathcal{L}} = -i\vec{x} \times \vec{\nabla}$ appears in the time components. Due to the Fourier representation of G, the time derivatives can be replaced by $-ip_0$, and a last simplification can be done by knowing that the time component of the surface normal vector n_γ is zero.

$$\mathcal{T}^{\mu\beta}(p_p, n_1, n_2, n_3) = \frac{1}{iR} x_\gamma \epsilon^{\mu\beta\gamma\alpha} \partial_\alpha \tag{4.36}$$

$$= \begin{pmatrix} 0 & \textcircled{\frac{\mathcal{L}_1}{R}} & \textcircled{\frac{\mathcal{L}_2}{R}} & \textcircled{\frac{\mathcal{L}_3}{R}} \\ \boxed{-\frac{\mathcal{L}_1}{R}} & 0 & p_0 n_3 & -p_0 n_2 \\ \boxed{-\frac{\mathcal{L}_2}{R}} & -p_0 n_3 & 0 & p_0 n_1 \\ \boxed{-\frac{\mathcal{L}_3}{R}} & p_0 n_2 & -p_0 n_1 & 0 \end{pmatrix} \tag{4.37}$$

Since the wrong Coulomb gauge means counting β and β' only from 1 to 3, the red boxed terms have to be set to zero in this gauge. On the other hand, the correct $\Psi_0 = 0$ gauge can be reached by setting the green circled terms to zero. Equation (4.35) and the operator (4.37) now lead to (4.31).

Due to $n\mathcal{T} = 0$ and $\mathcal{T}n = 0$, which means $\mathcal{T}$ projects onto the surface, the normal derivative ∂_r cancels out after replacing the Cartesian derivative by a derivative in spherical coordinates. In the end the $\mathcal{T}$ operator acts only on the spherical harmonics of G in (4.17) and not on the c_l coefficients. By defining $T_{lm} := \mathcal{T} Y_{lm}$, (4.35) reads

$$M_{22}^{\mu\nu}(p_0, \Omega, \Omega') = \sum_{lm} T_{lm}^{\mu\beta}(p_0, R, \Omega) c_l(p_0, R) T_{\beta\, lm}^{\dagger\nu}(p_0, R, \Omega') \,. \tag{4.38}$$

For calculating T explicitly, $\vec{\mathcal{L}}$ and n have to be rewritten in spherical tensor components $\tilde{\mu} = \{-1, 0, 1\}$.

$$\begin{aligned} \mathcal{L}_{\pm 1} &= \mp \tfrac{1}{\sqrt{2}} (\mathcal{L}_x \pm i\mathcal{L}_y) \\ \mathcal{L}_0 &= \mathcal{L}_z \\ n_{\pm 1} &= \mp \tfrac{1}{\sqrt{2}} (n_x \pm i n_y) \\ n_0 &= n_z \end{aligned} \tag{4.39}$$

The action of $\mathcal{L}$ on Y_{lm} is determined by the formula

$$\mathcal{L}_{\tilde{\mu}} Y_{l,m} = (-1)^{l+m+\tilde{\mu}+1} \sqrt{l(l+1)(2l+1)} \times \begin{pmatrix} l & 1 & l \\ m+\tilde{\mu} & -\tilde{\mu} & -m \end{pmatrix} Y_{l,m+\tilde{\mu}} \tag{4.40}$$

with the round bracket being a Wigner $3j$ symbol. This $3j$ symbol can be found in [36] and hence (4.40) results in the form

$$\mathcal{L}_{\pm 1} Y_{l,m} = \mp \frac{1}{\sqrt{2}} \sqrt{(l \mp m)(l \pm m + 1)} Y_{l,m\pm 1} \tag{4.41}$$

$$\mathcal{L}_0 Y_{l,m} = m Y_{l,m}\,, \tag{4.42}$$

whereby the $\mp\frac{1}{\sqrt{2}}$ comes from the convention in (4.39). For nY, an analogous expression can be obtained by knowing that $n_{\tilde{\mu}} = \sqrt{\frac{4\pi}{3}} Y_{1\tilde{\mu}}$. With the use of the product formula for spherical harmonics, also found in [36], nY can be expressed as

$$\begin{aligned} n_{\tilde{\mu}} Y_{l,m} =& (-1)^{l+m+\tilde{\mu}+1} \left[\sqrt{l+1} \begin{pmatrix} l & 1 & l+1 \\ m & \mu & -m-\tilde{\mu} \end{pmatrix} Y_{l+1,m+\tilde{\mu}} \right. \\ & \left. - \sqrt{l} \begin{pmatrix} l & 1 & l-1 \\ m & \tilde{\mu} & -m-\tilde{\mu} \end{pmatrix} Y_{l-1,m+\tilde{\mu}} \right]. \end{aligned} \tag{4.43}$$

This was done in [37]. After consulting [36] for these Wigner $3j$ symbols, equation (4.43) becomes

$$\begin{aligned} n_{\pm 1} Y_{l,m} =& \sqrt{\frac{(l \pm m + 1)(l \pm m + 2)}{2(2l+3)(2l+1)}} Y_{l+1,m\pm 1} \\ & - \sqrt{\frac{(l \mp m - 1)(l \mp m)}{2(2l+1)(2l-1)}} Y_{l-1,m\pm 1} \end{aligned} \tag{4.44}$$

$$\begin{aligned} n_0 Y_{l,m} =& \sqrt{\frac{(l-m+1)(l+m+1)}{(2l+3)(2l+1)}} Y_{l+1,m} \\ & + \sqrt{\frac{(l+m)(l-m)}{(2l+1)(2l-1)}} Y_{l-1,m} \end{aligned} \tag{4.45}$$

By putting (4.41), (4.42), (4.44), (4.45) and (4.39) together in (4.38) and calculating the sum up to a cutoff in l, a R and p_0 dependent 4×4 matrix is obtained, times the corresponding spherical harmonics of both points Ω and Ω'. From this, the matrix $S^{\mu\nu}_{lml'm'}(p_0, R, c_i)$ can be obtained by collecting all coefficients of $Y_{lm}(\Omega) Y^{\star}_{l'm'}(\Omega')$ for a special l ,m ,l' and m'. Because the inverse of S with respect to all indices will be needed, it is usefull to combine them to one superindex $A = (\mu, m, l)$ and $B = (\nu, m', l')$, counting from 1 to ∞.

A	1	2	3	4	5	6	7	8	9	10	11	12	13	14	15	16	17	...
μ	0	1	2	3	0	1	2	3	0	1	2	3	0	1	2	3	0	...
m	0				-1				0				1				-2	...
l	0				1												2	...

Table 1: Scheme of the used superindex notation.

This procedure leads to the matrix S_{AB}, plotted in the following figures:

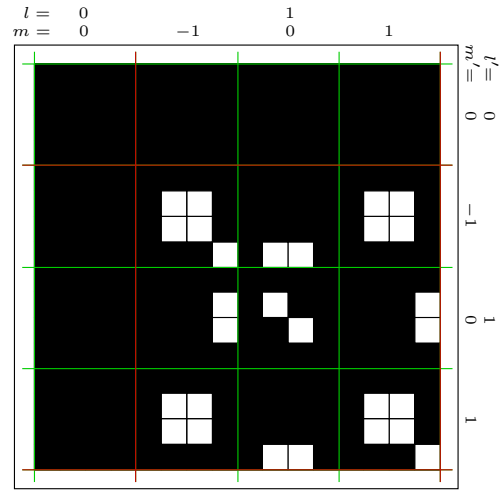

(a) S_{AB} with coefficients c_0

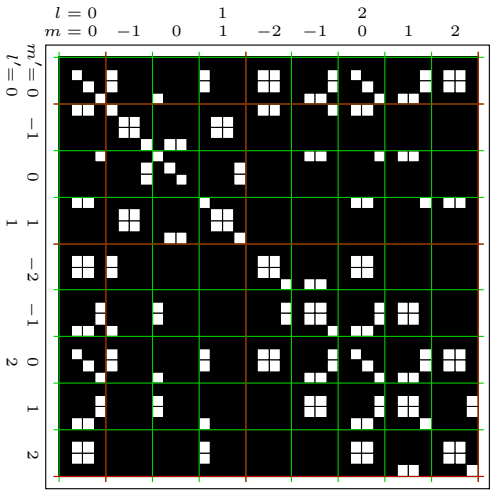

(b) S_{AB} with coefficients c_0 and c_1

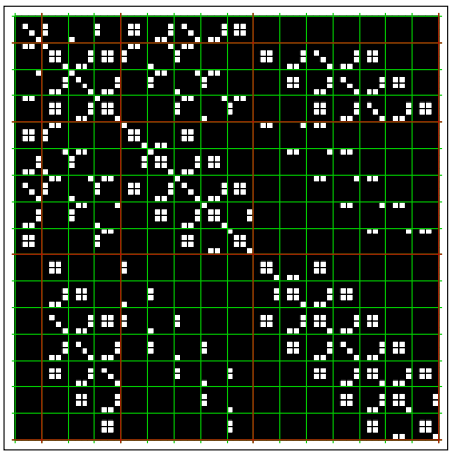

(c) S_{AB} with coefficients c_0 to c_2

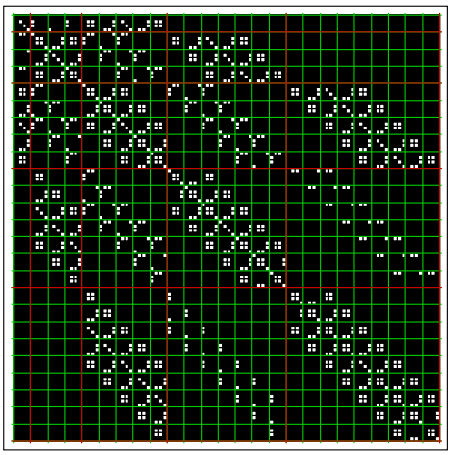

(d) S_{AB} with coefficients c_0 to c_3

Fig. 4.2: Scheme of matrix $S^{\mu\nu}_{lm,l'm'} \equiv S_{AB}$ for different expansion orders: black means zero and white non-zero. Every matrix is divided by red lines into separate parts corresponding to l and l'. Analogously, the green lines separate every red boxed submatrix into parts which correspond to m and m'. The inside of such a green boxed submatrix is a 4×4 matrix for the space-time-indices μ and ν.

The pictures show the matrix S_{AB} for different numbers of coefficients c_i. Furthermore the white non-zero components are polynomial in $(p_0^2, \frac{p_0}{R}, \frac{1}{R^2}) \times c_i$.

From the figures can be seen that the time-time components ($\{A, B | (A \mod 4 = 1) \cup (B \mod 4 = 1)\}$), where only $\frac{1}{R^2}$ terms come from, are placed on the diagonal $A = B$. Naturally, this results in the time-time components, because the angular momentum operators in (4.37) are placed at $\mu = 0$ and the product $TT^\dagger$ produces a product of $\frac{1}{R^2}\vec{\mathcal{L}}(\Omega)\vec{\mathcal{L}}^\star(\Omega')$. These operators only lift and lower the m and m' index in the spherical harmonics simultaneously. Analogous terms appear in the space-space components due to the $\vec{\mathcal{L}} \otimes \vec{\mathcal{L}}'$ there.

The $\frac{p_0}{R}$ and p_0^2 terms appear due to similar reasons. They come from the time-space and space-time components, where $TT^\dagger$ produces a product of $\frac{p_0}{R}\vec{\mathcal{L}} \times \vec{n}$, but also from the space-space components, where $TT^\dagger$ produces a product of $p_0 n_i(\Omega)$ and $p_0 n_j(\Omega')$. Not so obvious is the fact that $\frac{p_0}{R}$ only appears in the two branches where $|l - l'| = 1$ and p_0^2 appears in the three branches with $|l - l'| = 0$ or 2. Also remarkable is the fact that the outer areas $|l - l'| > 2$ are all zero. That implies a band structure respectively to the l index, which is necessary for the invertability of S_{AB} later.

The last thing that can be told about S_{AB} at the moment is the general allocation of the c_l coefficients showed in the following draft:

c_1	c_1	c_1	0	0	...
c_1	c_0, c_1, c_2	c_1, c_2	c_2	0	...
c_1	c_1, c_2	c_1, c_2, c_3	c_2, c_3	c_3	...
0	c_2	c_2, c_3	c_2, c_3, c_4	c_3, c_4	...
0	0	c_3	c_3, c_4	c_3, c_4, c_5	...
⋮	⋮	⋮	⋮	⋮	⋱

Table 2: Scheme of the c_l coefficient allocation in matrix S_{AB}. Separated are different l and l' indices.

Hence, only c_0 is an exception. It does not appear in $(l, l') = (0, 0)$, $(1, 0)$ and $(0, 1)$ because mathematically, the angular momentum operators vanish at this places due to $\vec{\mathcal{L}}Y_{00} = 0$. Physically this could be resulting because electromagnetic monopoles are not allowed in QED with no external electric charges. In the scalar case [31], where the monopole order is allowed, the corresponding energy was given by the c_0 coefficient.

4.5.3 The right truncation

S_{AB} is a quadratic matrix with dimension ∞. To get the inverse of it, a truncation has to be done, to make the dimension finite. One possible choice, which was already proposed, is to cut S_{AB} at a given number of c_l coefficients, because they determine the multipole order of the Casimir energy in the scalar case. Other truncations would be given by the number of used spherical harmonics or simply cutting S_{AB} at a given dimension. All these truncations result in the same energy by shifting the dimension to ∞, but the convergence behaviour, multipole order by multipole order, depends on the choice of the method.

The solution of this task is the following: The energy has to be calculated by taking the trace of a number of propagations. For example, the product $M_{12}M_{22}^{-1}$ is needed. M_{22}^{-1} has to be replaced by S_{AB}^{-1} and the corresponding spherical harmonics. On the one hand, S_{AB}^{-1} is the inverse of S_{AB}, and hence a truncation done with S_{AB} appears indirect in S_{AB}^{-1}. On the other hand, M_{12} is not expanded into this functional basis and will not be changed by a truncation of S_{AB}. So a discrepancy can be produced. Within the matrix product $M_{12}M_{22}^{-1}$, the integration $\int_\Omega M_{12}Y_{lm}S^{-1}_{lml'm'}$ will be done. This is a projection of M_{12} onto the basis of S_{AB} and thus it is in principle an expansion of M_{12} into these spherical harmonics given by the truncation of S_{AB}. If S_{AB} is cut, for example, at a specific number of coefficients c_i, M_{12} will be cut at a specific number of appearing spherical harmonics. To correct this influence, the truncation of S_{AB} has to be done in such a way, that, after the inversion, no additional spherical harmonics appear. The best choice to reach this, is to cut S_{AB} at a given maximal L_{max} like it is shown in the following figure:

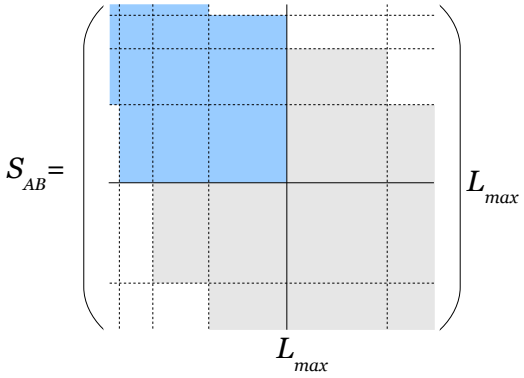

Fig. 4.3: Illustration of the cutting procedure. All spherical harmonics Y_{lm} with an index l higher than L_{max} have to be excluded.

4.5.4 Multipole analysis of the sphere-sphere propagator expansion

It is not necessary to calculate the matrix S_{AB}^{-1}, if only its dimension has to be obtained, which is maximally needed to determine a specific multipole energy. Because M_{22} only acts on the subspace of the surface, M_{22}^{-1} has to do the same. Thus by calculating S_{AB}, whose specific structure is basically determined by the surface normal vector[18], S_{AB}^{-1} can be assumed to have the same structure. But if it has the same structure, the leading power of R, which determines the multipole order, can be predicted for every entry of S_{AB}^{-1}.

In the worst case, which would contribute to the leading order in the energy, M_{22} has the structure

$$M_{22} \sim \begin{pmatrix} \frac{1}{R^2} & \frac{p_0}{R} & \frac{p_0}{R} & \frac{p_0}{R} \\ \frac{p_0}{R} & \star & \star & \star \\ \frac{p_0}{R} & \star & \star & \star \\ \frac{p_0}{R} & \star & \star & \star \end{pmatrix} \times \text{specific } c_i(R) \times \text{specific } Y_{lm} \tag{4.46}$$

with $\star = p_0^2$ in the case of $l, l' = 0$. Otherwise it is $\star = p_0^2 + \frac{1}{R^2}$. Hence S_{AB} is composed of such 4×4 blocks. As it was proven in section 4.4, the series expansion in a small radius of all c_l starts at $\frac{1}{R}$. Therefore, the series expansion of the 4×4 blocks of S_{AB} start at a known power. S_{AB}^{-1} has to have the same structure like S_{AB} in sense of zero and non-zero components. Thus the inverse matrix S_{AB}^{-1} expanded in a small radius should be composed of 4×4 blocks of the structure

$$\begin{pmatrix} R^3 s_{00} & R^2 s_{01} & R^2 s_{02} & R^2 s_{03} \\ R^2 s_{10} & \star s_{11} & \star s_{12} & \star s_{13} \\ R^2 s_{20} & \star s_{21} & \star s_{22} & \star s_{23} \\ R^2 s_{30} & \star s_{31} & \star s_{32} & \star s_{33} \end{pmatrix} \tag{4.47}$$

at all $|l - l'| \leq 2$. Here, in the case of $l, l' = 0$ the $\star$ equals $\star = R$ and otherwise it is $\star = R^3$. The $s_{\mu\nu}$ are arbitrary coefficients.

Furthermore, $M_{12}(\Omega)$ and $M_{21}(\Omega')$, which both are depending on R, have to be taken into account. By multiplying (4.47) from left and right with these matrices and expanding the whole expression for small R up to a given

[18]The normal vector $\vec{n}$ lifts and lowers the spherical harmonics and thus produces the central branch and the one with $|l - l'| = 2$. In addition, $\vec{n} \times \vec{\nabla}$ is the angular momentum operator and therefore produces the branch with $|l - l'| = 1$.

order, the integrations over the angles Ω and Ω' together with the spherical harmonics $Y_{lm}(\Omega)$ and $Y^{\star}_{l'm'}(\Omega')$ for given l, m, l' and m' can be carried out. The result is a matrix whose components are depending on several powers in R. By dereferencing with the use of $s_{\mu\nu}$, whose component in S_{AB} takes part in producing the leading order and writing this information in a matrix $\mathcal{O}_{AB}(R^{n_{max}})$, in the case of Feynman gauge, R^3 can only be produced by the spherical harmonics with l and l' being 0 up to 2 (see Fig. 4.4(a)). In this figure, all blue and green components can possibly produce R^3.

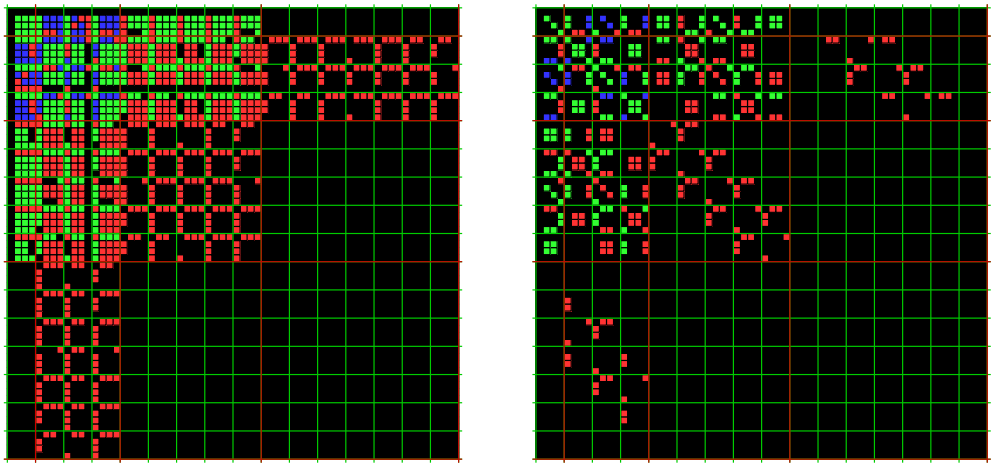

(a) plot of $\mathcal{O}_{AB}(R^4)$ (b) plot of $\tilde{\mathcal{O}}_{AB}(R^4)$

Fig. 4.4: Plotted are the components of S^{-1}_{AB} taking part in producing a given or higher power in R in the Casimir-Polder energy. Black components do not produce an energy up to the given maximal order R^4, blue ones mean the lowest contribution of this components is R^2, green $\equiv R^3$ and red $\equiv R^4$. $\mathcal{O}$ accounts only for the sphere integrals and $\tilde{\mathcal{O}}$ respects additionally the p_1 and p_2 integration for the plain plate.

In the matrix $\tilde{\mathcal{O}}_{AB}(R^{n_{max}})$ showed in Fig. 4.4(b), the plain plate is taken into account. There, the complete trace for the energy is calculated with above assumed S^{-1}_{AB} except for the p_θ and p_r integrals. Here, (p_r, p_θ, p_ϕ) is the spherical parametrisation of the plate momenta (p_1, p_2, p_0), which will be

used later on (see (4.54)). At last, the p_0 integral cannot be carried out since the c_l are depending on it.

From M_{12} and M_{21} only trigonometric functions in form of surface normal vector components occur (see (4.11)). They can be expanded in Y_{1m}. Together with M_{22}^{-1}, this results in a product of n spherical harmonics, which could be calculated out analytically.[19] Therefore, only the integration over the spherical harmonics determines, which part of S_{AB}^{-1} is needed for a special R power in the energy. This was the same mechanism in the scalar case [31], which determined that only c_0 contributes to the monopol order, even when all c_i start at $\frac{1}{R}$.

[19]For example, eq. (4.6.3) from [36] shows the product of three spherical harmonics.

4.5.5 Inverse sphere-sphere propagator

Because the sphere-sphere propagator is expanded into a functional basis, the needed inverse propagator can be calculated by inverting the expansion coefficients, or in this case, by inverting the whole expansion matrix S_{AB}. This will be done by calculating the Moore-Penrose inverse with the method described in D. That means the matrix will be inverted on the nonsingular subspace. This is easily done for small matrices. But for bigger ones, technical limits will be reached.

Dimension and rank

As an overview, the dimension and the corresponding rank of S_{AB} in two different truncations are listed in the following table, whereby $S_{AB}^{\{i\}}$ and $S_{AB}^{[L_{max}]}$ states S_{AB} with coefficients c_0 to c_i and truncated at L_{max} respectively:

$S_{AB}^{\{i\}}$ with coefficients c_0 to c_i or $S_{AB}^{[L_{max}]}$ truncated at $L_{max} = i + 1$		
i	$\dim(S_{AB})$	$\operatorname{rank} S_{AB}$
0	16×16	3
1	36×36	11
2	64×64	23
3	100×100	39
4	144×144	59
5	196×196	83
6	256×256	111
7	324×324	143

Table 3: Dimension and rank of matrix S_{AB} for "c_i and L_{max} truncation".

The dimension rises with the number of spherical harmonics involved by $4(i + 1)^2$, and, resulting from this checkup, the rank follows the rule $3(i+1)^2 - i^2$. Thus, taking the limit $i \to \infty$ leads to a rank-dimension ratio of $\frac{1}{2}$, as it should be for a rank(2) propagator. For finite dimensions, this ratio is always greater than $\frac{1}{2}$. That means there are interactions between the spherical harmonic modes, which are encoded by the off-diagonal matrix structure. These interactions can be minimised by a better choice of the basis in chapter 4.7.

The inverse

In the following figures, the first four inverse matrices S_{AB}^{-1} are plotted, whereby S_{AB} was truncated at a specific c_l:

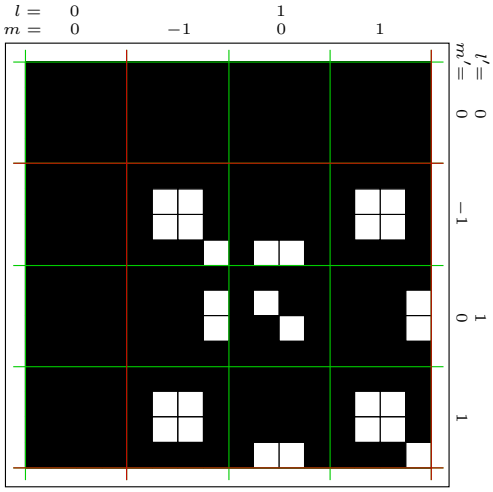

(a) Moore-Penrose inverse $S_{AB}^{-1\{0\}}$ of S_{AB} with coefficients c_0

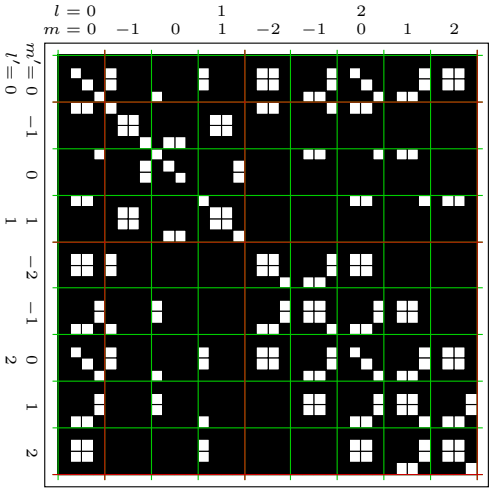

(b) Moore-Penrose inverse $S_{AB}^{-1\{1\}}$ of S_{AB} with coefficients c_0 and c_1

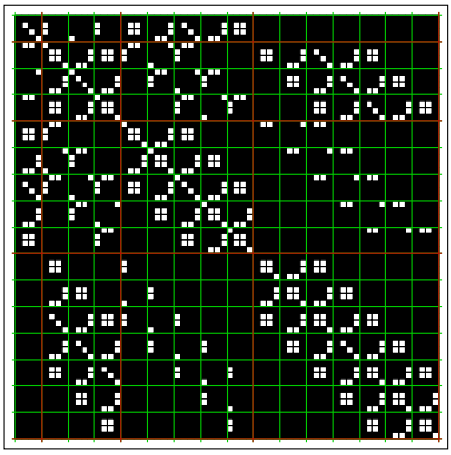

(c) Moore-Penrose inverse $S_{AB}^{-1\{2\}}$ of S_{AB} with coefficients c_0 and c_2

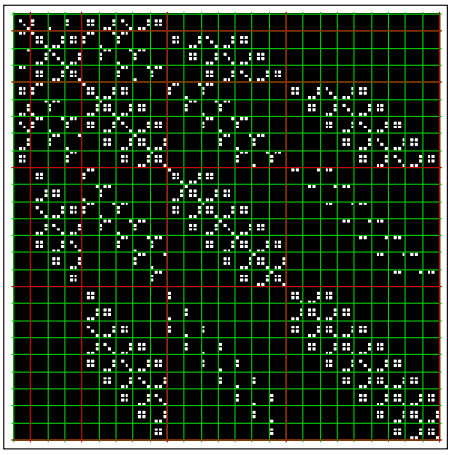

(d) Moore-Penrose inverse $S_{AB}^{-1\{3\}}$ of S_{AB} with coefficients c_0 and c_3

Fig. 4.5: Moore-Penrose inverse of matrix S_{AB} for different expansion orders. Black components are zero and the white ones are not zero.

As assumed, the (l, l') behaviour is the same as the one of S_{AB}. See for example $S_{AB}^{\{3\}}$ in Fig. 4.2(d) and ${S_{AB}^{-1}}^{\{3\}}$ in Fig. 4.5(d). In a next step, by knowing which parts contribute to the orders R to R^4 in the energy, any of the inverse matrices ${S_{AB}^{-1}}^{\{i\}}$ can be taken as a template for the matrices $\mathcal{O}_{AB}(R^4)$ and $\tilde{\mathcal{O}}_{AB}(R^4)$ in Fig. 4.4. This was done in Fig. 4.6.

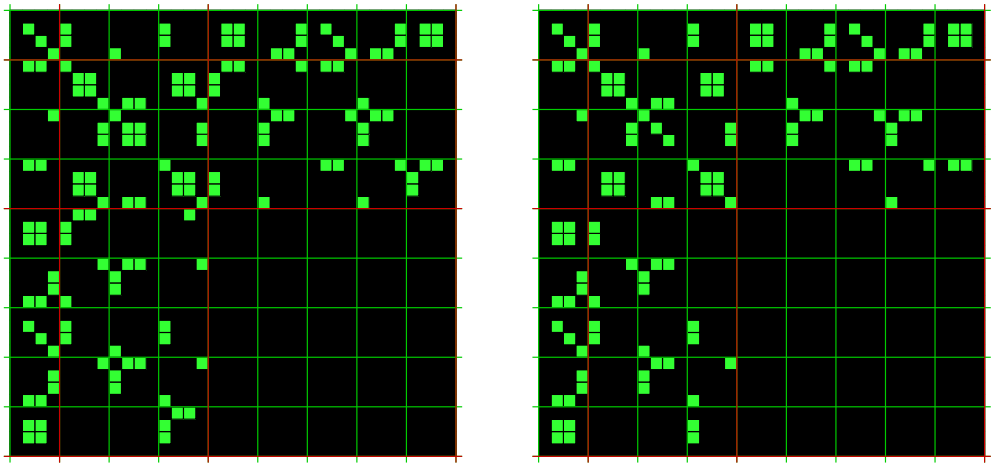

(a) ${S_{AB}^{-1}}^{\{3\}} \cap \mathcal{O}_{AB}(R^4)$ (b) ${S_{AB}^{-1}}^{\{3\}} \cap \tilde{\mathcal{O}}_{AB}(R^4)$

Fig. 4.6: The same plot as Fig. 4.4, but with Fig. 4.5(d) as template.

The blue and red components vanish, even for $\mathcal{O}_{AB}(R^4)$. That means, the sphere geometry (especially the integrals over the sphere surface) cancels out potential R^2 contributions to the energy at the blue points and R^4 at the red points. Of course R^4 can result from green components, too. But the R^4 energy results correctly, if R^3 is correct. However, the leading order in the Casimir energy has to start at R^3.

4.5.6 Casimir energy for a plain plate and a sphere

With the determined propagator matrices, the Casimir energy for a plain plate and a sphere can be calculated. An overview of these matrices can be found in Appendix C. However, it is usefull to implement the propagator expansion of M_{22} in the 1-loop Casimir energy, equation (4.7).

$$E_{\text{Cas}}^{1\text{ loop}} = \frac{\hbar c}{4}\frac{1}{(2\pi)^3}\int_{\Omega''}\int_{\Omega'''}\int_{\underline{p}}\sum_{lml'm'} Y_{lm}(\Omega'')Y^{\star}_{l'm'}(\Omega''') \\ M^{-1}_{11\,\mu\nu}(\underline{p})M^{\nu\rho}_{12}(\underline{p},R,\Omega'')S^{-1}_{lml'm'\,\rho\sigma}(p_0,R,\{c_i\})M^{\sigma\mu}_{21}(R,\Omega''',\underline{p}) \quad (4.48)$$

With this and the corresponding S^{-1}_{AB} from section 4.5.5, the resulting Casimir energy can be obtained to

$$E_{\text{Cas}}^{1\text{ loop}} = -\frac{\hbar c}{\pi H}\sum_{i=1} b_i \left(\frac{R}{H}\right)^i . \quad (4.49)$$

As a checkup, results for this setup obtained by others can be taken from [38]. Their coefficients are:

$$b_1 = 0 \quad b_2 = 0 \quad b_3 = \tfrac{9}{16} \quad b_4 = 0 \quad b_5 = \tfrac{25}{32} \quad . \quad (4.50)$$

In the following two tables, the results for the calculations in this thesis are given. On the one hand, the case of Feynman gauge with and without $\Psi_0 = 0$ gauge was used, and on the other hand, "c_l and L_{max} truncation" was sampled.

Truncation corresponding to c_l

maximal c_l	b_1	b_2	b_3	b_4	b_5
I - no additional gauge					
0	∞	∞	$\frac{11}{40}$	$\frac{3}{20}$	$\frac{1087}{10080}$
1	0	0	∞	0	$\frac{311}{224}$
2	0	0	$\frac{29}{28} \approx 0.54 \cdot \frac{9}{16}$	0	∞
3	0	0	$\frac{7881}{9344} \approx 0.67 \cdot \frac{9}{16}$		
II - $\Psi_0^{\text{plate}} = \Psi_0^{\text{sphere}} = 0$ gauge					
0	∞	∞	$\frac{11}{40}$	$\frac{3}{20}$	$\frac{1087}{10080}$
1	0	0	∞	0	$\frac{13}{7}$
2	0	0	$\frac{17}{32} \approx 0.94 \cdot \frac{9}{16}$	0	∞
3	0	0	$\frac{67}{128} \approx 0.93 \cdot \frac{9}{16}$		

Table 4: Results for the Casimir energy in the plain plate sphere setup. The shown coefficients determine the energy by the use of (4.49).

Truncation corresponding to L_{max}

L_{max}	b_1	b_2	b_3	b_4	b_5
III - no additional gauge					
0	0	0	$\frac{3}{16}$	0	$\frac{3}{16} \approx 0.24 \cdot \frac{25}{32}$
1	0	0	$\frac{9}{16}$	0	$\frac{191}{960} \approx 0.25 \cdot \frac{25}{32}$
2	0	0	$\frac{36043}{31536}$	0	$\frac{7448187949}{2071915200} \approx 4.60 \cdot \frac{25}{32}$
IV - $\Psi_0^{\text{plate}} = \Psi_0^{\text{sphere}} = 0$ gauge					
0	0	0	$\frac{3}{16}$	0	$\frac{3}{16} \approx 0.24 \cdot \frac{25}{32}$
1	0	0	$\frac{9}{16}$	0	$\frac{69848329}{355117455} \approx 0.25 \cdot \frac{25}{32}$
2	0	0	$\frac{9}{16}$	0	$\frac{559}{960} \approx 0.75 \cdot \frac{25}{32}$

Table 5: Results for the Casimir energy in the plain plate sphere setup. The shown coefficients determine the energy by the use of (4.49).

The longitudinal mode corresponding to b_1 and the monopole order corresponding to b_2 vanishes, independent of the chosen gauge or truncation method. They disappear because the integration over the sphere results in zero and in the case without $\Psi_0 = 0$ (case I and III) the coefficients become zero due to the leading R power of S_{AB}^{-1} is 3. In cases I and II with only c_0, b_1 and b_2 are divergent due to some integrals of the form $\int_{p_0} \frac{1}{p_0}$. But this can be explained with the mismatch of M_{12}, M_{22}^{-1} and M_{21} due to the truncation method. The other infinities in these cases appear for the same reason. As it was explained, "L_{max}-truncation" is the better choice.

Because R and R^2 cancels out at last after the sphere surface integration, the 1-loop and 2-loop propagators[20] starts with R^3 and R^6 respectively. This means b_3, b_4 and b_5 are completely determined by one propagation loop. Hence, the correct coefficient $\frac{9}{16}$ at R^3 is found for the "L_{max}-truncation" method. But in case III without $\Psi_0 = 0$ gauge, b_3 is not stable until $L_{max} = 2$ due to off-diagonal interaction terms in the time components of M_{22}^{-1}. In the situation of "c_l-truncation", the right coefficient is not reached, but again setting $\Psi_0 = 0$ gives the better convergence behaviour. In addition, the next coefficient $b_4 = 0$ is found correctly, too. But b_5 does not converge until $L_{max} = 2$, simply because more spherical harmonic orders of M_{22}^{-1} are needed.

Furthermore, these coefficients were calculated for the case of Coulomb gauge, too, to show that setting A_0 to zero leads to a wrong result. In

[20]The 1-loop propagator is $\frac{1}{2}\Delta\mathcal{M}^2 = M_{11}^{-1}M_{12}M_{22}^{-1}M_{21}$, which determines the 1-loop Casimir energy by equation (4.3), and two loops are determined by $\Delta\mathcal{M}^4$.

contrast to the above coefficients, the stable b_i for $A_0 = 0$ gauge are:

$$b_1 = \tfrac{5}{22} \quad b_2 = \tfrac{25}{242} \quad b_3 = \tfrac{355673}{1006236} \ ,$$

and together with $\Psi_0 = 0$ they are:

$$b_1 = \tfrac{5}{22} \quad b_2 = \tfrac{25}{242} \quad b_3 = \tfrac{151808}{251559} \ .$$

Obviously, $A_0 = 0$ gauge is incompatible to $\Psi_0 = 0$, because the b_3 differ from each other. But, of course, this gauge choice is simply wrong. As mentioned, the Weyl gauge is allowed in the QED for the case of pure vacuum, because there is no need of introducing a charge density A_0. Although, there was no input of matter in the setup, the boundary condition leads to a current term in the action (2.27). Thus, the vacuum is no free vacuum anymore and Weyl gauge results in unphysical longitudinal modes in the propagating photon fields, since these modes are not alowed due to the propagator itself is transversal: $M_{22}^{\mu\nu} n_\nu = 0$. Details are explained in section 2.5.

Otherwise, the correct energy up to R^4 was found and becomes stable within $\Psi_0 = 0$ gauge and $L_{max} = 1$ truncation, and the inverse propagator for the sphere in case IV can be given:

Explicit calculation for $L_{max} = 1$ and $\Psi_0 = 0$

After calculating the Moore-Penrose inverse of S_{AB}, truncated at $L_{max} = 1$ in the case of $\Psi_0 = 0$ gauge, the spherical harmonics can be added and the following inverse propagator for the sphere can be obtained:

$$\begin{aligned}
&R^4 \left(M_{22}(p_0, \Omega, \Omega') + \mathcal{O}(Y_{2,m}(\Omega)) + \mathcal{O}(Y^\star_{2,m'}(\Omega')) \right)^{-1} = \qquad (4.51)\\
&- \frac{3R}{8p_0^2\pi} \begin{pmatrix} 0 & 0 & 0 & 0 \\ 0 & 25(c_{\varphi+\Phi} + c_{\varphi-\Phi}) s_\theta s_\Theta - 3 & 25 s_\theta s_\Theta (s_{\varphi+\Phi} - s_{\varphi-\Phi}) & 50 c_\varphi s_\theta c_\Theta \\ 0 & 25 s_\theta s_\Theta (s_{\varphi+\Phi} + s_{\varphi-\Phi}) & 25(-c_{\varphi+\Phi} + c_{\varphi-\Phi}) s_\theta s_\Theta - 3 & 50 s_\varphi s_\theta c_\Theta \\ 0 & 50 c_\Phi c_\theta s_\Theta & 50 s_\Phi c_\theta s_\Theta & 25 c_\theta c_\Theta - 3 \end{pmatrix} \\
&- \frac{R^3}{1120\pi} \left\{ 5 \begin{pmatrix} 0 & 0 & 0 & 0 \\ 0 & (163 c_{\varphi+\Phi} + 37 c_{\varphi-\Phi}) s_\theta s_\Theta & s_\theta s_\Theta (163 s_{\varphi+\Phi} - 37 s_{\varphi-\Phi}) & 0 \\ 0 & s_\theta s_\Theta (163 s_{\varphi+\Phi} + 37 s_{\varphi-\Phi}) & (-163 c_{\varphi+\Phi} + 37 c_{\varphi-\Phi}) s_\theta s_\Theta & 0 \\ 0 & 0 & 0 & -126 c_{\varphi-\Phi} s_\theta s_\Theta \end{pmatrix} \right. \\
&\left. + 2 \begin{pmatrix} 0 & 0 & 0 & 0 \\ 0 & -252 - 315 c_\theta c_\Theta & 0 & 500 c_\varphi s_\theta c_\Theta + 315 c_\Phi c_\theta s_\Theta \\ 0 & 0 & -252 - 315 c_\theta c_\Theta & 500 s_\varphi s_\theta c_\Theta + 315 s_\Phi c_\theta s_\Theta \\ 0 & 500 c_\Phi c_\theta s_\Theta + 315 c_\varphi s_\theta c_\Theta & 500 s_\Phi c_\theta s_\Theta + 315 s_\Phi s_\theta c_\Theta & -252 \end{pmatrix} \right\} \\
&+ \mathcal{O}(R^4) + \mathcal{O}(Y_{2,m}(\Omega)) + \mathcal{O}(Y^\star_{2,m'}(\Omega')) \, .
\end{aligned}$$

(θ, φ) and (Θ, Φ) again are represented by Ω and Ω'. Together with M_{12} from (C.3) in $\Psi_0 = 0$ gauge and the corresponding M_{21}, firstly expanded into small R up to $\mathcal{O}(R^4)$, the sphere surface integrals $\int_\Omega \int_{\Omega'} M_{12} M_{22}^{-1} M_{21} = \int\int M_{12} M_{22}^{-1} M_{21}\, s_\theta d\theta d\varphi\, s_\Theta d\Theta d\Phi$ result in the following matrix.

$$\begin{aligned} M_{12}\Delta\mathcal{M}_{21} &= R^4 \int_\Omega \int_{\Omega'} M_{12}(p_0, p_{||}, \Omega) M_{22}^{-1}(p_0, \Omega, \Omega') M_{21}(p_0, q_{||}, \Omega') \\ &= \frac{\pi R^3}{2|\underline{p}||\underline{q}|} e^{-H(|\underline{p}|+|\underline{q}|)} \begin{pmatrix} 0 & 0 & 0 & 0 \\ 0 & \star_{11} & \star_{12} & 0 \\ 0 & \star_{21} & \star_{22} & 0 \\ 0 & 0 & 0 & 0 \end{pmatrix} \end{aligned} \tag{4.52}$$

$$\begin{aligned} \star_{11} &= \left(p_0^2 + \underline{p}^\mu \underline{q}_\mu + |\underline{p}||\underline{q}|\right)\left(p_0^2 + 2p_2q_2\right) - p_0^2\left(p_2^2 + q_2^2 - p_2q_2\right) \\ \star_{22} &= \left(p_0^2 + \underline{p}^\mu \underline{q}_\mu + |\underline{p}||\underline{q}|\right)\left(p_0^2 + 2p_1q_1\right) - p_0^2\left(p_1^2 + q_1^2 - p_1q_1\right) \\ \star_{12} &= -2\left(p_1p_2\left(p_0^2 + q_1^2\right) + q_1q_2\left(p_0^2 + p_2^2\right)\right) + p_2q_1\left(p_0^2 - 2|\underline{p}||\underline{q}|\right) \\ \star_{21} &= -2\left(p_1p_2\left(p_0^2 + q_2^2\right) + q_1q_2\left(p_0^2 + p_1^2\right)\right) + p_1q_2\left(p_0^2 - 2|\underline{p}||\underline{q}|\right) \end{aligned}$$

The plate momenta (p_1, p_2) of M_{12} and (q_1, q_2) of M_{21} were distinguished for the possibility of calculating more than one loop. But $p_0 = q_0$ can be set due to translation invariancy in time direction. R and R^2 vanished after carrying out the sphere surface integrals. Next, the inverse plate propagator (C.5) is needed to obtain one full loop.

$$\begin{aligned} \frac{1}{2}\Delta\mathcal{M}^2 &= M_{11}^{-1} M_{12}\Delta\mathcal{M}_{21} \\ &= \frac{\pi R^3}{|\underline{p}||\underline{q}|} e^{-H(|\underline{p}|+|\underline{q}|)} \begin{pmatrix} 0 & 0 & 0 & 0 \\ 0 & \star_{11} & \star_{12} & 0 \\ 0 & \star_{21} & \star_{22} & 0 \\ 0 & 0 & 0 & 0 \end{pmatrix} \end{aligned} \tag{4.53}$$

$$\begin{aligned} \star_{11} &= |\underline{p}|(2p_0^2 + p_1q_1 + 2q_2^2) + |\underline{q}|(p_0^2 + 2p_2q_2 + p_1^2) \\ \star_{22} &= |\underline{p}|(2p_0^2 + p_2q_2 + 2q_1^2) + |\underline{q}|(p_0^2 + 2p_1q_1 + p_2^2) \\ \star_{12} &= (p_1 - 2q_1)\left(|\underline{p}|q_2 + |\underline{q}|p_2\right) \\ \star_{21} &= (p_2 - 2q_2)\left(|\underline{p}|q_1 + |\underline{q}|p_1\right) \end{aligned}$$

For the Casimir energy (4.7) up to $\frac{R^3}{H^4}$, only the trace of $\frac{1}{2}\Delta\mathcal{M}^2$ has to be taken and multiplied with $-\frac{1}{2}\hbar c$. The "outside" momenta p and q were set equal due to a delta function resulting from the Fourier transformation of the trace, and a last integration over all remaining momenta has to be done. To be specific, the spherical coordinates

$$\begin{aligned} p_1 &= |\underline{p}| \cos\phi_{\underline{p}} \sin\theta_{\underline{p}} \\ p_2 &= |\underline{p}| \sin\phi_{\underline{p}} \sin\theta_{\underline{p}} \\ p_0 &= |\underline{p}| \cos\theta_{\underline{p}} \\ dp_0 dp_1 dp_2 &= \underline{p}^2 d|\underline{p}| \sin\theta_{\underline{p}} d\theta_{\underline{p}} d\phi_{\underline{p}} \end{aligned} \tag{4.54}$$

lead to solvable integrals.

$$E_{\text{Cas}} = -\frac{\hbar c}{2}\frac{1}{(2\pi)^3}\int_{\underline{p}} \text{tr}\left[\frac{1}{2}\Delta\mathcal{M}^2\right] + \mathcal{O}\left(R^4\right) \tag{4.55}$$

$$= -\frac{\hbar c}{2}\frac{1}{(2\pi)^3}\int 6\pi R^3 \underline{p} e^{-2|\underline{p}|H}\ \underline{p}^2 d\underline{p} \sin\theta_{\underline{p}} d\theta_{\underline{p}} d\phi_{\underline{p}} + \mathcal{O}\left(R^4\right) \tag{4.56}$$

$$= -\frac{9}{16}\frac{\hbar c}{\pi}\frac{R^3}{H^4} + \mathcal{O}\left(\frac{R^4}{H^5}\right) \tag{4.57}$$

This is the correct result and the inverse propagator M_{22}^{-1} for the sphere could be used to obtain $M_{12}M_{22}^{-1}M_{21}$ for a more general configuration like a sphere on top of a corrugated surface in position space. But there are different problems in calculating energy contributions of a higher order or even in inverting bigger matrices S_{AB}^{-1}. Also spherical harmonics up to $L_{max} = 1$ could not possibly suffice to determine the correct energy for arbitrary corrugated surfaces. Thus there is a need of a higher spherical harmonics order of the sphere propagator. In principle, this can be done with the methods described in the last sections. But there exists an easy possibility to simplify this inversion process, where in consequence the whole M_{22}^{-1} can be obtained explicitly up to any order (see section 4.7).

4.6 Rotated Cartesian basis

The idea is the following: The Cartesian basis for the matrices is the most general one and the easiest to implement, but it imposes not all symmetries of the problem. Precisely, it does not fit to the surface of the sphere, where the propagator M_{22} lives. To install this feature, spherical coordinates as matrix basis could be used, but they also impose metric coefficients in the matrix products, which then have to be taken into account at the functional inversion. Thus, a Cartesian basis for each point on the sphere is needed, where for example x_1 and x_2 are tangential to the surface and x_3 always points in the normal direction.

4.6.1 Sphere-sphere propagator explicitly

As already used in the last sections, the surface coordinates are represented in the best way by spherical coordinates.

$$\vec{\Omega} = R \begin{pmatrix} 0 \\ \cos\varphi \sin\theta \\ \sin\varphi \sin\theta \\ \cos\theta \end{pmatrix} = R\vec{n} \qquad \vec{\Omega}' = R \begin{pmatrix} 0 \\ \cos\Phi \sin\Theta \\ \sin\Phi \sin\Theta \\ \cos\Theta \end{pmatrix} = R\vec{n}' \tag{4.58}$$

$\vec{n}$ is the surface normal vector at the point $\vec{\Omega}$, described by the angles $\Omega \equiv (\theta, \phi)$ and the sphere radius R. In this case $|\vec{x}|$ in (4.30) becomes $R\sqrt{2(1-\cos\alpha)}$ and especially $G(p_0, \Omega, \Omega')$ depends only on α, the angle between the two vectors $\vec{\Omega}$ and $\vec{\Omega}'$, $0 \leq \alpha \leq \pi$.

$$\cos\alpha = \cos(\Phi - \varphi)\sin\theta\sin\Theta + \cos\theta\cos\Theta \tag{4.59}$$

$$\sin\alpha = +\sqrt{1-\cos^2\alpha} \tag{4.60}$$

It is usefull to rewrite $\vec{\Omega}$ and $\vec{\Omega}'$ in terms of rotation matrices $\mathcal{R}$, so $\vec{\Omega} = \mathcal{R}_\Omega \vec{e}_z$ and $\vec{\Omega}' = \mathcal{R}_{\Omega'} \vec{e}_z$ with $\mathcal{R}_\Omega = \mathcal{R}_z(\varphi)\mathcal{R}_y(\theta)$. $\mathcal{R}_y$ and $\mathcal{R}_z$ means rotation around the y- and z-axis respectively.

$$\mathcal{R}_y(\theta) = \begin{pmatrix} 1 & 0 & 0 & 0 \\ 0 & \cos\theta & 0 & \sin\theta \\ 0 & 0 & 1 & 0 \\ 0 & -\sin\theta & 0 & \cos\theta \end{pmatrix} \quad \mathcal{R}_z(\varphi) = \begin{pmatrix} 1 & 0 & 0 & 0 \\ 0 & \cos\varphi & -\sin\varphi & 0 \\ 0 & \sin\varphi & \cos\varphi & 0 \\ 0 & 0 & 0 & 1 \end{pmatrix} \tag{4.61}$$

The rotation which connects $\vec{\Omega}$ and $\vec{\Omega}'$ will be named $\mathcal{R}_{\alpha\beta}$, so $\mathcal{R}_{\Omega'} = \mathcal{R}_\Omega \mathcal{R}_{\alpha\beta}$. α again describes the angle between $\vec{\Omega}$ and $\vec{\Omega}'$ and β is the angle describing the

direction of the propagation. The coordinates described by α and β should be chosen in such a way that M_{22} equals its Hermitian transposed with exchange of Ω and Ω'. Therefore, $\mathcal{R}_{\alpha\beta}$ has to satisfy the relation $\mathcal{R}_{\alpha\beta} = \mathcal{R}_{\alpha\beta}^T$. A definition, which solves this problem, is $\mathcal{R}_{\alpha\beta} = \mathcal{R}_z(\beta)\mathcal{R}_y(\alpha)\mathcal{R}_z(\pi - \beta)$. With this $\mathcal{R}_{\alpha\beta}^T = \mathcal{R}_z(\beta - \pi)\mathcal{R}_y(-\alpha)\mathcal{R}_z(-\beta)$ and hence is the same as $\mathcal{R}_z(\beta)\mathcal{R}_z(\pi)\mathcal{R}_y(-\alpha)\mathcal{R}_z(-\beta) = \mathcal{R}_z(\beta)\mathcal{R}_y(\alpha)\mathcal{R}_z(\pi)\mathcal{R}_z(-\beta) = \mathcal{R}_{\alpha\beta}$. With this, β can be calculated as a function of Ω and Ω'.

$$\cos\beta = \frac{\cos\theta\sin\Theta\cos(\Phi-\varphi) - \sin\theta\cos\Theta}{\sin\alpha} \tag{4.62}$$

$$\sin\beta = \frac{\sin(\Phi-\varphi)\sin\Theta}{\sin\alpha} \tag{4.63}$$

Equipped with this system of rotation matrices, M_{22} can be simplified in such a way that it can be written out explicitly. For example, by rotating the coordinate system at the points $\vec{\Omega}$ and $\vec{\Omega}'$ with the use of $R_\Omega^T M_{22} R_{\Omega'}$, the local z-axis points in normal direction (see Fig. 4.7).

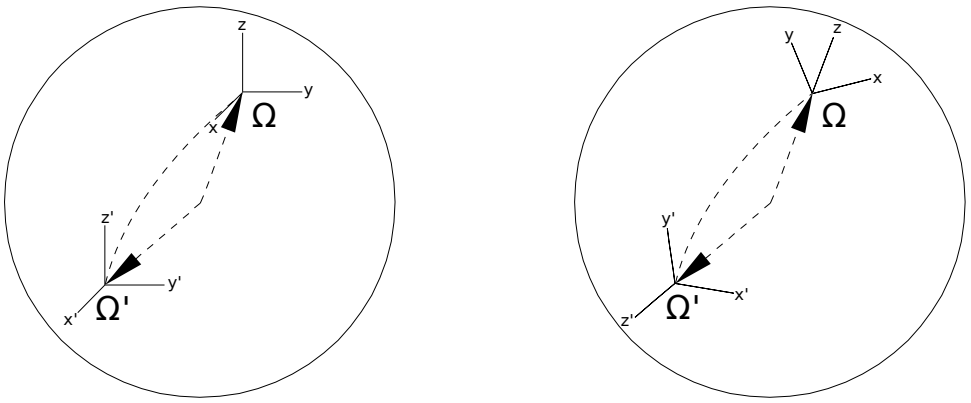

(a) M_{22} (b) $R_\Omega^T M_{22} R_{\Omega'}$

Fig. 4.7: Matrix axes of M_{22} rotated by different rotation matrices

$$R_\Omega^T M_{22} R_{\Omega'} = G(p_0, R, c_\alpha)p_0^2\times \tag{4.64}$$

$$\begin{pmatrix} \frac{2R^2p_0^2s_\alpha^2+(3-c_\alpha)\left(1+R|p_0|\sqrt{2(1-c_\alpha)}\right)}{4R^2p_0^2(1-c_\alpha)} & \frac{-is_\alpha c_\beta\left(R|p_0|\sqrt{2(1-c_\alpha)}+1\right)}{2Rp_0(1-c_\alpha)} & \frac{-is_\alpha s_\beta\left(R|p_0|\sqrt{2(1-c_\alpha)}+1\right)}{2Rp_0(1-c_\alpha)} & 0 \\ \frac{is_\alpha c_\beta\left(R|p_0|\sqrt{2(1-c_\alpha)}+1\right)}{2Rp_0(1-c_\alpha)} & \star_{11} & \star_{21} & 0 \\ \frac{is_\alpha s_\beta\left(R|p_0|\sqrt{2(1-c_\alpha)}+1\right)}{2Rp_0(1-c_\alpha)} & \star_{12} & \star_{22} & 0 \\ 0 & 0 & 0 & 0 \end{pmatrix}$$

$$\star_{11} = \frac{(2p_0^2R^2s_\beta^2c_\alpha^2-((-8p_0^2R^2+1)c_\beta^2-1+4p_0^2R^2)c_\alpha-(6p_0^2R^2+5)c_\beta^2+3+2p_0^2R^2)\sqrt{2(1-c_\alpha)}-2p_0(1-c_\alpha)(s_\beta^2c_\alpha+5c_\beta^2-3)R}{4\sqrt{2(1-c_\alpha)}(1-c_\alpha)R^2p_0^2}$$

$$\star_{22} = \frac{((2p_0^2R^2c_\alpha^2+(1-8p_0^2R^2)c_\alpha+5+6p_0^2R^2)c\beta^2-2+4p_0^2c_\alpha R^2-4p_0^2R^2)\sqrt{2(1-c_\alpha)}+2R(1-c_\alpha)p_0((c_\alpha+5)c_\beta^2-2)}{4\sqrt{2(1-c_\alpha)}(1-c_\alpha)R^2p_0^2}$$

$$\star_{12} = \star_{21} = \frac{((-2p_0^2R^2c_\alpha^2+(8p_0^2R^2-1)c_\alpha-6p_0^2R^2-5)\sqrt{2(1-c_\alpha)}-2p_0R(c_\alpha+5)(1-c_\alpha))c_\beta s_\beta}{4\sqrt{2(1-c_\alpha)}(1-c_\alpha)R^2p_0^2}$$

The new z-components in the matrix are zero, which means, there is no propagation leaving the surface. It was mentioned that β represents a direction on the sphere. That can be easily seen by a second rotation around the new z-axis in such a way, that the x-axis points in the direct direction to the other point.

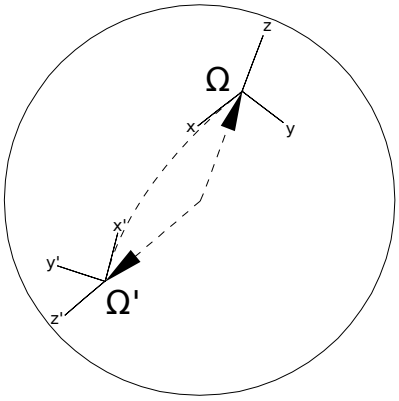

Fig. 4.8: Matrix axes of M_{22} rotated by $R_z^T(\beta)R_\Omega^TM_{22}R_{\Omega'}R_z(\beta)$

In this case, M_{22} becomes independent of β, because the physics in this setup only depends on the distance between the two points.

$$R_z^T(\beta)R_\Omega^TM_{22}R_{\Omega'}R_z(\beta) = G(p_0,R,c_\alpha)p_0^2\times \tag{4.65}$$

$$\begin{pmatrix} \frac{2R^2p_0^2s_\alpha^2+(3-c_\alpha)\left(1+R|p_0|\sqrt{2(1-c_\alpha)}\right)}{4R^2p_0^2(1-c_\alpha)} & \frac{-is_\alpha\left(R|p_0|\sqrt{2(1-c_\alpha)}+1\right)}{2Rp_0(1-c_\alpha)} & 0 & 0 \\ \frac{is_\alpha\left(R|p_0|\sqrt{2(1-c_\alpha)}+1\right)}{2Rp_0(1-c_\alpha)} & \star_{11} & 0 & 0 \\ 0 & 0 & \star_{22} & 0 \\ 0 & 0 & 0 & 0 \end{pmatrix}$$

$$\star_{11} = \frac{1}{2R^2p_0^2(1-c_\alpha)} + \frac{1}{R|p_0|\sqrt{2(1-c_\alpha)}} + 1$$

$$\star_{22} = \frac{1}{4}\frac{2R|p_0|(1-c_\alpha)(3+c_\alpha)+\sqrt{2(1-c_\alpha)}(2R^2p_0^2(1+c_\alpha^2)+(1-4p_0^2R^2)c_\alpha+3)}{R^2p_0^2(1-c_\alpha)\sqrt{2(1-c_\alpha)}}$$

To calculate the Casimir energy in a setup with a sphere, the functional inverse of the corresponding propagator matrix M_{22} for the auxiliary fields Ψ on the surface is needed. Thus, one could say, (4.65) only depends on $\cos\alpha$ and therefore could be expanded into Legendre polynomials $P_l(\cos\alpha)$ to get the inverse M_{22}^{-1}. Therefore, (4.65) has to be multiplied with $P_l(\cos\alpha)$ and the integral over $\cos\alpha$ leads to the expansion coefficient, analogue to the way it was done in the scalar case [31]. Afterwards, every $P_l(\cos\alpha)$ can be replaced with spherical harmonics $\frac{4\pi}{2l+1}\sum_{m=-l..l} Y_{lm}(\Omega)Y^{\star}_{lm}(\Omega')$ and the expansion of M_{22} into spherical harmonics would be obtained. With the time-time and the space-space components of (4.65), this can be done. But the integrals at the time-space component diverge due to an integral of the type $\int_0^1 \frac{1}{x}dx$. The reason for this is, in the end, a mistake in the assumption itself.

The inverse is defined in equation (D.1):

$$\int_\Omega M_{22}^{-1}(\Omega',\Omega)M_{22}(\Omega,\Omega'') = \mathbb{1}\delta(\Omega'-\Omega'')\,. \tag{4.66}$$

Next, arbitrary rotation matrices like $R_{\Omega''}$ and $R_{\Omega'}$ can be attached to (4.66), which do not depend on the integrand Ω. In addition, in-between M_{22}^{-1} and M_{22}, a representation of $\mathbb{1}$ like for example $R_\Omega R_\Omega^\dagger$ can be inserted. But the transformation used in (4.65) is not allowed, because $R_z(\beta)$ intrinsically depends on both points Ω and Ω', and the integration in (D.1) has to be done over one of these points. The best transformation which is allowed to be done is (4.64).

4.6.2 Sphere-sphere propagator expanded into spherical harmonics

With the transformation $R_\Omega^T M_{22} R_{\Omega'} \to \tilde{M}_{22}$, equation (4.66) becomes:

$$\int_\Omega \tilde{M}_{22}^{-1}(\Omega',\Omega)\tilde{M}_{22}(\Omega,\Omega'') = \mathbb{1}\delta(\Omega'-\Omega'')\,. \tag{4.67}$$

Together with the expansion method described in chapter 4.5.2, this transformation can be translated into a transformation of the boundary conditions including operator $\mathcal{T}$ (4.36): $\mathcal{T}(\Omega) = R_\Omega\tilde{\mathcal{T}}(\Omega)$. $\tilde{T}_{lm}$ can be obtained by calculating the action of $\mathcal{T}$ on a given spherical harmonic $Y_{lm}(\Omega)$, and then multiplying it with R_Ω. This $\tilde{T}_{lm}$ has to be expanded into spherical harmonics a second time to follow the formalism in chapter 4.5.2 and furthermore to get the expansion $\tilde{S}_{AB}$ of $\tilde{M}_{22}$.

This procedure was applied to the transformed $\tilde{M}_{22}$ in (4.64). A plot of the resulting coefficient matrix $\tilde{S}_{AB}$ is shown in figure Fig. 4.9.

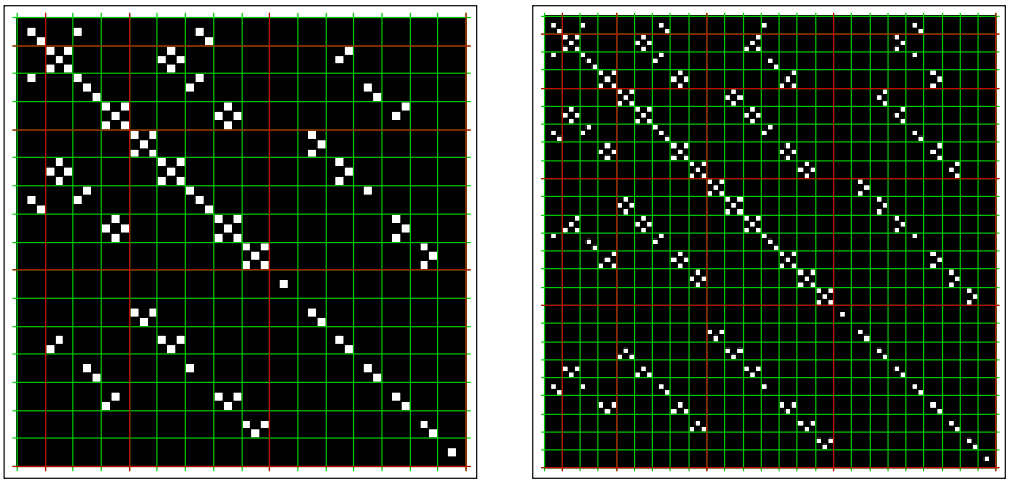

(a) $\tilde{S}_{AB}$ with coefficients c_0 to c_2 (b) $\tilde{S}_{AB}$ with coefficients c_0 to c_3

Fig. 4.9: Matrix $\tilde{S}_{AB}$ for different expansion orders, black means zero and white non-zero

These matrices now consist of 3×3 submatrices corresponding to the space time indices. The radial component is zero and therefore not plotted here. But as it can be seen, this matrix is not diagonal and there is no chance to obtain the exact inverse for a given subspace. In addition, the c_l are placed everywhere between Y_{00} and Y_{ll}. Thus, with the use of more and more coefficients, the inverse changes everytime in every component. This inflation is caused to the fact that the normalised tangential vectors of the surface, which come into play at the second expansion of $\tilde{T}_{lm}$, are not expandable into a finite number of spherical harmonics. Therefore, this way was not assumed to work right. Otherwise, if an orthonormal basis would be found which fulfils the above explained requirements, this scheme could be a possible method to calculate the Casimir energy, too.

4.7 Vector spherical basis

Until now, all matrix expansions were done in Cartesian coordinates. A change of the coordinate axes in a way that they lie on the surface is possible, but does not result in some well behaved propagator matrices. However, in the case of a sphere, a change of the functional basis $Y_{lm} \to \mathcal{V}_{lm}$ can be done, too. The $\mathcal{V}_{lm}$ are vector spherical harmonics or vector multipoles, which are orthonormalized vector functions for the scalar product of the space $L_1^2(S^2)$. One possible definition can be found in the article [39], equation (24a - 24c), in the case of a sphere with radius R and normal vector $\vec{n}$.

$$\mathfrak{E}^T_{lm} = \mathcal{V}^1_{lm} = \gamma_l^{-1} R\vec{\nabla} Y_{lm} \tag{4.68}$$

$$\mathfrak{M}^T_{lm} = \mathcal{V}^2_{lm} = \gamma_l^{-1} \vec{\mathcal{L}} Y_{lm} \tag{4.69}$$

$$\mathfrak{E}^L_{lm} = \mathcal{V}^3_{lm} = \vec{n} Y_{lm} \tag{4.70}$$

They satisfy the orthogonality relation $\int\limits_\Omega \mathcal{V}^{\star\, si}_{lm}(\Omega)\mathcal{V}^{s'}_{i\,l'm'}(\Omega) = \delta^{ss'}\delta_{ll'}\delta_{mm'}$, whereby the space indices $i = 1\ldots 3$ has to be summed up. s and s' label the sort of the vector multipoles and γ_l is a normalisation constant by construction.

$$\gamma_l = \sqrt{l(l+1)} \tag{4.71}$$

Within this definition, they are called transverse electric $\mathfrak{E}^T_{lm}$, transverse magnetic $\mathfrak{M}^T_{lm}$ and longitudinal electric $\mathfrak{E}^L_{lm}$ modes respectively.

But in this work, the matrices are of the dimension 4×4. Thus, a fourth orthonormal vector multipole has to be found. This one is

$$\mathcal{V}^0_{lm} = e_t Y_{lm}\,. \tag{4.72}$$

With $\mathcal{V}^0_{lm}$ the four vector spherical harmonics are optimised for a 3D sphere surface S^2 in a 4D spacetime, which all satisfy the orthogonality relation

$$\int_\Omega \mathcal{V}^{\star\, s\mu}_{lm}(\Omega)\mathcal{V}^{s'}_{\mu\, l'm'}(\Omega) = \delta^{ss'}\delta_{ll'}\delta_{mm'}\,. \tag{4.73}$$

Now s, s' and μ count from 0 to 3.

Because these harmonics fit well into the setup, M_{22}, which expanded into them, may have coefficients that do not depend on m and which are diagonal in l ($l' = l$). Thus, a method analogue to the scalar case [31] could be used to expand $M^{\mu\nu}_{22}(R\vec{n} - R\vec{n}')$ into the "tensorial Legendre Functions"

$$\mathcal{P}^{ss'\,\mu\nu}_l(\vec{n} - \vec{n}') = \frac{4\pi}{2l+1}\sum_m \mathcal{V}^{s\,\mu}_{lm}(\vec{n})\mathcal{V}^{\star\, s'\,\nu}_{lm}(\vec{n}')\,. \tag{4.74}$$

These functions are the generalisation of the Legendre Functions in the sense of changing scalar fields to vector fields or $Y_{lm} \to \mathcal{V}^{s\mu}_{lm}$. As it will turn out, this assumption is correct. But without a proof, M_{22} still has to be expanded into vector multipoles.

4.7.1 Propagator invertion with vector spherical basis

At first, the expansion into vector multipoles has to result in a matrix coefficient, which can be inverted afterwards. Thus, the representations

$$M_{22}^{\mu\nu}(p_0,\Omega,\Omega') = \sum_{\substack{l=0\dots\infty \\ m=-l\dots l \\ l'=0\dots\infty \\ m'=-l'\dots l'}} \mathcal{V}^{s\mu}_{lm}(\Omega) C_{ss'\,lm\,l'm'} \mathcal{V}^{\star\,s'\nu}_{l'm'}(\Omega') \tag{4.75}$$

$$= \mathcal{V}^{A\mu}(\Omega) C_{AB} \mathcal{V}^{\star\,B\nu}(\Omega') \tag{4.76}$$

and

$$M_{22}^{-1\,\mu\nu}(p_0,\Omega,\Omega') = \mathcal{V}^{A\mu}(\Omega) B_{AB} \mathcal{V}^{\star\,B\nu}(\Omega') \tag{4.77}$$

are assumed to be analogous to (4.32). Again, Ω and Ω' represent the angles of the two points on the sphere. $C^{ss'}_{lm\,l'm'}$ corresponds to the object $S^{\mu\nu}_{lm\,l'm'}$ from section 4.5.2 and therefore has the same superindex notation C_{AB}. This time, such a superindex combines s, l and m to a capital letter A. Afterwards, the inversion can be done by inverting the coefficient matrix C_{AB} due to the relation

$$\begin{aligned}
\delta(\vec{\Omega}-\vec{\Omega}')\mathbb{1}^{\mu\kappa}_{\text{sphere}} =& R^4 \int_{\Omega'} M_{22}^{-1\,\mu}{}_{\nu}(\Omega,\Omega') M_{22}^{\nu\kappa}(\Omega',\Omega'') \\
=& R^4 \mathcal{V}^{A\mu}(\Omega) B_{AB} \underbrace{\int_{\Omega'} \mathcal{V}^{\star\,B}{}_{\nu}(\Omega') \mathcal{V}^{C\nu}(\Omega')}_{=\delta^{BC}} C_{CD} \mathcal{V}^{\star\,D\kappa}(\Omega'') \qquad (4.78) \\
=& \mathcal{V}^{A\mu}(\Omega) R^4 B_{AB} C^{B}{}_{D} \mathcal{V}^{\star\,D\kappa}(\Omega'')\,. \qquad (4.79)
\end{aligned}$$

The left hand side can be replaced by $\tilde{\mathbb{1}}_{ss''} \sum_{lm} \mathcal{V}^{s\mu}_{lm} \mathcal{V}^{\star\,s''\kappa}_{lm}$, where the $\tilde{\mathbb{1}}$ has a zero on the sort indices $s = s' = 3$ for no longitudinal electric modes $\mathfrak{E}^L$. The propagator actually has rank 2 and therefore a diagonalisation of the coefficient matrix results in a second zero. For example in $\Psi_0 = 0$ gauge, this zero lies on the $s = 0$ axis. But, again, this problem can be avoided by using the Moore-Penrose inverse, because due to the definition (4.76) C_{AB} has to be Hermitian. Thus, only the inversion of C_{AB} has to be done to obtain B_{AB}:

$$B_{AB} = \frac{C^{-1}_{AB}}{R^4}\,. \tag{4.80}$$

4.7.2 Sphere-sphere propagator expanded into vector spherical basis

The following task is to expand the propagator matrix M_{22} for a sphere into vector spherical harmonics. Using the orthogonality relation (4.73) and (4.75), the coefficient C can be obtained by

$$C^{ss'}_{lm\,l'm'} = \int_{\Omega,\Omega'} \mathcal{V}^{\star s}_{lm\mu}(\Omega) M^{\mu\nu}_{22}(\Omega,\Omega') \mathcal{V}^{s'}_{l'm'\nu}(\Omega')\,. \tag{4.81}$$

This direct expansion is not such an easy task as it was in chapter (4.5.2) with S_{AB}. But again, the following representation (4.38) of M_{22} can be used:

$$M^{\mu\nu}_{22}(p_0,\Omega,\Omega') = \sum_{lm} T^{\mu\beta}_{lm}(p_0,R,\Omega) c_l(p_0,R) T^{\dagger\nu}_{\beta\,lm}(p_0,R,\Omega')\,. \tag{4.82}$$

Here $T^{\mu\beta}_{lm}$ is $\mathcal{T}^{\mu\beta}Y_{lm}$, whereby the $\mathcal{T}$ is the operator in (4.36), which can be written in the following compact form:

$$\mathcal{T} = \frac{1}{R}\begin{pmatrix} 0 & \vec{\mathcal{L}}^T \\ -\vec{\mathcal{L}} & p_0(\vec{e}_i \times \vec{x})^T \end{pmatrix} \tag{4.83}$$

The $\vec{e}_i \times \vec{x}$ symbolises the cross product between the unit vector in Cartesian coordinates $\vec{e}_i$ and $\vec{x}$. It has to be read in the following way: $T^{ij} = \frac{p_0}{R}\epsilon^{ijk}x_k$. Again, the green circled angular momentum operator $\vec{\mathcal{L}} = -i\vec{x} \times \vec{\nabla}$ has to be set to zero in the case of $\Psi_0 = 0$ gauge, and $\vec{x}$ is $R\vec{n}$. Inserting (4.82) into (4.81) leads to integrals of the kind

$$t^{s\beta}_{lm\,l'm'} = \int_{\Omega} \mathcal{V}^{\star s}_{lm\mu}(\Omega) T^{\mu\beta}_{l'm'}(\Omega)\,. \tag{4.84}$$

Afterwards C can be obtained through

$$C^{ss''}_{lm\,l''m''} = \sum_{l'm'} t^{s\beta}_{lm\,l'm'} c_{l'} t^{\star s''}_{l'm'\,l''m''\,\beta}\,. \tag{4.85}$$

The summation over l' goes in principle from 0 to ∞ and m' runs from $-l'$ to l', but as it turns out, there are only at most three possibilities for l' for a given l or l'', where the summand is not zero. Thus, the $t^{s\beta}_{lm\,l'm'}$ matrix can be calculated, component by component.

For $\beta = 0$, this is an easy task, because in this case $T^{\mu 0}_{l'm'} = -R^{-1}\vec{\mathcal{L}}Y_{l'm'}$ $= -R^{-1}\gamma_{l'}\mathcal{V}^{2\mu}_{l'm'}$ and the integral (4.84) gives

$$t^{s0}_{lm\,l'm'} = -R^{-1}\gamma_{l'}\delta^{s2}\delta_{ll'}\delta_{mm'}\,. \tag{4.86}$$

In the other cases, where β is a spacelike i, different integrals for each s has to be carried out.

In the case of $s = 0$, the integral

$$t^{0i}_{lm\,l'm'} = R^{-1}\int Y^{\star}_{lm}\mathcal{L}^i Y_{l'm'} \tag{4.87}$$

has to be solved. This can be done by using the decomposition of $\vec{\mathcal{L}}Y_{lm}$ into Y_{lm} with the coefficients of (4.41) and (4.42).

The next component is $s = 1$, where the integral $\int\gamma_l^{-1}(\vec{\nabla}Y_{lm})^{\star}p_0(\vec{e}_i\times\vec{x})Y_{l'm'}$ has to be calculated. The cross product can be permutated to $\gamma_l^{-1}p_0\int(\vec{x}\times\vec{\nabla}Y_{lm})^{\star}\vec{e}_iY_{l'm'}$, thus an angular momentum operator appears, which acts on $Y^{\star}_{lm}$. Therefore, this component becomes

$$t^{1i}_{lm\,l'm'} = -ip_0\gamma_l^{-1}\int(\mathcal{L}^iY_{lm})^{\star}Y_{l'm'}\,, \tag{4.88}$$

which is the same as $-ip_0R\gamma_l^{-1}(-1)^{m+m'}t^{0i}_{l',-m',l,-m}$. Because of this symmetry, the coefficients later obtain rank 2 and not 3. $\Psi_0 = 0$ gauge, of course, easily sets $t^{0i}_{l'm'\,lm}$ to zero.

By going further with $s = 2$, the integral $\int\gamma_l^{-1}p_0(\vec{\mathcal{L}}Y_{lm})^{\star}(\vec{e}_i\times\vec{x})Y_{l'm'}$ has to be solved. The cross product can be permutated between $\vec{x}$ and $\vec{\mathcal{L}}$ and a term $\vec{x}\times(\vec{x}\times\vec{\nabla})$ arises. This one is the same as $(\vec{x}\vec{x})\vec{\nabla} - \vec{x}(\vec{x}\vec{\nabla})$ and hence can be simplified to $R^2\vec{\nabla}$. The second term is zero, because it vanishes under the integral:

$$\int\underbrace{\vec{x}}_{\propto\vec{n}}(\underbrace{\vec{x}}_{\propto\vec{n}}\underbrace{\vec{\nabla}Y_{lm}}_{\propto\mathfrak{E}^T_{lm}})^{\star}Y_{l'm'}\propto\int\underbrace{\vec{n}Y_{l'm'}}_{\propto Y_{l'\pm1,m'+m''}}(\vec{n}\mathfrak{E}^{T\star}_{lm})\propto\int\underbrace{\vec{n}Y_{l'\pm1,m'+m''}}_{\propto\mathfrak{E}^L_{l'\pm1,m'+m''}}\mathfrak{E}^{T\star}_{lm}. \tag{4.89}$$

This integral vanishes due to the orthogonality relation (4.73). Therefore, the first term above is left and t^{2i} becomes

$$t^{2i}_{lm\,l'm'} = -ip_0\gamma_l^{-1}\int(R\nabla^iY_{lm})^{\star}Y_{l'm'}\,. \tag{4.90}$$

To solve this integral, again, the paper [37] can be used. There, the authors give the action of $\vec{\nabla}$ on a spherical harmonic in form of Wigner 3j symbols

$$\begin{aligned} R\nabla_{\tilde{\mu}} Y_{l,m} =&(-1)^{l+m+\tilde{\mu}} \left[l\sqrt{l+1} \begin{pmatrix} l & 1 & l+1 \\ m & \tilde{\mu} & -m-\tilde{\mu} \end{pmatrix} Y_{l+1,m+\tilde{\mu}} \right. \\ &\left. +(l+1)\sqrt{l} \begin{pmatrix} l & 1 & l-1 \\ m & \tilde{\mu} & -m-\tilde{\mu} \end{pmatrix} Y_{l-1,m+\tilde{\mu}} \right] , \end{aligned} \tag{4.91}$$

with $\tilde{\mu}$ being the spherical tensor component index counting from -1 to 1.

$$\nabla_{\pm 1} = \mp \frac{1}{\sqrt{2}} (\nabla_x \pm i\nabla_y) \tag{4.92}$$

$$\nabla_0 = \nabla_z \tag{4.93}$$

These $3j$ symbols are already known from (4.43) and hence (4.91) becomes

$$\begin{aligned} R\nabla_{\pm 1} Y_{l,m} =& - l\sqrt{\frac{(l \pm m + 1)(l \pm m + 2)}{2(2l+3)(2l+1)}} Y_{l+1,m\pm 1} \\ &- (l+1)\sqrt{\frac{(l \mp m - 1)(l \mp m)}{2(2l+1)(2l-1)}} Y_{l-1,m\pm 1} \end{aligned} \tag{4.94}$$

$$\begin{aligned} R\nabla_0 Y_{l,m} =& - l\sqrt{\frac{(l-m+1)(l+m+1)}{(2l+3)(2l+1)}} Y_{l+1,m} \\ &+ (l+1)\sqrt{\frac{(l+m)(l-m)}{(2l+1)(2l-1)}} Y_{l-1,m} \,. \end{aligned} \tag{4.95}$$

With this, the integral (4.90) and consequently $t^{2i}_{lm\,l'm'}$ can be obtained.

In the last component $s = 3$, the integral of a longitudinal electric mode $\mathfrak{E}^L$ with something tangential to the surface has to be determined: $\int p_0 R^{-1} (\vec{x} Y_{lm})^\star (\vec{e}_i \times \vec{x}) Y_{l'm'}$. Therefore it is zero and

$$t^{3i}_{lm\,l'm'} = 0 \,. \tag{4.96}$$

In the end, $t^{s\beta}_{lm\,l'm'}$ at most connects a given l with $l' = l-1, l, l+1$ and equation (4.85) can be written as

$$C^{ss''}_{lm\,l''m''} = \sum_{l'=\max(0,l-1)}^{l+1} \sum_{m'} t^{s\beta}_{lm\,l'm'} c_{l'} t^{\star s''}_{l'm'\,l''m''\,\beta} \,. \tag{4.97}$$

But that means C_{AB} has a band structure with $|l-l'| \leq 2$ like in the Cartesian case and additional zero rows and columns for the longitudinal electric modes like in the rotated Cartesian case. Calculating C_{AB} now gives the surprising result shown in the following figure Fig. 4.10.

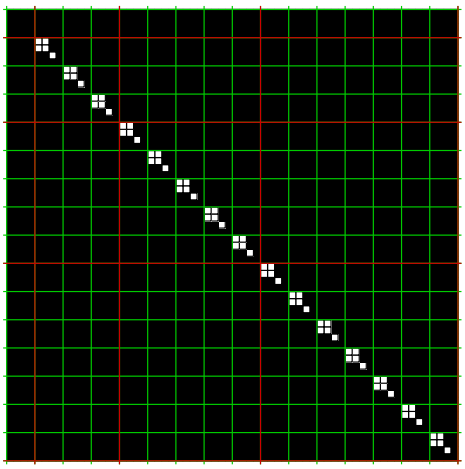

Fig. 4.10: Expansion of M_{22} into the coefficient matrix C_{AB} with the truncation $L_{max} = 3$.

The matrix $C^{ss'}_{lm\,l'm'}$ is diagonal in the sense of $\delta_{ll'}$ and $\delta_{mm'}$, which means the coefficients in (4.97) cancel within. Additionally, every $C^{ss'}_{lm\,l'm'} = C^{ss'}_{lm}\delta^l_{l'}\delta^m_{m'}$ is the same for a given l, does not depend on m, and therefore can be rewritten as $C^{ss'}_l = C^{ss'}_{lm}$. This was tested by the above expansion scheme up to $L_{max} = 7$. So M_{22} can be decomposed into above tensorial Legendre Functions (4.74).

$$M^{\mu\nu}_{22}(\vec{x} - \vec{x}') = \frac{2l+1}{4\pi} C_{ss'l} \mathcal{P}^{ss'\,\mu\nu}_l(\vec{n} - \vec{n}') \tag{4.98}$$

$$M^{-1\,\mu\nu}_{22}(\vec{x} - \vec{x}') = \frac{1}{R^4}\frac{2l+1}{4\pi} C^{-1}_{ss'l} \mathcal{P}^{ss'\,\mu\nu}_l(\vec{n} - \vec{n}') \tag{4.99}$$

This behaviour can be assumed to be a feature of a more general class of functions. Hence, whenever a propagator matrix depending on the difference of two points living on a sphere has to be expanded in some functional basis, there should exist a system of Tensor Legendre Functions in which the propagator becomes diagonal. But this is only an assumption and not prooven. Back to $C^{ss'}_l$:

Monopole order $l = 0$ is cancelled out completely, as it can be seen in

Fig. 4.10. The fourth component is zero which responds to no longitudinal electric modes.

Also, the summation (4.97) seems to be not easy, *Maple 11* is able to give an explicit sum formula for the diagonal components, which can be simplified afterwards. From this one, the coefficient matrices for $l \geq 1$ can be calculated by

$$C_l^{ss'} = \begin{pmatrix} \frac{l(l+1)c_l}{R^2} & \frac{i\sqrt{l(l+1)}c_l p_0}{R} & 0 & 0 \\ -\frac{i\sqrt{l(l+1)}c_l p_0}{R} & p_0^2 c_l & 0 & 0 \\ 0 & 0 & \frac{p_0^2((l+1)c_{l-1}+lc_{l+1})}{2l+1} + \frac{l(l+1)c_l}{R^2} & 0 \\ 0 & 0 & 0 & 0 \end{pmatrix}. \quad (4.100)$$

The first coefficients are the following:

$$C_0^{ss'} = 0 \quad (4.101)$$

$$C_1^{ss'} = \begin{pmatrix} \frac{2c_1}{R^2} & \frac{i\sqrt{2}c_1 p_0}{R} & 0 & 0 \\ -\frac{i\sqrt{2}c_1 p_0}{R} & p_0^2 c_1 & 0 & 0 \\ 0 & 0 & \frac{2p_0^2 c_0 R^2 + 6c_1 + p_0^2 c_2 R^2}{3R^2} & 0 \\ 0 & 0 & 0 & 0 \end{pmatrix} \quad (4.102)$$

$$C_2^{ss'} = \begin{pmatrix} \frac{6c_2}{R^2} & \frac{i\sqrt{6}c_2 p_0}{R} & 0 & 0 \\ -\frac{i\sqrt{6}c_2 p_0}{R} & p_0^2 c_2 & 0 & 0 \\ 0 & 0 & \frac{3p_0^2 c_1 R^2 + 30c_2 + 2p_0^2 c_3 R^2}{5R^2} & 0 \\ 0 & 0 & 0 & 0 \end{pmatrix} \quad (4.103)$$

$$C_3^{ss'} = \begin{pmatrix} \frac{12c_3}{R^2} & \frac{i2\sqrt{3}c_3 p_0}{R} & 0 & 0 \\ -\frac{i2\sqrt{3}c_3 p_0}{R} & p_0^2 c_3 & 0 & 0 \\ 0 & 0 & \frac{4p_0^2 c_2 R^2 + 84c_3 + 3p_0^2 c_4 R^2}{7R^2} & 0 \\ 0 & 0 & 0 & 0 \end{pmatrix}. \quad (4.104)$$

This matrix $C^{ss'}$ is an analogy to (4.65). In (4.65), $M_{22}(\Omega, \Omega')$ was rotated in the way that the new x-axis local to the point Ω faces in the direct direction to Ω'. The z-axis points in normal direction and the y-axis is orthogonal to x and z. Here, the same result is received by using the $\vec{\nabla}$ "direction" as x-, $\vec{n}$ as z- and $\vec{\mathcal{L}}$ as y-axis, because $\vec{\nabla}$ gives something like a flow direction from one point to the other.

By knowing C up to any order, the inverse coefficient can be calculated, too. For the case of only Feynman gauge, this is

$$C_l^{-1\,ss'} = \begin{pmatrix} \frac{R^2 l(l+1)}{c_l(p_0^2R^2+l(l+1))^2} & \frac{i\sqrt{l(l+1)}R^3p_0}{c_l(p_0^2R^2+l(l+1))^2} & 0 & 0 \\ -\frac{i\sqrt{l(l+1)}(\underline{p})R^3p_0}{c_l(p_0^2R^2+l(l+1))^2} & \frac{R^4p_0^2}{c_l(p_0^2R^2+l(l+1))^2} & 0 & 0 \\ 0 & 0 & \frac{R^2(2l+1)}{l(l+1)(2l+1)c_l+R^2p_0^2((l+1)c_{l-1}+lc_{l+1})} & 0 \\ 0 & 0 & 0 & 0 \end{pmatrix} \quad (4.105)$$

and with an additional $\Psi_0 = 0$ gauge, it simplifies to

$$C_l^{-1\,ss'} = \begin{pmatrix} 0 & 0 & 0 & 0 \\ 0 & \frac{1}{p_0^2c_1} & 0 & 0 \\ 0 & 0 & \frac{R^2(2l+1)}{l(l+1)(2l+1)c_l+R^2p_0^2((l+1)c_{l-1}+lc_{l+1})} & 0 \\ 0 & 0 & 0 & 0 \end{pmatrix}. \quad (4.106)$$

The c_l are known to start at R^{-1} in a series expansion for small R. Consequently, all $C_l^{-1\,ss'}$ with $\Psi_0 = 0$ start in component $(1,1)$ at R and in component $(2,2)$ they start at R^3. But the $C_l^{-1\,ss'}$ without this gauge all have R^3 as their lowest contribution. By consideration of M_{12} and M_{21}, the energy has to start at least at R^3, because it does not depend on the chosen gauge.

4.7.3 Casimir energy for a plain plate and a sphere

With the new basis (4.68) to (4.72), the Casimir energy for a plain plate and a sphere can be simply calculated also for higher orders than only R^4. But at first, it is useful to implement the propagator expansion (4.99) into the equation for the 1-loop propagator $\frac{1}{2}\Delta\mathcal{M}^2(p_0, p_{||}, q_{||}) = \Delta\mathcal{M}_{12}\Delta\mathcal{M}_{21}$ and the energy. Altogether,

$$\frac{1}{2}\Delta\mathcal{M}^2 = R^4 \int_{\Omega,\Omega'} M_{11}^{-1}(\underline{p}) M_{12}(\underline{p}, R, \Omega) M_{22}^{-1}(p_0, \Omega, \Omega') M_{21}(\Omega', p_0, q_{||}) \quad (4.107)$$

$$\frac{1}{2}(\Delta\mathcal{M}^2)_\mu^\kappa = \sum_{l\geq 1} \frac{2l+1}{4\pi} M_{11\,\mu\nu}^{-1} C_{ss'l}^{-1} \int_{\Omega,\Omega'} M_{12}^{\nu\rho}(\Omega) \mathcal{P}_{l\,\rho\sigma}^{ss'}(\vec{\Omega} - \vec{\Omega}') M_{21}^{\sigma\kappa}(\Omega') \quad (4.108)$$

can be obtained, with $p_{||}$ and $q_{||}$ being the corresponding surface momenta on the plate. Again, this object can be calculated, if M_{12} (and M_{21}) is expanded into a series for small R, and of course a truncation like $l = 1 \ldots L_{max}$ is set. To get the N-loop energy, the Nth power of $\Delta\mathcal{M}^2$ has to be taken, always including the Fourier integrals for the connecting surface momenta[21]. These integrals can all be calculated by using polar coordinates

$$q_1 = |q_{||}| \cos\phi_{q_{||}} \quad (4.109)$$

$$q_2 = |q_{||}| \sin\phi_{q_{||}} \quad (4.110)$$

and the substitution $\sqrt{p_0^2 + q_{||}^2} = \tilde{q_{||}}$. For this reason, the Casimir energy up to arbitrary numbers of loops can be calculated analogue to section 4.2 by the following equation:

$$E_{\mathrm{Cas}} = -\frac{\hbar c}{2} \frac{1}{(2\pi)^3} \int_{p_0, p_{||}} \sum_{n\geq 1} \frac{1}{n} \frac{1}{(2\pi)^{2n-2}} \int_{\overbrace{q_{||}, q'_{||}, \ldots, q''_{||}}^{n}} \underbrace{\Delta\mathcal{M}_\mu^{2\nu}(p_0, p_{||}, q_{||}) \Delta\mathcal{M}_\nu^{2\rho}(p_0, q_{||}, q'_{||}) \ldots \Delta\mathcal{M}_\sigma^{2\mu}(p_0, q''_{||}, p_{||})}_{n} . \quad (4.111)$$

With this, the following results can be obtained. Again, the energy can be expressed as

$$E_{\mathrm{Cas}}^{1\text{ loop}} = -\frac{\hbar c}{\pi H} \sum_{i=3} b_i \left(\frac{R}{H}\right)^i . \quad (4.112)$$

In addition for the 1-loop calculations, a lower cutoff $l \geq L_{min}$ was used.

[21] The appearing $(2\pi)^2$ has to be taken into account.

N-loop $-$ L_{min} $-$ L_{max}	b_3	b_4	b_5	b_6	b_7
$1-1-1$	$\frac{9}{16}$	0	0	$\frac{45}{64}$	0
$1-2-2$	0	0	$\frac{25}{32}$	0	$\frac{385}{1152}$
$1-3-3$	0	0	0	0	$\frac{7007}{7200}$
$2-1-1$				$\frac{143}{4096}$	0
$\sum$	$\frac{9}{16}$	0	$\frac{25}{32}$	$\frac{3023}{4096}$	$\frac{12551}{9600}$

Table 6: Results for the Casimir energy in the plain plate sphere setup. The shown coefficients determine the energy by the use of (4.112).

All the coefficients in the last line are the same as the one in [38]. Also, the chosen gauge did not influence these results. In this calculations $L_{max} = 1$ sufficed to determine b_3. Thus, the vector spherical basis seems to be the correct one and $l = 1$ could be called the dipole order. With R^3 as the first contribution in the matrix $\Delta\mathcal{M}^2$, also b_4 and b_5 are determined by this one propagation loop. But again, R^4 cancels out completely even in the matrix $\Delta\mathcal{M}^2$, and therefore the coefficient b_7 is determined by only one loop, too. But for b_6, one more propagation loop $\Delta\mathcal{M}^4$ is needed.

The following results for the energy are obtained:

- R^3 is determined by one loop of dipole order $l = 1$
- R^5 is determined by one loop of quadrupole order $l = 2$
- R^6 is determined by two loops of dipole order $l = 1$
- R^7 is determined by one loop of quadrupole and hexapole order $l = 2, 3$.

From the inverse propagator M_{22}^{-1} to the R^3 energy

The full R^3 energy is given by only $l = 1$. Therefore, the complete inverse propagator M_{22}^{-1} up to this order can be given. In Feynman gauge without $\Psi_0 = 0$, M_{22}^{-1} up to dipole order is:

$$R^4 M_{22}^{-1}(p_0, \Omega, \Omega') = -\frac{9R^3}{16\pi} \times \tag{4.113}$$
$$\begin{pmatrix} 2s_\theta s_\Theta c_{(\varphi-\Phi)} + 2c_\theta c_\Theta & 0 & 0 & 0 \\ 0 & c_\theta c_\Theta + s_\varphi s_\theta s_\Phi s_\Theta & -s_\varphi s_\theta s_\Theta c_\Phi & -c_\theta s_\Theta c_\Phi \\ 0 & -s_\theta c_\varphi s_\Phi s_\Theta & c_\theta c_\Theta + s_\theta c_\varphi s_\Theta c_\Phi & -c_\theta s_\Theta s_\Phi \\ 0 & -c_\Theta c_\varphi s_\theta & -c_\Theta s_\theta s_\varphi & s_\theta s_\Theta c_{(\varphi-\Phi)} \end{pmatrix}$$
$$+ \mathcal{O}(R^4) + \mathcal{O}(\mathcal{P}_{l=2}) \,,$$

and with additional $\Psi_0 = 0$ gauge it becomes:

$$R^4 M_{22}^{-1}(p_0, \Omega, \Omega') = -\frac{9R}{8p_0^2\pi} A - \frac{9R^3}{80\pi} B + \mathcal{O}(R^4) + \mathcal{O}(\mathcal{P}_{l=2}) \tag{4.114}$$

with

$$\begin{aligned}
A_{1,1} &= (1 - s_\theta^2 c_\varphi^2)(1 + c_\Theta)(c_\Theta - 1)c_\Phi^2 + c_\varphi(s_\varphi s_\Phi(c_\theta - 1)(c_\theta + 1)c_\Theta^2 + c_\theta s_\theta c_\Theta s_\Theta + s_\varphi s_\Phi - c_\theta^2 s_\varphi s_\Phi)c_\Phi + 1 - s_\theta^2 c_\varphi^2 \\
A_{2,2} &= (c_\Theta + 1)(c_\Theta - 1)(s_\Phi s_\varphi(c_\theta - 1)(c_\theta + 1)c_\varphi c_\Phi - (s_\theta^2 c_\varphi^2 + c_\theta^2)c_\Phi^2) + c_\Theta(c_\Theta(s_\theta^2 c_\varphi^2 + c_\theta^2) + s_\theta s_\Theta c_\theta s_\varphi s_\Phi) \\
A_{3,3} &= -s_\theta^2 c_\Theta^2 + c_\theta s_\Theta s_\theta(c_\varphi c_\Phi + s_\varphi s_\Phi)c_\Theta + s_\theta^2 \\
A_{2,1} &= (c_\theta - 1)(c_\theta + 1)(c_\varphi s_\varphi - (c_\Theta - 1)(c_\Theta + 1)(c_\varphi s_\varphi c_\Phi^2 - c_\Phi s_\Phi c_\varphi^2)) + c_\theta(s_\Theta^2 s_\Phi c_\theta + s_\theta s_\Theta c_\Theta s_\varphi)c_\Phi \\
A_{1,2} &= (c_\Theta - 1)(c_\Theta + 1)(c_\Phi s_\Phi - (c_\theta - 1)(c_\theta + 1)(c_\Phi s_\Phi c_\varphi^2 - c_\varphi s_\varphi c_\Phi^2)) + c_\Theta(s_\theta^2 s_\varphi c_\Theta + s_\Theta s_\theta c_\theta s_\Phi)c_\varphi \\
A_{3,1} &= s_\Theta c_\Phi c_\Theta c_\theta^2 - ((c_\varphi c_\Theta^2 - c_\varphi)c_\Phi^2 + s_\Phi s_\varphi(c_\Theta - 1)(c_\Theta + 1)c_\Phi + c_\varphi)c_\theta s_\theta - s_\Theta c_\Phi c_\Theta \\
A_{1,3} &= s_\theta c_\varphi c_\theta c_\Theta^2 - ((c_\Phi c_\theta^2 - c_\Phi)c_\varphi^2 + s_\varphi s_\Phi(c_\theta - 1)(c_\theta + 1)c_\varphi + c_\Phi)c_\Theta s_\Theta - s_\theta c_\varphi c_\theta \\
A_{3,2} &= s_\Theta c_\Theta c_\theta^2 s_\Phi + ((s_\varphi s_\Phi^2 + c_\varphi s_\Phi c_\Phi)s_\Theta^2 - s_\varphi)s_\theta c_\theta - s_\Theta s_\Phi c_\Theta \\
A_{2,3} &= s_\theta c_\theta c_\Theta^2 s_\varphi + ((s_\Phi s_\varphi^2 + c_\Phi s_\varphi c_\varphi)s_\theta^2 - s_\Phi)s_\Theta c_\Theta - s_\theta s_\varphi c_\theta \\
B_{1,1} &= 4((1 - s_\theta^2 c_\varphi^2)(c_\Theta + 1)(c_\Theta - 1)c_\Phi^2 + (s_\Phi s_\varphi(c_\theta - 1)(c_\theta + 1)c_\Theta^2 + c_\theta s_\theta c_\Theta s_\Theta + s_\theta^2 s_\varphi s_\Phi)c_\varphi c_\Phi - s_\theta^2 c_\varphi^2 + 1) \\
&\quad + 5(s_\theta s_\Theta s_\varphi s_\Phi + c_\theta c_\Theta) \\
B_{2,2} &= 4((s_\Phi s_\varphi((c_\theta - 1)(c_\theta + 1)c_\Theta^2 + s_\theta^2) + \tfrac{5}{4} s_\theta s_\Theta)c_\varphi c_\Phi - (c_\Theta + 1)(s_\theta^2 c_\varphi^2 + c_\theta^2)(c_\Theta - 1)c_\Phi^2 \\
&\quad + c_\Theta(c_\Theta s_\theta^2 c_\varphi^2 + c_\theta(c_\theta c_\Theta + s_\theta s_\Theta s_\varphi s_\Phi + \tfrac{5}{4}))) \\
B_{3,3} &= 4(c_\theta s_\Theta s_\theta(c_\varphi c_\Phi + s_\Phi s_\varphi)c_\Theta - c_\theta^2 - s_\theta^2 c_\Theta^2 + 1) + 5 s_\theta(c_\varphi c_\Phi + s_\Phi s_\varphi)s_\Theta \\
B_{2,1} &= 4(((c_\theta - 1)(c_\theta + 1)(c_\Theta - 1)(c_\Theta + 1)(c_\Phi c_\varphi s_\varphi - s_\Phi c_\varphi^2) + c_\theta(-s_\Theta^2 s_\Phi c_\theta + s_\theta s_\Theta c_\Theta s_\varphi))c_\Phi - c_\varphi(\tfrac{5}{4} s_\theta s_\Theta s_\Phi + s_\varphi s_\theta^2)) \\
B_{1,2} &= 4(((c_\Theta - 1)(c_\Theta + 1)(c_\theta - 1)(c_\theta + 1)(c_\varphi c_\Phi s_\Phi - s_\varphi c_\Phi^2) + c_\Theta(-s_\theta^2 s_\varphi c_\Theta + s_\Theta s_\theta c_\theta s_\Phi))c_\varphi - c_\Phi(\tfrac{5}{4} s_\Theta s_\theta s_\varphi + s_\Phi s_\Theta^2)) \\
B_{3,1} &= 4 s_\Theta c_\Phi c_\Theta c_\theta^2 - 4 s_\theta(-c_\varphi s_\Theta^2 c_\Phi^2 + s_\Phi s_\varphi(c_\Theta - 1)(c_\Theta + 1)c_\Phi + c_\varphi)c_\theta - 4 s_\Theta c_\Phi c_\Theta - 5 s_\theta c_\Theta c_\varphi \\
B_{1,3} &= 4 s_\theta c_\varphi c_\theta c_\Theta^2 - 4 s_\Theta(-c_\Phi s_\theta^2 c_\varphi^2 + s_\varphi s_\Phi(c_\theta - 1)(c_\theta + 1)c_\varphi + c_\Phi)c_\Theta - 4 s_\theta c_\varphi c_\theta - 5 s_\Theta c_\theta c_\Phi \\
B_{3,2} &= -4 c_\theta s_\theta(c_\varphi s_\Phi c_\Phi + s_\varphi s_\Phi^2)c_\Theta^2 - (5 s_\theta s_\varphi + 4 s_\theta^2 s_\Theta s_\Phi)c_\Theta + 4 c_\theta s_\theta c_\Phi(c_\varphi s_\Phi - s_\varphi c_\Phi) \\
B_{2,3} &= -4 c_\Theta s_\Theta(c_\Phi s_\varphi c_\varphi + s_\Phi s_\varphi^2)c_\theta^2 - (5 s_\Theta s_\Phi + 4 s_\Theta^2 s_\theta s_\varphi)c_\theta + 4 c_\Theta s_\Theta c_\varphi(c_\Phi s_\varphi - s_\Phi c_\varphi)\,.
\end{aligned}$$

Matrix (4.113) or (4.114) together with the corresponding M_{11}^{-1} (C.2) or (C.5), the M_{12} from (C.3) and the corresponding M_{21} determine the correct Casimir energy for a plain plate and a sphere up to dipole order. In the next step, the product $M_{12}M_{22}^{-1}M_{21} \equiv R^4 \int_{\Omega,\Omega'} M_{12}(\Omega)M_{22}^{-1}(\Omega,\Omega')M_{21}(\Omega')$ has to be carried out by first expanding M_{12} and M_{21} up to $\mathcal{O}(R^4)$, and afterwards solving the Ω and Ω' integrals. By multiplying the result with $M_{11}^{-1}(p_0, p_{||})$, the 1-loop propagator $\frac{1}{2}\Delta\mathcal{M}^2(p_0, p_{||}, q_{||})$ is obtained. In the case of $\Psi_0 = 0$ gauge, this is exactly the same as equation (4.53) in section 4.5.6 and hence the Casimir energy results correctly, too. In contrast, without $\Psi_0 = 0$ gauge,

the 1-loop propagator becomes more complicated:

$$\frac{1}{2}\Delta\mathcal{M}^2 = \frac{\pi R^3}{\underline{p}^2|\underline{q}|}e^{-H(|\underline{p}|+|\underline{q}|)}\begin{pmatrix} \star_{00} & \star_{01} & \star_{02} & 0 \\ \star_{10} & \star_{11} & \star_{12} & 0 \\ \star_{20} & \star_{21} & \star_{22} & 0 \\ 0 & 0 & 0 & 0 \end{pmatrix} \tag{4.115}$$

$$\begin{aligned}
\star_{00} &= (|\underline{p}||\underline{q}| + 2p_0^2)(p_1q_1 + p_2q_2) + (p_1^2 + p_2^2)(q_1^2 + q_2^2) \\
\star_{11} &= (|\underline{p}||\underline{q}| + p_1q_1)(p_0^2 + 2p_2q_2) + 2(p_0^2 + q_2^2)(p_0^2 + p_2^2) \\
\star_{22} &= (|\underline{p}||\underline{q}| + 2p_2q_2)(p_0^2 + p_1q_1) + |\underline{p}||\underline{q}|p_1q_1 + 2(p_0^2 + p_1^2)(p_0^2 + q_1^2) \\
\star_{10} &= -((|\underline{p}||\underline{q}| + 2(p_0^2 + p_2^2))p_0q_1 + (q_1^2 + q_2^2 - 2p_2q_2)p_0p_1) \\
\star_{01} &= -((|\underline{p}||\underline{q}| + 2(p_0^2 + q_2^2))p_0p_1 + (p_1^2 + p_2^2 - 2p_2q_2)p_0q_1) \\
\star_{20} &= -((|\underline{p}||\underline{q}| + 2(p_0^2 + p_1^2))p_0q_2 + (q_1^2 + q_2^2 - 2p_1q_1)p_0p_2) \\
\star_{02} &= -((|\underline{p}||\underline{q}| + 2(p_0^2 + q_1^2))p_0p_2 + (p_1^2 + p_2^2 - 2p_1q_1)p_0q_2) \\
\star_{21} &= -((|\underline{p}||\underline{q}| + p_1q_1 + p_2q_2)2p_1q_2 + 2(p_1p_2 + q_1q_2 - q_1p_2)p_0^2) \\
\star_{12} &= -((|\underline{p}||\underline{q}| + p_1q_1 + p_2q_2)2q_1p_2 + 2(p_1p_2 + q_1q_2 - p_1q_2)p_0^2)
\end{aligned}$$

But of course, taking the trace of (4.115) and using the spherical coordinates (4.54) to solve the appearing integral results in the same energy

$$\begin{aligned}
E_{\text{Cas}} &= -\frac{\hbar c}{2}\frac{1}{(2\pi)^3}\int_{\underline{p}} \text{tr}\left[\frac{1}{2}\Delta\mathcal{M}^2\right] + \mathcal{O}\left(R^4\right) && (4.116) \\
&= -\frac{\hbar c}{2}\frac{1}{(2\pi)^3}\int 6\pi R^3 \underline{p}e^{-2|\underline{p}|H}\ \underline{p}^2 d\underline{p}\sin\theta_{\underline{p}}d\theta_{\underline{p}}d\phi_{\underline{p}} + \mathcal{O}\left(R^4\right) && (4.117) \\
&= -\frac{9}{16}\frac{\hbar c}{\pi}\frac{R^3}{H^4} + \mathcal{O}\left(\frac{R^4}{H^5}\right). && (4.118)
\end{aligned}$$

5 Casimir-Polder force for an atom and a uniaxial structured plate

Meanwhile, the propagator matrix and its inverse for a perfectly conducting plain plate and a perfectly conducting sphere is already known. The next step is to implement the corresponding calculations numerically and compare them with known results. At the same time, a deformation of the plate in one direction with an arbitrary amplitude is assumed.

5.1 Setup

A perfectly conducting sphere with radius R above a perfectly conducting uniaxial structured plate is assumed. The mean distance between them shall be denoted by H, where "mean" means the shortest distance between the center of the sphere and the midaxis of the plate. See Fig. 5.1.

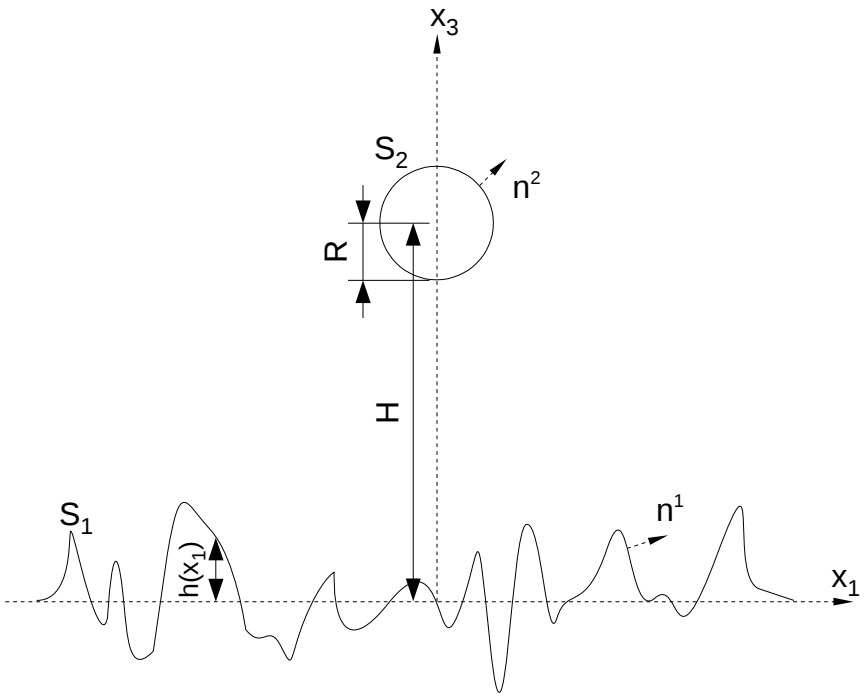

Fig. 5.1: One uniaxial corrugated plate and a sphere of radius R above are set on a distance H. Both are assumed to be perfect conductors. Coordinates for the plate are Cartesian and those for the sphere are spherical ones. x_1, x_2 and $x_3 = h(x_1)$ are the coordinates on the plate, θ and ϕ are the coordinates on the sphere. n^1 and n^2 are the normal vectors.

The plate S_1 is described by the Cartesian coordinates x_1 and x_2. In x_3 direction it is shaped by a height function $h(x_1)$. Furthermore, the sphere S_2 with its center at the point $(x_0, 0, 0, H)$ implies spherical coordinates φ and θ, which are abstracted by Ω. Again the normal vectors have to face each other by convention, thus n^1 points in positive x_3 direction and n^2 points outside the sphere. Within this parametrisation, the surface normal vectors are given by

$$n^1_\gamma = \delta^3_\gamma = \frac{1}{\sqrt{g}} \begin{pmatrix} 0 \\ -h' \\ 0 \\ 1 \end{pmatrix} \qquad n^2_{\gamma'}(\Omega) = \begin{pmatrix} 0 \\ \cos\varphi \sin\theta \\ \sin\varphi \sin\theta \\ \cos\theta \end{pmatrix} \tag{5.1}$$

$$\sqrt{g} = \sqrt{1 + h'^2}\,. \tag{5.2}$$

The h' represents the derivative $\partial_{x_1} h(x_1)$. On the one hand, $\sqrt{g}$ is the normalisation of n^1, and on the other hand it is the square root of the induced surface metric, which will be needed for the surface integral

$$\int_{x_1} f(x_1) = \int_{-\infty}^{\infty} \sqrt{g(x_1)} f(x_1) dx_1\,. \tag{5.3}$$

5.2 Preliminaries

Again, the change in the symmetry of the problem leads to a slightly different strategy to achieve the Casimir energy. As usual, propagators between the surfaces have to be calculated and functionally inverted. The sphere propagator M_{22} fits best in the vector spherical basis (4.68) to (4.72), in which its inverse up to dipole order can be given by (4.113) or in the case of $\Psi_0 = 0$ gauge results in (4.114). In addition, the two propagators M_{12} and M_{21} between the plate and the sphere, and the one connecting two points on the plate M_{11} can be calculated analytically. However, the inverse of M_{11} in the case of a nontrivial structure can only be obtained numerically, because there is no known functional basis in which it can be expanded analytically. Also, if a periodic structure could be assumed to fit well into Fourier modes, the appearing coefficients would intrinsically depend on one of both points as it is already discussed in [31], and therefore this method is not considered for now. Otherwise, the uniaxial structure implies a translation invariance in x_2 direction, of which naturally advantage has to be taken. With this, even if the four sphere surface integrals can be calculated analytically, the Casimir

energy up to dipole order is determined by four integrals, one for the surface coordinate x_1' in the product $M_{11}^{-1}M_{12}$, and three for the trace: x_1 and the momenta p_0 and p_2.

Analogue to section 4.2, the 1-loop Casimir energy is given by

$$E_{\text{Cas}}^{1\text{ loop}} = -\frac{\hbar c}{2T_E}\text{Tr}\left[\Delta\mathcal{M}_{12}\Delta\mathcal{M}_{21}\right] \tag{5.4}$$

$$= -\frac{\hbar c}{2}\frac{R^4}{(2\pi)^2}\int_{p_0,p_2,x_1}\int_{x_1'}\int_{\Omega}\int_{\Omega'}\text{tr}\left[M_{11}^{-1}(p_0,p_2,x_1,x_1')\right.$$
$$\left.M_{12}(p_0,p_2,x_1',\Omega)M_{22}^{-1}(p_0,\Omega,\Omega')M_{21}(p_0,p_2,\Omega',x_1)\right]. \tag{5.5}$$

Now M_{22}^{-1} has to be inserted, but instead of using (4.113), (4.114) or (4.99) and the tensorial Legendre polynomials, it is more convenient to first multiply M_{12} with the vector spherical basis of M_{22}^{-1} and to carry out one Ω integral.

$$(M\mathcal{V})_{12\,lm}^{\mu s} = \int_{\Omega} M_{12\,\nu}^{\mu}(\Omega)\mathcal{V}_{lm}^{s\nu}(\Omega) \tag{5.6}$$

Afterwards, the corresponding object $(\mathcal{V}M)_{21} = \int \mathcal{V}^{\star}M_{21}$ can be obtained by simply adjoining $(M\mathcal{V})_{12}$: $(\mathcal{V}M)_{21} = (M\mathcal{V})_{12}^{\dagger}$. The energy now reads

$$E_{\text{Cas}}^{1\text{ loop}} = -\frac{\hbar c}{2}\frac{1}{(2\pi)^2}\int_{p_0,p_2,x_1}\int_{x_1'}\sum_{lm}\text{tr}\left[M_{11}^{-1}(p_0,p_2,x_1,x_1')\right.$$
$$\left.(M\mathcal{V})_{12\,lm}(p_0,p_2,x_1')C_l^{-1}(p_0,R)(M\mathcal{V})_{12\,lm}^{\dagger}(p_0,p_2,x_1)\right]. \tag{5.7}$$

From this point, it is convenient to choose the pure Feynman gauge without $\Psi_0^{\text{sphere}} = 0$ on the sphere side and the one with $\Psi_0^{\text{plate}} = 0$ on the plate side.[22] On the one hand, in this case, the coefficients $C_l^{ss'\,-1}$ in (4.105) have R^3 as their lowest contribution. Hence, to reach R^3 in the energy, M_{12} and M_{21} only have to be expanded up to $\mathcal{O}(R)$, which can be obtained by simply setting $R = 0$. Then, the full R dependence up to R^3 can be factored out from equation (5.7) and in addition, the integral (5.6) becomes analytically solvable. Otherwise, the R dependence would have to be considered and (5.6) has to be solved numerically. On the other hand, $\Psi_0^{\text{plate}} = 0$ simply lowers the number of terms in M_{11}, which have to be inverted numerically.

[22] In chapter 2.5, the $\Psi_0 = 0$ gauge was found to be allowed for each surface separately. That means, instead of using a "global" $\Psi_0 = 0$ for all surfaces, this gauge can be separately switched on and off for each surface. This can be done by simply setting the time components of the corresponding inverse propagators M_{aa}^{-1} to zero. In principle, also the propagators between the surfaces have to be changed, but by taking the product $\text{tr}[M_{11}^{-1}M_{12}M_{22}^{-1}M_{21}]$, the chosen gauge automatically applies to them.

So far, everything except the M_{11}^{-1} can be obtained analytically. By restriction to the dipole order, only the $C_{l=1}^{-1}$ contributes to the energy and therefore the lm summation only runs for m from -1 to 1. The C_1^{-1} expanded up to $\mathcal{O}(R^4)$ is

$$C_1^{-1} = \frac{3R^3}{2} \begin{pmatrix} 1 & 0 & 0 & 0 \\ 0 & 0 & 0 & 0 \\ 0 & 0 & 1 & 0 \\ 0 & 0 & 0 & 0 \end{pmatrix} + \mathcal{O}(R^4)\,. \tag{5.8}$$

Next, the integrals have to be discretised and replaced by summations like for example

$$\int_a^b f(x)dx = \Delta x \left[\frac{1}{2}f(a) + \sum_{i=1}^{i_{max}-1} f(x_i) + \frac{1}{2}f(b)\right] \tag{5.9}$$
$$\Delta x = \frac{b-a}{i_{max}}\,, \quad x_i = \Delta x\, i + a\,, \quad i = 0 \ldots i_{max}\,.$$

Hence, the plate has to get a finite size in x_1 direction and the infinite large case can only be obtained as a limit. But this opens up the possibility to study edge effects. The same problem exists for the momenta integrals, too. Thus, a cut-off for high momenta has to be introduced. In the scalar case, only $\sqrt{p_0^2 + p_2^2}$ terms appeared under the integrals and therefore a change to polar coordinates

$$p_0 = |\underset{\sim}{p}| \cos p_\phi \tag{5.10}$$
$$p_2 = |\underset{\sim}{p}| \sin p_\phi \tag{5.11}$$
$$dp_0 dp_2 = |\underset{\sim}{p}| d|\underset{\sim}{p}| dp_\phi \tag{5.12}$$

led to only one integral of the type $2\pi \int_0^\infty |\underset{\sim}{p}| f(|\underset{\sim}{p}|) d|\underset{\sim}{p}|$. However, in the QED case, such a simplification cannot be done and both momenta integrals have to be carried out numerically. Nevertheless, polar coordinates are used, too, because they give the possibility to choose a symmetrically cut-off p_{max} and a lower one p_{min} to avoid divergences at $|\underset{\sim}{p}| = 0$.

5.3 The propagator between a corrugated plate and a sphere

To obtain the Casimir energy from equation (5.7), the propagator $M_{12}(x - x')$ between the corrugated plate and the sphere is needed, which is additionally transformed to momentum space in the following way: $x_0 - x_0' \to p_0$ and

$x_2 \to p_2$. Therefore, the free propagator G has to be transformed in this way, too:

$$G(\underset{\sim}{p}, x_1-x_1', x_2', x_3-x_3') = \int_{x_0-x_0', x_2} G(x-x') e^{i((x_0-x_0')p_0+x_2p_2)} \tag{5.13}$$

$$= \frac{e^{ip_2x_2'}}{2\pi} K_0\left(|\underset{\sim}{p}|\sqrt{(x_1-x_1')^2+(x_3-x_3')^2}\right) \tag{5.14}$$

$$G(x-x') = \frac{1}{(2\pi)^2}\int_{\underset{\sim}{p}} G(\underset{\sim}{p}, x_1-x_1', x_2', x_3-x_3') e^{-i((x_0-x_0')p_0+x_2p_2)} \tag{5.15}$$

with $\underset{\sim}{p} = (p_0, p_2)$. Equation (5.15) and the normal vectors (5.1) have to be put in (2.32), which leads to M_{12}. After inserting the surface coordinates,

$$M_{12}(\underset{\sim}{p}, x_1, \Omega) = \frac{1}{\sqrt{g(x_1)}}\left[\mathcal{D}G(\underset{\sim}{p}, x_1-x_1', x_2', x_3-x_3')\right]\Big|\begin{array}{l} x_3 = h(x_1) \\ x' = x'(\Omega)\end{array} \tag{5.16}$$

can be obtained, whereby $\mathcal{D}$ is the following operator in components:

$$\begin{aligned}
\mathcal{D}_{0,0} =\ & h'(x_1)\, c_\varphi s_\theta \partial_{x_3}^2 + (c_\varphi s_\theta - h'(x_1)\, c_\theta)\, \partial_{x_1}\partial_{x_3} - c_\theta \partial_{x_1}^2 \\
& + p_2 (i h'(x_1)\, s_\varphi s_\theta \partial_{x_1} - i s_\varphi s_\theta \partial_{x_3} + p_2 (c_\theta - h'(x_1)\, c_\varphi s_\theta)) \\
\mathcal{D}_{1,0} =\ & i p_0 (c_\varphi s_\theta \partial_{x_3} - c_\theta \partial_{x_1}) \\
\mathcal{D}_{2,0} =\ & p_0 (i s_\varphi s_\theta \partial_{x_3} - i h'(x_1)\, s_\varphi s_\theta \partial_{x_1} + p_2 (h'(x_1)\, c_\varphi s_\theta - c_\theta)) \\
\mathcal{D}_{3,0} =\ & i h'(x_1)\, p_0 (c_\varphi s_\theta \partial_{x_3} c_\theta \partial_{x_1}) \\
\mathcal{D}_{0,1} =\ & p_0 (h'(x_1)\, s_\varphi s_\theta p_2 - i c_\theta \partial_{x_1} - i h'(x_1)\, c_\theta \partial_{x_3}) \\
\mathcal{D}_{1,1} =\ & c_\theta \underset{\sim}{p}^2 - i s_\varphi s_\theta p_2 \partial_{x_3} \\
\mathcal{D}_{2,1} =\ & h'(x_1)\, s_\varphi s_\theta p_0^2 - i c_\theta p_2 \partial_{x_1} - (i h'(x_1)\, c_\theta p_2 + s_\varphi s_\theta (\partial_{x_1} + h'(x_1)) \partial_{x_3})\, \partial_{x_3} \\
\mathcal{D}_{3,1} =\ & h'(x_1)\left(c_\theta \underset{\sim}{p}^2 - i s_\varphi s_\theta p_2 \partial_{x_3}\right) \\
\mathcal{D}_{0,2} =\ & p_2 p_0 (h'(x_1)\, c_\varphi s_\theta - c_\theta) \\
\mathcal{D}_{1,2} =\ & i p_2 (c_\varphi s_\theta \partial_{x_3} - c_\theta \partial_{x_1}) \\
\mathcal{D}_{2,2} =\ & (c_\varphi s_\theta - h'(x_1)\, c_\theta)\, \partial_{x_1}\partial_{x_3} + c_\theta (p_0^2 - \partial_{x_1}^2) + h'(x_1)\, c_\varphi s_\theta (\partial_{x_3}^2 - p_0^2) \\
\mathcal{D}_{3,2} =\ & i h'(x_1)\, p_2 (c_\varphi s_\theta \partial_{x_3} - c_\theta \partial_{x_1}) \\
\mathcal{D}_{0,3} =\ & p_0 s_\theta (i c_\varphi \partial_{x_1} + s_\varphi p_2 + i h'(x_1)\, c_\varphi \partial_{x_3}) \\
\mathcal{D}_{1,3} =\ & s_\theta \left(i s_\varphi p_2 \partial_{x_1} - c_\varphi \underset{\sim}{p}^2\right) \\
\mathcal{D}_{2,3} =\ & s_\theta \left(s_\varphi (\partial_{x_1}^2 + h'(x_1)\, \partial_{x_1}\partial_{x_3} - p_0^2) + i c_\varphi p_2 \partial_{x_1} + i h'(x_1)\, c_\varphi p_2 \partial_{x_3}\right) \\
\mathcal{D}_{3,3} =\ & h'(x_1)\left(i s_\varphi p_2 \partial_{x_1} - c_\varphi \underset{\sim}{p}^2\right) s_\theta\,.
\end{aligned} \tag{5.17}$$

The derivatives ∂_{x_1} and ∂_{x_3} in (5.17), which act on the free propagator G in equation (5.16), have to be carried out before x_3 is set to $h(x_1)$.

5.4 The propagator for a corrugated plate

In a next step, the propagator $M_{11}(\underset{\sim}{p}, x_1, x_1')$ has to be calculated. Therefore, the following free photon propagator has to be inserted in (2.32):

$$G(x-x') = \frac{1}{(2\pi)^2}\int_{\underset{\sim}{p}} G(\underset{\sim}{p}, x_1-x_1', x_3-x_3')e^{-i((x_0-x_0')p_0+(x_3-x_3')p_2)} \tag{5.18}$$

with

$$G(\underset{\sim}{p}, x_1-x_1', x_3-x_3') = \int_{x_0-x_0', x_2-x_2'} G(x-x')e^{i((x_0-x_0')p_0+(x_2-x_2')p_2)} \tag{5.19}$$

$$= \frac{1}{2\pi}K_0\left(|\underset{\sim}{p}|\sqrt{(x_1-x_1')^2+(x_3-x_3')^2}\right). \tag{5.20}$$

Together with the normal vectors for the plate, $n_\gamma^1(x)$ and $n_\gamma^1(x')$ from (5.1), M_{11} can be obtained.

$$M_{11}(\underset{\sim}{p}, x_1, x_1') = \frac{1}{\sqrt{g(x_1)}\sqrt{g(x_1')}}\left[\mathcal{D}G(\underset{\sim}{p}, x_1-x_1', x_3-x_3')\right]\Big|_{\substack{x_3=h(x_1)\\ x_3'=h(x_1')}} \tag{5.21}$$

$\mathcal{D}$ is the following operator in components:

$$\begin{aligned}
\mathcal{D}_{0,0} &= p_2^2 - (h'(x_1)+h'(x_1'))\,\partial_{x_1}\partial_{x_3} - \partial_{x_1}^2 + h'(x_1)h'(x_1')\left(p_2^2-\partial_{x_3}^2\right)\\
\mathcal{D}_{1,0} &= -ip_0\left(\partial_{x_1}+h'(x_1')\partial_{x_3}\right)\\
\mathcal{D}_{2,0} &= -p_2p_0\left(1+h'(x_1)h'(x_1')\right)\\
\mathcal{D}_{3,0} &= -ih'(x_1)p_0\left(\partial_{x_1}+h'(x_1')\partial_{x_3}\right)\\
\mathcal{D}_{0,1} &= -ip_0\left(\partial_{x_1}+h'(x_1)\partial_{x_3}\right)\\
\mathcal{D}_{1,1} &= \underset{\sim}{p}^2\\
\mathcal{D}_{2,1} &= -ip_2\left(\partial_{x_1}+h'(x_1)\partial_{x_3}\right)\\
\mathcal{D}_{3,1} &= \underset{\sim}{p}^2h'(x_1)\\
\mathcal{D}_{0,2} &= -p_2p_0\left(1+h'(x_1)h'(x_1')\right)\\
\mathcal{D}_{1,2} &= -ip_2\left(\partial_{x_1}+h'(x_1')\partial_{x_3}\right)\\
\mathcal{D}_{2,2} &= p_0^2 - (h'(x_1)+h'(x_1'))\,\partial_{x_1}\partial_{x_3} - \partial_{x_1}^2 + h'(x_1)h'(x_1')\left(p_0^2-\partial_{x_3}^2\right)\\
\mathcal{D}_{3,2} &= -ih'(x_1)p_2\left(\partial_{x_1}+h'(x_1')\partial_{x_3}\right)\\
\mathcal{D}_{0,3} &= -ih'(x_1')p_0\left(\partial_{x_1}+h'(x_1)\partial_{x_3}\right)\\
\mathcal{D}_{1,3} &= \underset{\sim}{p}^2h'(x_1')\\
\mathcal{D}_{2,3} &= -ih'(x_1')p_2\left(\partial_{x_1}+h'(x_1)\partial_{x_3}\right)\\
\mathcal{D}_{3,3} &= \underset{\sim}{p}^2h'(x_1)h'(x_1').
\end{aligned} \tag{5.22}$$

5.5 The numerical implementation for obtaining the Casimir energy for a uniaxial corrugated plate and a sphere

With the use of (5.7), (5.8), (5.16) and (5.21) the Casimir energy can be obtained numerically within the numerical accuracy for arbitrary height functions h and arbitrary distances H up to dipole order. The remaining task is to invert M_{11} numerically, collecting everything together and carrying out all remaining integrals. But before, one last simplification can be done: To obtain an algorithm, which is independent from the used scale, every dimensionful variable has to be rescaled by H. This means

$$\begin{array}{llll} x &= [eV^{-1}] &= H\hat{x} & \qquad M_{12} = [eV^2] = H^{-2}\hat{M}_{12} \\ p &= [eV] &= H^{-1}\hat{p} & \qquad M_{11} = [eV^2] = H^{-2}\hat{M}_{11} \\ h &= [eV^{-1}] &= H\hat{h} & \qquad M_{11}^{-1} = [eV^0] = \hat{M}_{11}^{-1} \\ R &= [eV^{-1}] &= H\hat{R} & \end{array} \quad . \tag{5.23}$$

The hatted variable is dimensionless. With this, the energy in (5.7) can be rewritten by the dimensionless energy coefficient Σ

$$E_{\text{Cas}}^{1\text{ loop}} = -\frac{3\hbar c}{4(2\pi)^2}\frac{R^3}{H^4}\Sigma\,. \tag{5.24}$$

$$\Sigma = \int_{\underset{\sim}{\hat{p}},\hat{x}_1,\hat{x}_1'} \sum_{m=-1}^{1} \text{tr}\left[\hat{M}_{11}^{-1}(\underset{\sim}{\hat{p}},\hat{x}_1,\hat{x}_1')(\hat{M}\mathcal{V})_{12\,m}^{l=1}(\underset{\sim}{\hat{p}},\hat{x}_1')\begin{pmatrix}1&0&0&0\\0&0&0&0\\0&0&1&0\\0&0&0&0\end{pmatrix}(\hat{M}\mathcal{V})_{12\,m}^{\dagger\,l=1}(\underset{\sim}{\hat{p}},\hat{x}_1)\right] \tag{5.25}$$

From now on, the hats, the index "1" from x_1 and x_1', the index "11" from $\hat{M}_{11}$ and $\hat{M}_{11}^{-1}$, and the index "$l = 1$" and "12" from $(\hat{M}\mathcal{V})_{12\,m}^{l=1}$ are removed for simplicity. Additionally, the momenta are expressed in the polar coordinates $p_0 = |\underset{\sim}{p}|\cos\phi_{\underset{\sim}{p}}$ and $p_2 = |\underset{\sim}{p}|\sin\phi_{\underset{\sim}{p}}$, and hence "$|\underset{\sim}{p}|$" is renamed with "$p$". Also, the index "$\underset{\sim}{p}$" from $\phi_{\underset{\sim}{p}}$ is removed. In a next step, the following discretisation can be done:

$$x \to x_u = \Delta x\, u - L + \epsilon \quad , \quad u = 0 \ldots N_x \quad , \quad \Delta x = \frac{2L}{N_x} \tag{5.26}$$

$$x' \to x'_v = \Delta x'\, v - L - \epsilon \quad , \quad v = 0 \ldots N_x \quad , \quad \Delta x' = \frac{2L}{N_x} \tag{5.27}$$

$$p \to p_i = \Delta p\, j + p_{min} \quad , \quad i = 0 \ldots N_p \quad , \quad \Delta p = \frac{p_{max} - p_{min}}{N_p} \tag{5.28}$$

$$\phi \to \phi_j = \Delta\phi\, j \quad , \quad j = 0 \ldots N_\phi \quad , \quad \Delta\phi = \frac{2\pi}{N_\phi} \tag{5.29}$$

$$M(p,\phi,x,x') \to M^{ijuv} = M(p_i,\phi_j,x_u,x'_v) \tag{5.30}$$
$$(M\mathcal{V})_m(p,\phi,x') \to (M\mathcal{V})_m^{ijv} = (M\mathcal{V})_m(p_i,\phi_j,x'_v) \tag{5.31}$$
$$\sqrt{g}(x) \to \sqrt{g_u} = \sqrt{g}(x_u) \quad , \tag{5.32}$$

whereby the plate is placed at $x \in [-L, L]$, p_{min} and p_{max} are the lower and the higher cutoff of p, and N_x, N_p and N_ϕ are resolution parameters. The ϵ parameter is included because it is the easiest possibility to circumvent the divergent behaviour of $M(p,\phi,x,x')$ at $x = x'$ [31].[23] In the following, i and j are called the "momentum indices", and u and v are the "position indices". The next step is to combine the space-time index μ and the position index u to a super index $A = (\mu, u)$, whereby the A counts from 1 to $4(N_x + 1)$. The B is analogue. Only the integrals are left and have to be discretised like it was done in (5.9) by considering (5.12). Thus, the $\int$ has to be replaced by a $\sum$. The Δx becomes a Δx_A, which includes the factors $\frac{1}{2}$ at $u = 0$ and $u = N_x$. This is the same for Δp. Only $\Delta\phi$ can remain $\Delta\phi$ due to the periodicity in ϕ. Within this discretisation, the energy coefficient Σ from (5.25) reads

$$\Sigma = \sum_{\substack{i=0\ldots N_p \\ j=0\ldots N_\phi-1 \\ m=-1\ldots 1 \\ A,B}} \Delta p_i \Delta\phi\, p_i \left[\sqrt{g_A}\Delta x_A M_{AB}^{-1\,ij} \Delta x_B \sqrt{g_B} (M\mathcal{V})_m^{ij\,Bs} (\delta_{1s}\delta_{1s'} + \delta_{3s}\delta_{3s'}) (M\mathcal{V})_m^{ij\,\dagger s'A}\right]. \tag{5.33}$$

$M_{AB}^{-1\,ij}$ is the discretisation of the functional inverse $M^{-1}(\underset{\sim}{p}, x, x')$ and not the matrix inverse of M_{AB}^{ij}. This becomes clear by writing out the discretised equation (D.1):

$$\sum_B M_{AB}^{-1\,ij} \Delta x_B \sqrt{g_B} M_{BC}^{ij} = \frac{1}{\Delta x_A \sqrt{g_A}} \delta_{AC}\,. \tag{5.34}$$

Hence, the complete object $(\sqrt{g_A}\Delta x_A M_{AB}^{-1\,ij} \Delta x_B \sqrt{g_B})$ can be obtained by inverting M_{AB}^{ij}. This matrix inverse of M_{AB}^{ij} is named $M_{AB}^{ij\,-1}$ and can be calculated within the numerical precision since M_{AB}^{ij} is only a matrix of numbers. The energy coefficient Σ now reads

$$\Sigma = \sum_{\substack{i=0\ldots N_p \\ j=0\ldots N_\phi-1 \\ m=-1\ldots 1}} \Delta p_i \Delta\phi\, p_i \left[M_{AB}^{ij\,-1} (M\mathcal{V})_m^{ij\,Bs} (\delta_{1s}\delta_{1s'} + \delta_{3s}\delta_{3s'}) (M\mathcal{V})_m^{ij\,\dagger s'A}\right]. \tag{5.35}$$

[23] In [31], also a regularisation of the divergent Bessel function in M is proposed, whereby ϵ can be set to zero. But this second method becomes more complex when it is applied to the matrix valued propagators of this thesis.

This is one possibility to obtain the first order of the Casimir energy for a sphere in front of a uniaxial shaped surface.

An enhancement to arbitrary 2D corrugated surfaces is possible, too. Then, there is no translation invariance in x_2 direction, which has to be considered. Thus, the utilised free photon propagator is (4.9). In addition, the used normal vectors and $\sqrt{g}$ changes by a derivative of h in x_2 direction. Therefore, the propagators M_{11} and M_{12} have to be recalculated. Next, the momentum integral $\int_{p_2}$ changes to a surface integral $\int_{x_2}$, which has to be discretised. Thus, the plate becomes finite in this direction, too. The superindex A combines both discretisation indices u and u' and the matrix index μ to (μ, u, u'). It might be the case that the combination of u and u' has to be done in an elegant way for reaching maximal numerical stability within the algorithms. But, in the end, that should not be a problem and the energy coefficient Σ will be given by

$$\Sigma = \sum_{\substack{i=0\ldots N_p \\ m=-1\ldots 1}} \Delta p_i \left[M^{i\,-1}_{AB} (M\mathcal{V})^{i\,Bs}_{m} (\delta_{1s}\delta_{1s'} + \delta_{3s}\delta_{3s'}) (M\mathcal{V})^{i\,\dagger s'A}_{m} \right]. \tag{5.36}$$

The real task would be to invert a bigger matrix M^i_{AB}, whose dimension d grows up quadratically with the discretisation parameters $d \propto N_{x_1} N_{x_2}$. That means, finally, only the numerical cost grows.

6 Résumé

The aim of this thesis was to extend the non-perturbative calculation scheme for Casimir-Polder potentials induced by scalar fields [31] in the case of arbitrarily structured surfaces to abelian gauge fields and to apply this to the quantum-electrodynamic case.

Hence, the method for the quantum field theoretical handling of fluctuating gauge fields in the presence of boundaries was derived within the functional integral formalism. For the generating functional $\mathcal{Z}$ the Euclidian Maxwell-Yang-Mills action was utilised and the free photon propergator G was obtained due to the usage of the gauge breaking term $\frac{1}{2\alpha}(\partial A)^2$ in the Lagrangian. For reasons of simplicity, Feynman gauge was chosen for the calculations afterwards.

Then, boundary conditions for perfectly conducting surfaces, which are dictated by Maxwell's equations, were reviewed. However, also non-local conditions for general frequency dependent dielectrics were obtained in the way described by [35] and ascribed to local ones clearly arranged in index notation.

From these, the constraints for perfectly conducting surfaces were chosen and inserted via a delta functional into $\mathcal{Z}$. Due to a Fourier transformation of this delta constraint, a set of auxiliary vector fields Ψ, defined only on the surfaces, was introduced, which led to a current term in the action. This term broke the concept of an external current- and charge-free vacuum, so Weyl gauge for the vector field potential A (which in combination with Feynman gauge leads to Coulomb gauge) was discussed to be allowed only for plain surfaces, which therefore are translation invariant in all directions tangential to the surfaces. In addition, an analogue to this gauge but for the fields Ψ was proven. This was called the $\Psi_0 = 0$ gauge, which can be applied to each surface separately.

The constrained action was transformed in a way that Gaussian integrals for the physical and the auxiliary fields could be evaluated and the known trace-log formula for the Casimir energy and force was obtained. The logarithm of the appearing normalised super-propagator $\mathcal{M}_{\mathrm{BC}}$ for all Ψ fields on all surfaces resulted through a Taylor expansion around the self-interaction contribution in a sum of every possible propagation circle, which passes all surfaces.

Afterwards, this method was applied to two parallel perfectly conducting plain plates in momentum space and the well-known Casimir force for this setup was obtained.

Then, the main focus was shifted to Casimir-Polder type problems. Thus,

one of the above plates was exchanged with a perfectly conducting sphere for representing an atom in front of a plain plate. Hence, the above propagator for a plain plate was used. For the sphere, a propagator had been calculated and functionally inverted, so the time was transformed to momentum space. Since the inversion can become arbitrarily complicated, three different coordinate systems were discussed and utilised for explicit calculations, whereby for the first two, spherical harmonics were used:

After firstly introducing a scheme for decomposing the corresponding propagator into spherical harmonics, Cartesian coordinates led to a sophisticated expansion matrix. But in the end, the standard Casimir-Polder result up to dipole order was obtained. Because this expansion matrix is infinite-dimensional, for the inversion of it, the right truncation had to be found. Also, the needed dimension before the inversion was estimated. In addition, due to the arithmetic costs, the Moore-Penrose inverse was introduced as an effective way of inverting Hermitian singular matrices with a large dimension analytically.

Obtaining the energy within rotated Cartesian coordinates, whose axes lies tangential and normal to the sphere surface, failed due to the requirement of calculating the complete inverse propagator at once. But thirdly, a vector spherical basis was introduced, which fitted best to a S^2-sphere symmetry in a 4D spacetime. Thus, a well-behaving coefficient matrix was obtained, which yielded in the full expression for the inverse sphere propagator up to any multipole order and sphere radius. Also, tensorial Legendre functions were found and interpreted as the naturally basis for matrix valued 2-point-functions when changing from scalar to vector fields. With the latter basis, the next four correct energy contributions compared to [38] were calculated and decomposed to the corresponding multipole order.

At last, the method was applied to a sphere in front of a uniaxial corrugated surface. Therefore the corresponding propagators for the corrugated surface and the numerical method was presented. It was shown that for the case of using no $\Psi_0 = 0$ gauge on the sphere side, the sphere surface integrals needed for the Casimir energy in the leading order $\frac{R^3}{H^4}$ can be derived analytically and hence only the integrations over the plate-side remain.

7 Outlook

A sequel to the presented work is possible in several directions: Consequently, the above numerical implementation of the corrugated surface setup has to be applied, customised and improved. But an implementation of two dimensional corrugated surfaces is possible, too, which only goes along with an increased numerical work. Also the study of edge effects is possible.

A still remaining problem upon discretisation is the divergent behaviour of the propagators as it was described. Therefore, several regularisation methods can be checked. Also, if there is no functional basis in which the corrugated plate propagator can be decomposed analytically, this possibly can be done numerically with high precision. Then, only the coefficient matrix would have to be inverted, but the divergent behaviour of the propagators could be circumvented.

Furthermore, an analytical extension with the above boundary conditions for general dielectric functions is feasible. This would provide the possibility to compare the calculations with existing experimental measurements. Finite temperature can be included to the method [40], as well as other geometrical objects like a cylinder or a torus. Instead of corrugating the plate by a height function h, also the sphere surface can possibly be structured and inverted within the vector spherical basis. And, of course, also other fluctuating gauge fields could be studied by this method.

A Dimensional checkup

In natural dimensions $\hbar = c = 1$, the scalings of space, time and momentum can be expressed as eV. Meter and second become eV^{-1} and the momentum has dimension eV. With respect to the dimension, the propagator matrix M for the auxiliary fields Ψ (cf. section 2) is only twice the derivative of the free photon propagator $M \propto \partial\partial G$. G is one over the distance squared and therefore has the dimension eV^2. Thus M, or better $M(x, x')$, in position space becomes eV^4. By taking the Fourier transformations into account, the dimension of M is lowered by one power of eV for each change to momentum space. In this thesis the following Fourier transformations were used for a plain plate (index 1) and a sphere (index 2).

$$M_{11}(x,x') = \frac{1}{(2\pi)^3}\int_{\underline{p}} M_{11}(\underline{p}) e^{-i\underline{p}(\underline{x}-\underline{x}')} \quad \rightarrow \quad M_{11}(\underline{p}) \propto eV^1 \tag{A.1}$$

$$M_{12}(x,x') = \frac{1}{(2\pi)^3}\int_{\underline{p}} M_{12}(\underline{p},\vec{x}') e^{-i\underline{p}\underline{x}+ip_0x_0'} \quad \rightarrow \quad M_{12}(\underline{p},\vec{x}') \propto eV^1 \tag{A.2}$$

$$M_{22}(x,x') = \frac{1}{2\pi}\int_{p_0} M_{22}(p_0,\vec{x},\vec{x}') e^{-ip_0(x_0-x_0')} \rightarrow M_{22}(p_0,\vec{x},\vec{x}') \propto eV^3 \tag{A.3}$$

$$M_{21}(x,x') = \frac{1}{(2\pi)^3}\int_{\underline{p}} M_{21}(\vec{x},\underline{p}) e^{-ip_0x_0+i\underline{p}\underline{x}'} \quad \rightarrow \quad M_{21}(\vec{x},\underline{p}) \propto eV^1 \tag{A.4}$$

With a short look on (D.1), having in mind $\int_{\Omega'}$ is dimensionless, $\int_{t'} \propto eV^{-1}$, and $R \propto eV^{-1}$, the inverse propagators can be seen to have the dimensions

$$M_{11}^{-1}(x,x') \propto eV^2 \tag{A.5}$$

$$M_{11}^{-1}(\underline{p}) \propto eV^{-1} \tag{A.6}$$

$$M_{22}^{-1}(x,x') \propto eV^2 \tag{A.7}$$

$$M_{22}^{-1}(p_0,\vec{x},\vec{x}') \propto eV^1\,. \tag{A.8}$$

Now with the use of equation (2.51), a cross checkup can be done.

$$E_{\mathrm{Cas}} = -\frac{\hbar c}{2T_E}\sum_{n=2}^{\infty}\frac{(-1)^n}{n}\,\mathrm{Tr}\left[\Delta\mathcal{M}^n\right] \propto eV \tag{A.9}$$

With $\hbar = c = 1$, the Euclidean timelength T_E got the dimension eV^{-1}, so the trace $\mathrm{Tr}[\Delta\mathcal{M}^n]$ has to be dimensionless.

B Calculation of the plate-sphere-propagator

As it turns out, the propagator matrices between a plate and a plate or a plate and a sphere are easy expressions and can be calculated out by hand. But for

two spheres, the very amount of terms makes this calculation a little bit of a nasty job. Therefore, a computer algebra system like *Maple* or *Mathematica* should be used. By using the example of component $(\mu, \nu) = (0, 1)$ of the propagator matrix M_{12} for a plain plate and a sphere, the calculation, which in principle needs to be done, can easily be understood. Considering equation (2.32) and $L^{-1}_{\beta\beta'} = \delta_{\beta\beta'}G$, this term becomes

$$M^{01}_{12} = n^1_\gamma n^2_{\gamma'} \epsilon^{\gamma 0 \alpha \beta} \epsilon^{\gamma' 1 \alpha' \beta'} \delta_{\beta\beta'} \partial_\alpha \partial'_{\alpha'} G \,. \tag{B.1}$$

Because the normal vector of the plate only points along the x_3 axis, γ can be set to 3 and n^1_3 to 1. Also, β can neither be 0 due to $\mu = 0$, nor 1, because of $\beta = \beta'$ and $\nu = 1$. Therefore, the first ϵ tensor is only for $\alpha = 1$ and $\beta = 2$ nonzero. $\{3012\}$ is an odd permutation of $\{0123\}$, so this tensor is -1.

$$M^{01}_{12} = 1 n^2_{\gamma'} (-1) \epsilon^{\gamma' 1 \alpha' 2} \partial_1 \partial'_{\alpha'} G \tag{B.2}$$

But now, the second ϵ tensor can give only nonzero contributions with $\alpha' = 0$, $\gamma' = 3$ and $\alpha' = 3$, $\gamma' = 0$. However, γ' is the component of the normal vector and thus n^2_0 is zero. Consequently, only $\epsilon^{3102} = 1$ contributes to this component. In fact, the complicated looking expression (B.1) above has only one nontrivial summand.

$$M^{01}_{12} = -n^2_3 \partial_1 \partial'_0 G = -\cos\theta (-ip_1)(ip_0) G = -\cos\theta p_0 p_1 G \tag{B.3}$$

But, in the case of the sphere-sphere-propagator, both normal vectors have three components. Therefore, there are much more nontrivial contributions. In component $(1, 1)$, $(2, 2)$ and $(3, 3)$, there are only two summands, and component $(1, 2)$, $(1, 3)$ and $(2, 3)$ even got only one term. But in $(0, 1)$, $(0, 2)$ and $(0, 3)$, there are four terms left and in $(0, 0)$, there are 12 of them. Now keeping in mind the derivatives of G and the normal vectors in spherical coordinates, the expressions will become slightly complex and computer algebra programs will be the tool of choice.

C Propagator matrices

In every case, Feynman gauge $\alpha = 1$ is assumed. In the case of $\Psi_0 = 0$ M_{ab} can be obtained by simply setting the time components to zero and therefore only M^{-1}_{aa} will be shown here. $(0, n_1, n_2, n_3)$ is the normal vector on the sphere, which is positioned at the distance H above the plate in the origin. $M_{21} = M^\dagger_{12}$.

C.1 Feynman gauge

plain plate → plain plate

$$M_{ab}(\underline{p},H) = \frac{(-1)^{a+b}}{2|\underline{p}|} e^{-|\underline{p}||H(a-b)|} \begin{pmatrix} p_1^2+p_2^2 & -p_0\,p_1 & -p_0\,p_2 & 0 \\ -p_0\,p_1 & p_0^2+p_2^2 & -p_1\,p_2 & 0 \\ -p_0\,p_2 & -p_1\,p_2 & {p_0}^2+p_1^2 & 0 \\ 0 & 0 & 0 & 0 \end{pmatrix} \tag{C.1}$$

$$M_{aa}^{-1}(\underline{p}) = \frac{2}{|\underline{p}|^3} \begin{pmatrix} p_1^2+p_2^2 & -p_0\,p_1 & -p_0\,p_2 & 0 \\ -p_0\,p_1 & p_0^2+p_2^2 & -p_1\,p_2 & 0 \\ -p_0\,p_2 & -p_1\,p_2 & {p_0}^2+p_1^2 & 0 \\ 0 & 0 & 0 & 0 \end{pmatrix} \tag{C.2}$$

plain plate → sphere

$$M_{12}(\underline{p},\Omega) = \frac{e^{iR\left(n_1p_1+n_2p_2+\left|n_3+\frac{H}{R}\right| i|\underline{p}|\right)}}{2|\underline{p}|} \times \tag{C.3}$$

$$\begin{pmatrix} n_3(p_1^2+p_2^2)-(n_1p_1+n_2p_2)\,i|\underline{p}| & -n_3p_0\,p_1 & -n_3p_0\,p_2 & p_0\,(n_1p_1+n_2p_2) \\ p_0(n_1i|\underline{p}|-n_3p_1) & n_3(p_0^2+p_2^2)-n_2p_2i|\underline{p}| & p_2(n_1i|\underline{p}|-n_3p_1) & n_2p_1p_2-n_1(p_0^2+p_2^2) \\ p_0(n_2i|\underline{p}|-n_3p_2) & p_1(n_2i|\underline{p}|-n_3p_2) & n_3(p_0^2+p_1^2)-n_1p_1i|\underline{p}| & n_1p_1p_2-n_2(p_0^2+p_1^2) \\ 0 & 0 & 0 & 0 \end{pmatrix}$$

sphere → sphere

$$M_{22}(p_0,\Omega,\Omega') = \begin{pmatrix} R^{-2}\vec{L}\vec{L}'^{\star} & ip_0R^{-1}(\vec{L}\times\vec{n}')^T \\ -ip_0R^{-1}\vec{n}\times\vec{L}'^{\star} & p_0^2(\vec{n}'\otimes\vec{n}-\vec{n}\vec{n}'\mathbb{1}_3)+R^{-2}\vec{L}\otimes\vec{L}'^{\star} \end{pmatrix} G \tag{C.4}$$

C.2 Feynman gauge and $\Psi_0 = 0$

plain plate → parallel plate

$$M_{aa}^{-1}(\underline{p}) = \frac{2}{|\underline{p}|p_0^2} \begin{pmatrix} 0 & 0 & 0 & 0 \\ 0 & p_0^2+p_1^2 & p_1\,p_2 & 0 \\ 0 & p_1\,p_2 & {p_0}^2+p_2^2 & 0 \\ 0 & 0 & 0 & 0 \end{pmatrix} \tag{C.5}$$

D Inversion of singular Hermitian matrices

During this thesis, it is necessary to get the functional matrix inverse of a given propagator, whose definition is

$$\int_{x'} \mathcal{M}^{-1}(x,x')\mathcal{M}(x',x'') = \mathbb{1}\delta(x-x'')\,. \tag{D.1}$$

Because $\mathcal{M}$ has to be a physical propagator, its eigenvalues have to be real. Also, $\mathcal{M}$ is a propagator for a photon coming from a surface a and flying to the same surface. Thus it is quadratic, too, or in the complex case it has to be Hermitian. But, because it is a matrix acting on a surface, it has zero eigenvalues corresponding to the normal direction, for instance. Thus, $\mathcal{M}$ is a singular matrix. In such a case, the $\mathbb{1}$ in (D.1) has to be an identity matrix living on the same surface a. But this can become a problem, because the $\mathbb{1}$ and $\mathcal{M}$ would have to be diagonalised. Later on, when the inverse of the corresponding propagator for a plain plate is needed, $\mathcal{M}$ can be Fourier transformed to momentum space and hence the functional inversion becomes a usual matrix inversion of such a singular and Hermitian matrix with dimension 4×4. Here, it is no big task to apply a principal axis transformation on $\mathcal{M}$, but for a corrugated surface, such a momentum space does not exist except in time direction because of stationarity, and the matrix basis needs to be changed to a functional basis. In this one, $\mathcal{M}$ is expanded in infinitely many orthonormal functions, for example spherical harmonics for a sphere, and this expansion coefficients can be combined to a singular and Hermitian matrix with dimension $\infty\times\infty$. Therefore, an inversion cannot be given up to any order in general, but truncations can be found to make the dimension finite. Thus there are big matrices, which have to be inverted on the subspace, where no eigenvalue is zero. One possibility of solving this problem is to diagonalise the coefficient matrix later on called S_{AB}. Therefore, eigenvalues λ_A and normalised eigenvectors $v_B^{\{\lambda_A\}} =: v_{BA}$ have to be calculated in a way, that $S_{AB} = v^\dagger_{AC}\,\mathrm{diag}(\lambda_i|i=1\ldots\infty)^C_{\ D}v^D_{\ B}$. In this case the subspace inverse S^{-1}_{AB} is

$$S^{-1}_{AB} = v^\dagger_{AC}\,\mathrm{diag}(\{\frac{1}{\lambda_i}|\lambda_i\neq 0\}\cup\{0|\lambda_i=0\}|i=1\ldots\infty)^C_{\ D}v^D_{\ B}\,. \tag{D.2}$$

But here technical limits will be reached. This work mainly was done with the computer algebra system *Maple 11* on a desktop PC with 8GB working memory. After the truncation is shifted and S_{AB} becomes bigger, in this configuration *Maple 11* is able to calculate the first 59 eigenvalues. Eventually, it is able to calculate the corresponding eigenvectors, too. But then the expressions become that big that in this example *Maple 11* is not able

to handle and simplify the expressions, because the working memory is full. Thus, another way has to be found.

A method that works well also for big matrices is based on the so-called Moore-Penrose or Pseudo inverse. This is defined by

$$\int_{x'}\int_{x''} \mathcal{M}^{-1}(x,x')\mathcal{M}(x',x'')\mathcal{M}^{-1}(x'',x''') = \mathcal{M}^{-1}(x,x''') \tag{D.3}$$

$$\int_{x'}\int_{x''} \mathcal{M}(x,x')\mathcal{M}^{-1}(x',x'')\mathcal{M}(x'',x''') = \mathcal{M}(x,x''') \tag{D.4}$$

$$\int_{x'} \mathcal{M}^{-1}(x,x')\mathcal{M}(x',x'') = \left[\int_{x'} \mathcal{M}^{-1}(x,x')\mathcal{M}(x',x'')\right]^{\dagger} \tag{D.5}$$

$$\int_{x'} \mathcal{M}(x,x')\mathcal{M}^{-1}(x',x'') = \left[\int_{x'} \mathcal{M}(x,x')\mathcal{M}^{-1}(x',x'')\right]^{\dagger}. \tag{D.6}$$

(D.3) and (D.4) do not suffice to determine $\mathcal{M}^{-1}$, therefore the Hermiticity conditions (D.5) and (D.6) are needed. Then this method becomes the same as inverting the nonzero eigenvalues. In the sense of the coefficient matrix S_{AB}, this inverse is consequently defined as

$$S_{AB}^{-1}S_{BC}S_{CD}^{-1} = S_{AD}^{-1} \tag{D.7}$$

$$S_{AB}S_{BC}^{-1}S_{CD} = S_{AD} \tag{D.8}$$

$$S_{AB}^{-1}S_{BC} = \left[S_{AB}^{-1}S_{BC}\right]^{\dagger} \tag{D.9}$$

$$S_{AB}S_{BC}^{-1} = \left[S_{AB}S_{BC}^{-1}\right]^{\dagger}. \tag{D.10}$$

Hence there is no need of explicitly calculating eigenvalues and eigenvectors. Only a matrix has to be found which determines the above four conditions. One possibility to get such a matrix is by using the LU-decomposition of S_{AB}. Assuming, a square matrix S of dimension $n\times n$ and with rank $k \leq n$ is given, it can be split up into two matrices A and B of dimension $n\times k$ and $k\times n$ with both having rank k in this way, that afterwards $S_{\{n\times n\}}$ equals $A_{\{n\times k\}}B_{\{k\times n\}}$. *Maple 11* LU-decomposes the matrix into three matrices called p, L and U, where p is a permutation matrix, L a lower triangular matrix and U an upper triangular matrix. Especially U collects the row space of S and therefore has the form

$$U = \begin{pmatrix} \star & & \cdots & & \star \\ 0 & \ddots & & & \vdots \\ \vdots & \ddots & \star & \cdots & \star \\ 0 & \cdots & 0 & \cdots & 0 \end{pmatrix}_{\{n\times n\}} \tag{D.11}$$

with k non-zero rows. Putting the zero rows aside, A and B can be calculated by $A_{\{n\times k\}} = p_{\{n\times n\}}L_{\{n\times k\}}$ and $B_{\{k\times n\}} = U_{\{k\times n\}}$. Now the inverse of S is given by

$$S^{-1} = B^{\dagger}(BB^{\dagger})^{-1}(A^{\dagger}A)^{-1}A^{\dagger}\,, \tag{D.12}$$

where the only task is to invert two nonsingular $k \times k$ matrices by a simple Gauss algorithm. This Moore-Penrose inverse now has the same relationships as equations (D.7) to (D.10).

List of Figures

List of Tables

References

[1] R. K. Eisenschitz, F. London. Über das Verhältnis der VAN DER WAALSschen Kräfte zu den homöopolaren Bindungskräften. *Z. Physik*, 60(491), 1930.

[2] F. London. *Z. Physik*, 63(245), 1930.

[3] H. B. G. Casimir. *On the attraction between two perfectly conducting plates.* Proc. K. Ned. Akad. Wetensch., 1948.

[4] P. W. Milonni. *The Quantum Vacuum.* Academic Press, San Diego, CA, 1994.

[5] D. P. Craig, T. Thirunamachandran. *Molecular Quantum Electrodynamics.* Dover, Mineola, NY, 1998.

[6] M. Fisher, P. de Gennes. Phenomenes aux parois dans un melange binaire critique. *Acad. Sci. Paris B*, 287:207, 1978.

[7] C. Hertlein, L. Helden, A. Gambassi, S. Dietrich, C. Bechinger. Direct measurement of critical Casimir forces. *Nature*, 451(7175):172–175, 2008.

[8] S. K. Lamoreaux. *Rep. Prog. Phys.*, 68:201, 2005.

[9] V. Sandoghdar, C.I. Sukenik, E.A. Hinds, S. Haroche. *Phys. Rev. Lett.*, 68:3432, 1992.

[10] C.I. Sukenik, M.G. Boshier, D. Cho, V. Sandoghdar, E.A. Hinds. *Phys. Rev. Lett.*, 70:560, 1993.

[11] V. Druzhinina, M. DeKieviet. *Phys. Rev. Lett.*, 91:193202, 2003.

[12] D.M. Harber, J.M. Obrecht, J.M. McGuirk, E.A. Cornell. *Phys. Rev. A*, 72:033610, 2005.

[13] J.M. Obrecht, R.J. Wild, M. Antezza, L.P. Pitaevskii, S. Stringari, E.A. Cornell. *Phys. Rev. Lett.*, 98:063201, 2007.

[14] C.J. Coakley, D. Tabor. *J. Phys. D: Appl. Phys.*, 11:L77, 1978.

[15] M.A. Bevan, D.C. Prieve. *Langmuir*, 15:7925, 1999.

[16] E.J.W. Verwey, J.Th.G. Overbeek. *Theory of the Stability of Lyophobic Colloids.* Dover Publications, 2003.

[17] H. B. Chan, V. A. Aksyuk, R. N. Kleiman, D. J. Bishop, F. Capasso. Quantum Mechanical Actuation of Microelectromechanical Systems by Casimir Force. *Science*, 291(5510):1941–1944, 2001.

[18] D. Iannuzzi, M. Lisanti, J.M. Munday, F. Capasso. *Solid State Comm.*, 135:618, 2005.

[19] B. V. Derjaguin, I. I. Abrikosova, and E. M. Lifshitz. Direct measurement of molecular attraction between solids separated by a narrow gap. *Q. Rev. Chem. Soc.*, 10:295–329, 1956.

[20] J. Blocki, J. Randrup, W. Swiatecki, C. Tsang. Proximity forces. *Ann. Phys.*, 105:427–462, 1977.

[21] M. Schaden, L. Spruch. Infinity-free semiclassical evaluation of Casimir effects. *Phys. Rev. A*, 58(2):427–462, 1998.

[22] H. Gies, K. Langfeld, L. Moyaerts. Casimir effect on the worldline. *JHEP*, 0306(06):018, 2003.

[23] L. Moyaerts, K. Langfeld, H. Gies. Worldline approach to the Casimir effect. 2003.

[24] R. L. Jaffe, A. Scardicchio. Casimir Effect and Geometric Optics. *Phys. Rev. Lett.*, 92(7):070402, 2004.

[25] A. Scardicchio and R. Jaffe. Casimir Effects: An Optical Approach I. Foundations and Examples. *Nucl. Phys. B*, 704(3):552–582, 2005.

[26] H. Gies, K. Klingmüller. Casimir Effect for Curved Geometries: Proximity-Force-Approximation Validity Limits. *Phys. Rev. Lett.*, 96(22):220401, 2006.

[27] M. Bordag. Casimir effect for a sphere and a cylinder in front of a plane and corrections to the proximity force theorem. *Phys. Rev. D*, 73(12):125018, 2006.

[28] A. Bulgac, P. Magierski, A. Wirzba. Scalar Casimir effect between Dirichlet spheres or a plate and a sphere. *Phys. Rev. D*, 73(2):025007, 2006.

[29] T. Emig, N. Graham, R. L. Jaffe, M. Kardar. Casimir Forces between Arbitrary Compact Objects. *Phys. Rev. Lett.*, 99(17):170403, 2007.

[30] M. Bordag, U. Mohideen, V. M. Mostepanenko. New Developments in the Casimir Effect. *Phys.Rept.*, 353:1–205, 2001.

[31] B. Döbrich. Non-perturbative access to Casimir-Polder potentials in nontrivial geometries. Diplomarbeit, Universitaet Heidelberg, 2008.

[32] V. Droujinina. On Quantum Reflection and The Casimir Effect. Dissertation, University of Heidelberg, 2003.

[33] U. Warring. Auf der Suche nach dem perfekten Quantenreflex. Diploma thesis, University of Heidelberg, 2006.

[34] L. H. Ryder. *Quantum Field Theory*. Cambridge University Press, 2 edition, 1996. p.146.

[35] T. Emig, R.F Büscher. Towards a theory of molecular forces between deformed media. *Nuclear Physics B*, 696(3):468 – 491, 2004.

[36] A. R. Edmonds. *Angular Momentum in Quantum Mechanics*. B-I-Hochschultaschenbücher, 1957.

[37] Frank J. Zerilli. Tensor Harmonics in Canonical Form for Gravitational Radiation and Other Applications. *Journal of Mathematical Physics*, 11(7):2203 – 2208, 1970.

[38] T. Emig. Fluctuation-induced quantum interactions between compact objects and a plane mirror. *Journal of Statistical Mechanics: Theory and Experiment*, 2008(04):P04007 (33pp), 2008.

[39] M. Daumens, P. Minnaert. Tensor spherical harmonics and tensor multipoles. I. Euclidean space. *Journal of Mathematical Physics*, 17(10):1903–1909, 1976.

[40] K. Klingmüeller, H. Gies. Geothermal Casimir Phenomena. 2007.

[41] John D. Jackson. *Klassische Elektrodynamik*. de Gruyter, 4$^{\text{th}}$ edition, 2006.

[42] Milton Abramowitz, Irene A. Stegun, editor. *Handbook of Mathematical Functions: with Formulas, Graphs, and Mathematical Tables*. Dover Publications, 1965.

[43] M. E. Peskin, D. V. Schroeder. *An Introduction to Quantum Field Theory*. Westview Press, 1995.

Acknowledgement

It has been a pleasure to work with Prof. Dr. Holger Gies in his research group, who enabled me to do this diploma thesis at the Institute of Theoretical Physics in Jena. I am grateful to him for his encouragement and various hints during the time.

Priv.-Doz. Dr. Maarten DeKieviet from the University in Heidelberg deserves gratitude for his increased interest in my work and his suggestions for solving the plain plate-sphere problem.

I am indebted to Babette Döbrich, who was always willing to listen to my concerns, for her patience, the numerous discussions and helpful suggestions.

My further thanks goes to my colleagues, who allowed me to use their computer resources and supported me in any way during my work on this thesis.

Eidesstattliche Erklärung

Ich erkläre, dass ich die vorliegende Arbeit

> *Non-perturbative access to Casimir-Polder potentials for nontrivial geometries in QED*

selbstständig verfasst und keine andere als die angegebenen Quellen und Hilfsmittel benutzt habe.

Jena, den 14. Mai 2010 _____
Frank Glowna

Seitens des Verfassers bestehen keine Einwände, die vorliegende Diplomarbeit für die öffentliche Nutzung in der Thüringer Universitäts- und Landesbibliothek zur Verfügung zu stellen.

Jena, den 14. Mai 2010 _____
Frank Glowna